Large-N_c Consistency of Chiral Nuclear Forces

Masterarbeit

im

Studiengang

„Master of Science“

im Fach Physik

an der Fakultät für Physik und Astronomie

der Ruhr-Universität Bochum

von

Christopher Körber

aus

Bochum

Bochum 2014

Abstract

Large-N_c Konsistenz von chiralen Nukleon-Kräften

Ziel dieser Arbeit ist die Prüfung der Konsistenz von Nukleon-Nukleon Kräften, welche durch zwei verschiedene Approximationen der Quanten Chromodynamik (QCD) bestimmt werden. Dargestellt werden hierbei die Herleitung des Nukleon-Nukleon Potentials durch die Chirale Störungstheorie (χPT) sowie der QCD im large-N_c limes. Die Konsistenz des chiralen Potentials, bestimmt durch unitäre Transformationen, wird für die chiralen Ordnungen Q^ν für $\nu = 0,2,4$ bewiesen. Methoden der Überprüfung sowie Aussichten für höhere Ordnungen werden präsentiert.

Large-N_c consistency of chiral nuclear forces

The work tests the consistency of nucleon-nucleon forces derived by two different approximation schemes of Quantum Chromodynamics (QCD)—the chiral perturbation theory (χPT) and large-N_c QCD. The approximation schemes and the derivation of the potential are demonstrated in this work. The consistency of the chiral potential, derived using the method of unitary transformation, is verified for chiral orders Q^ν for $\nu = 0,2,4$. Used methods as well as possible extensions for higher orders are presented.

Contents

Part I

Introduction

Introduction

The standard model of particle physics is currently the most successful model to describe interactions in the regime of subnuclear physics. By predicting the Higgs particle, one was able to verify the applicability of this model in high precision. The hadronic part of the model—the so-called Quantum Chromodynamics (QCD)—is the theory which describes the interaction of hadrons (e.g. nucleons) and mesons (e.g. pions) on a subhadronic scale. Elementary particles in this theory, the quarks, carry the so-called quantum number *color*. As a result of measurements, one can describe the currently known physics by the following observations:

- there are three different color quantum-numbers: $N_c = 3$ and
- all hadrons—as compound quark-states—are color neutral.

Though one is able to make predictions of such dynamics in the high-energy regime using a perturbative ansatz, solutions below a regime specific scale can currently not be computed in a conventional way. To overcome this obstacle, different approximations were used to find solutions of low-energy QCD problems. Two of those theories are the so-called large-N_c limit of QCD and the Chiral Perturbation Theory (χPT).

The large-N_c limit of QCD assumes that the number of colors N_c is large and $1/N_c$ accordingly small. Thus one can start to evaluate the theory as a perturbation over $1/N_c$ (['t Hooft, 1974]). Knowing that the world can be described by $N_c = 3$, one hopes that qualitative results of large-N_c QCD are also valid for regular QCD.
While [Witten, 1979] has shown that general hadron-meson-scattering-amplitudes have to scale with N_c, [Kaplan and Savage, 1996] and [Kaplan and Manohar, 1997] were able to make further predictions for nuclear potential: the large-N_c scaling of the nuclear potential is depending on spin and isospin structures of the asymptotic states (KSM counting rules).

In contrast to the large-N_c ansatz, the χPT is effectively a colorless theory. To construct an effective theory of QCD, one demands that the new theory has the same symmetry properties as the more fundamental theory [Weinberg, 1968]. As the name already suggests χPT is based on the chiral symmetry quarks. The particles which are used to formulate the theory, the degrees of freedom, are hadrons only and thus colorless.

Though, from a naive point of view, those two theories cannot be compared, the symmetry analysis of the nucleon-nucleon potential in large-N_c QCD and χPT makes it possible to draw comparisons between both theories.

While [Banerjee et al., 2002] have shown that the chiral approximation of QCD in the limit of large-N_c supports the KSM counting rules up to chiral order $\nu = 2$, some problems still arise on higher chiral orders [Belitsky and Cohen, 2002]. To solve this problem [Cohen, 2002] suggests a different, energy independent, approach for computing nuclear forces.

In this work, the method of unitary transformation ([Epelbaum et al., 1998]) is used to derive the nuclear potential and it is shown that this potential is consistent with the KSM counting rules in the limit of large-N_c up to chiral order $\nu = 4$.

1 Quantum Chromodynamics

1.1 Gauge theory of strong interactions

In the early sixties Gell-Mann was able to resolve the so-called particle zoo problem. The variety of new possible elementary particles could be systematically ordered by introducing three more fundamental building blocks—the so-called up, down and strange quarks. Using the conservation of specific quantum numbers, Gell-Mann noticed that at that time known particles can be expressed as weights of a $SU(3)$-representation, the so-called flavor-$SU(3)$. Thus the u,d and s quarks correspond to the fundamental weights of this representation. Later on, further quark flavors where introduced to be able to explain newly discovered particles at higher energy scales. Currently, all known hadronic particles can be build out of the three light quarks and additionally the more heavy charm bottom and top quark (see table 1.1).

flavor	u *up*	d *down*	s *strange*	c *charmed*	b *bottom*	t *top*
Mass (MeV)	$2.3^{+0.7}_{-0.5}$	$4.8^{+0.7}_{-0.3}$	95 ± 5	1275 ± 25	4180 ± 30	$160^{+5}_{-4} \cdot 10^3$

Table 1.1: The six flavors of quarks as the building block of current hadronic particles. The masses are calculated using the $\overline{MS}$-scheme at scale $\mu = 2GeV$ (extracted from [Beringer et al., 2012]).

Though one was able to describe particles in a more compactified theory, a major problem still arises: acknowledging the quarks as fermions, some compound quark objects did not obey the Pauli statistics any more. As a simple example on could mention the Δ_{++} resonance: the Δ_{++} is build out of three up quarks and can carry the spin $S = 3/2$. Thus all up quarks (which are described by a two dimensional spin representation) have to be aligned with the same spin. Since all quantum-numbers are the same, this would be a violation of the Pauli statistics.

To resolve this problem, another quantum-number was introduced: the so-called color of quarks. Similar to the flavor, quarks transform like $SU(3)$ representations under color. Also it is important to mention, that observable particles are color neutral. While mesons are build out of a quark and an antiquark, color and the according anti-color, baryons are made up out of three different colors. Both add up to the color „white“[1]. The observation of colorless particles is also known as the color confinement. Also to express the importance of colors, the theory to describe the strong interactions between hadrons is called Quantum Chromodynamics.

[1] This analogy is considered to be the reason for the name color $SU(3)$.

1.2 QCD Lagrangian

This section basically summarizes briefly some facts about QCD and is following [Peskin and Schroeder, 1995], [Scherer and Schindler, 2012] as well as [Zee, 2003].

As a summary to statements in the previous section, the three light quarks have to transform according to

$$SO(3,1)_{Lorentz} \times SU(3)_{flavor} \times SU(3)_{color} \,. \tag{1.1}$$

Therefore, if one wants to describe a model inhabiting the three light quarks, one has to acknowledge nine times the free Dirac equation for each quark state:

$$\mathscr{L}_{\text{light quarks}} = \sum_{F=1}^{3} \sum_{a=1}^{3} \sum_{\alpha=1}^{4} \left(\bar{q}_F^a\right)_\alpha \left(i\partial\!\!\!/ - m_F\right)_{\alpha\beta} \left(q_F^a\right)_\beta \,. \tag{1.2}$$

Hereby the upper case letters refer to the quark flavors, the lower case letters to the quark colors and the Greek letters to the Dirac spinor components.

As a crucial feature of hadron physics, it is known that states are asymptotically free: at large distances, the interaction between quarks is non-existing. As Quantum Electrodynamics already has introduced the principle of gauge theories, it was known that only a non-abelian gauge theory could provide such asymptotic freedom. Thus the color $SU(3)$, as a local symmetry of QCD, should fulfill those requirements.

Since each quark flavor in each Dirac component has to obey the gauge principle individually, one can formulate the transformation under the color $SU(3)$ by suppressing the Dirac spinor index as

$$q_F \mapsto U_g q_F \, U_g^\dagger = D(g) q_F = \exp\left(-ig(x)\right) q_F \,. \tag{1.3}$$

Note that the unitary operators U directly act on the Fock-space[2], while D is the representation of this transformation which is acting on color space. The matrix $g(x) = \theta^a(x)\lambda^a/2$ is a local generator of $SU(3)$, which generates the so-called Gell-Mann algebra $\mathfrak{su}(3)$. Using that U is unitary, one can see that the Lagrangian density of equation (1.2) is currently not invariant under transformations of equation (1.3) since the derivative is also acting on $U = U(x)$. To provide the correct transformation law, one introduces a covariant derivative D_μ which should transform according to

$$D_\mu \, q_F(x) \mapsto U(D_\mu \, q_F(x)) U^\dagger \stackrel{!}{=} U(x) D_\mu \, q_F(x) \,. \tag{1.4}$$

A solution to this transformation law is generated by introducing the gauge field $\mathcal{A}_\mu$[3]

$$D_\mu \, q_F(x) := \left(\partial_\mu + ig\mathcal{A}_\mu\right) q_F(x) \,, \tag{1.5}$$

and solving for the transformation law of $\mathcal{A}_\mu$ one gets

$$\mathcal{A}_\mu \mapsto \hat{U}\mathcal{A}_\mu\hat{U}^\dagger = U(x)\mathcal{A}_\mu U^\dagger(x) + \frac{i}{g}\left(\partial_\mu U(x)\right) U^\dagger(x) \,. \tag{1.6}$$

For infinitesimal transformations $U(x) \approx 1 - i\theta_a(x)\lambda_a/2$ it is also useful to decompose $\mathcal{A}_\mu$ into its $SU(3)$ components:

$$\begin{aligned} \hat{U}\mathcal{A}_\mu^a\hat{U}^\dagger\frac{\lambda^a}{2} &= \mathcal{A}_\mu^a\frac{\lambda^a}{2} + i\mathcal{A}_\mu^b\theta^c\left[\frac{\lambda^b}{2}\,,\,\frac{\lambda^c}{2}\right] - \frac{1}{g}\partial_\mu\theta^a\frac{\lambda^a}{2} \\ &= \left(\mathcal{A}_\mu^a + \frac{i}{2}\mathcal{A}_\mu^b\theta^c f^{abc} - \frac{1}{g}\partial_\mu\theta^a\right)\frac{\lambda^a}{2} \,, \end{aligned} \tag{1.7}$$

[2] Acting on the Fock-space is equivalent to transforming creation and annihilation operators.

[3] Note that the gauge field $\mathcal{A}_\mu$ also has to able to act on Fock-space, since otherwise it would not be possible to provide this kind of transformation behavior, e.g. $U\mathcal{A}_\mu U^\dagger = \mathcal{A}'_\mu$. Thus this gauge field is able to create and annihilate quarks. The intermediate "exchange" particles corresponding to the gauge field will be called gluons later on.

where the so-called structure constants f^{abc} of the algebra $\mathfrak{su}(3)$ have been introduced.

Since one has introduced a further object acting on the Fock-space, one has to include $\mathcal{A}_\mu$ such that the symmetries of the Lagrangian remain unchanged. Doing so one finally obtains the full[4] gauge invariant QCD Lagrangian

$$\mathscr{L}_{QCD} = \sum_F \bar{q}_F \left(i\not{D} - m_F\right) q_F - \frac{1}{4}\mathrm{Tr}\left[\mathcal{G}_{\mu\nu}\mathcal{G}^{\mu\nu}\right] , \tag{1.8}$$

where the trace is acting on color space for the non-abelian field-strength tensor

$$\mathcal{G}^a_{\mu\nu} = \partial_\mu \mathcal{A}^a_\nu - \partial_\nu \mathcal{A}^a_\mu - g f^{abc} \mathcal{A}^b_\mu \mathcal{A}^c_\nu \, . \tag{1.9}$$

It is also important to mention that the last term of (1.9) makes it possible to have three- and four-vertices of gauge fields only (see figure 1.2). Thus the gauge boson of QCD, also-called gluon, is able to interact with itself and poses a major problem for low energy computations.

Gluon-Fermion Vertex	Three-Gluon Vertex	Four-Gluon Vertex
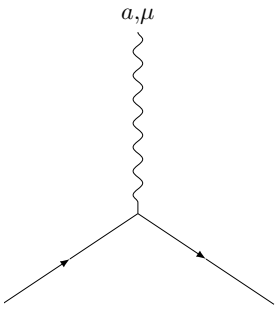	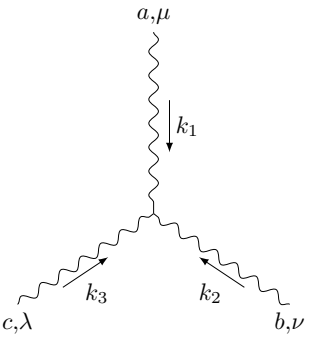	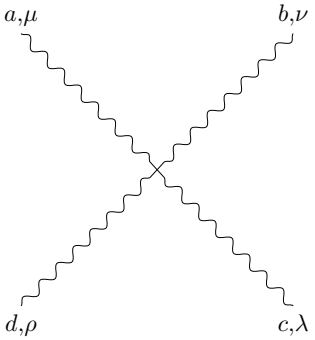
$ig\gamma^\mu\lambda^a$	gf^{abc} $\times\Big[\; g^{\mu\nu}(k_1-k_2)^\lambda$ $+g^{\lambda\nu}(k_2-k_3)^\mu$ $+g^{\mu\lambda}(k_3-k_1)^\nu\Big]$	$-ig^2$ $\times\Big[\; f^{abe}f^{cde}(g^{\mu\lambda}g^{\nu\rho}-g^{\mu\rho}g^{\nu\lambda})$ $+f^{ade}f^{cbe}(g^{\mu\lambda}g^{\nu\rho}-g^{\mu\nu}g^{\rho\lambda})$ $+f^{ace}f^{bde}(g^{\mu\nu}g^{\lambda\rho}-g^{\mu\rho}g^{\nu\lambda})\Big]$

Table 1.2: Possible fermion-gluon and pure gluon vertices for Lagrangian density given by (1.8). Fermions are represented by directed straight lines while gluons are represented by curly lines.

[4] In principle one could also include a so-called θ-term proportional to θ^a which violates P and CP symmetry.

1.3 Running coupling and renormalization group flow

To explain the difficulty in the low-energy regime of QCD, it is useful to discuss the description of physical quantities in renormalized theories. When making predictions for physical quantities Q_1 and Q_2, one has to find the relation between Q_1 and Q_2

$$Q_1 = f\left(Q_2\right) . \tag{1.10}$$

The measurement of just one quantity is equivalent to making a definition of the meaning of the quantity itself. As an example, the Milikan experiment has defined what one has to understand as a fundamental charge e. This feature is even more evident in quantum field theories since, in general, those quantities depend on scheme specific, non-physical parameters.

The ϕ^4-theory as an example, has two parameters: the bare mass $\mathring{m}$ and the bare coupling $\mathring{\lambda}$ of a scalar field ϕ. It is important to mention that the $\mathring{m}$ and $\mathring{\lambda}$ do not have to be physical (measurable) parameters as the physical mass of the particle

$$\mathscr{L} = \frac{1}{2}\left(\partial_\mu\phi\,\partial^\mu\phi - \mathring{m}\phi^2\right) + \frac{\mathring{\lambda}}{4!}\,\phi^4 . \tag{1.11}$$

To find the physical correspondence of those parameters, one could measure scattering processes of the ϕ-particle. For example one could measure $p_1 + p_2 \mapsto p_3 + p_4$ processes to find the physical coupling λ_P. Accordingly the most general type of λ_P is given by

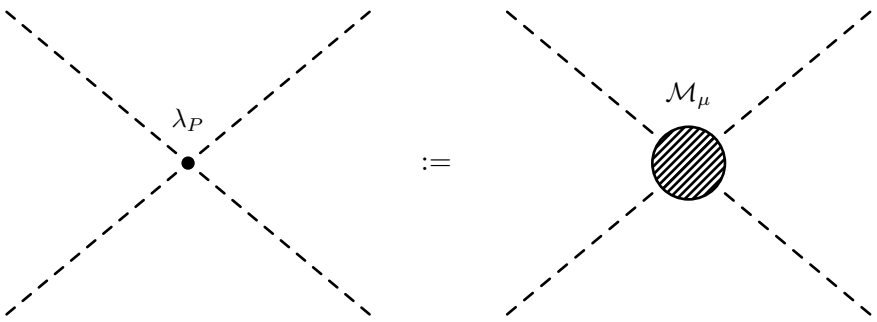

Figure 1.1: Definition of the physical coupling λ_P in a ϕ^4-theory in terms scattering amplitude $\mathcal{M}$ measured at momentum scale μ.

$$\lambda_P\big|_\mu = \lambda_P\left(\mathring{\lambda},\mathring{m},p=\mu\right) , \tag{1.12}$$

where μ is the momentum scale where the external momenta p_i's are measured.

Furthermore, when computing the scattering amplitude for such a process, one recognizes divergences. Since one tries to find a relation between λ_P and m_P one can not assume that λ_P as a function of non-physical parameters $\mathring{\lambda}$ and $\mathring{m}$ has to be well-defined—just the definition of λ_P in terms of physical parameters has to be well-defined[5]. Thus, to avoid divergences, it is essential to introduce a regularization scheme depending on a non-physical scale or cutoff parameter Λ[6], which makes it possible to compare λ_P and m_P with each other. Accordingly the most general form for the physical parameters is given by:

$$m_P = f_{m_P}(\mathring{m},\mathring{\lambda},\mu,\Lambda) \qquad \lambda_P = f_{\lambda_P}(\mathring{m},\mathring{\lambda},\mu,\Lambda) , \tag{1.13}$$

[5] In fact this is only possible if a theory is renormalizable in the sense of subtracting divergences.

[6] To understand the meaning of Λ some physicist share the believe that each QFT is an effective field theory of a more fundamental theory. Thus it is not shocking that the current theory is just valid in a specific energy regime. To evaluate the theory in the according regime, a cutoff Λ is introduced. Particles with an energy higher than Λ do not contribute to any processes.

or in terms of physical parameters for a renormalizable theory

$$m_P\big|_{\mu_1} := f_{m_P}\left(m_P|_{\mu_2}, \lambda_P|_{\mu_3}, \mu_1\right) \qquad \lambda_P\big|_{\mu_1} := f_{\lambda_P}(m_P|_{\mu_2}, \lambda_P|_{\mu_3}, \mu_1)\,, \tag{1.14}$$

where the μ_i's correspond to the measurement of the physical parameters at a given momentum scale μ. Note that the physical parameters should be independent of the cutoff Λ.

Obviously one would expect that for a measurement at the same scale $\mu_i = \mu$ that

$$f_{m_P}\left(m_P|_{\mu}, \lambda_P|_{\mu}, \mu\right) \stackrel{!}{=} m_P|_{\mu}\,, \tag{1.15}$$

and thus one might be interested in the μ-scaling of the physical parameters, if one has measured the couplings at a given different scale μ_0. The differential equation describing the flow of a physical parameter in terms of the measuring scale μ is called the renormalization group flow equation

$$\mu\frac{\mathrm{d}}{\mathrm{d}\mu}g_{P,j}\big|_{\mu} = f_j\left(g_{P,i}\big|_{\mu}\right)\,. \tag{1.16}$$

Hereby the „constants“ $g_{P,i}\big|_{\mu}$ are physical parameters evaluated at a momentum scale μ.

As it can be found in literature, the so-called running coupling at scale μ in QCD, is given by (suppressing the index P)

$$\mu\frac{\mathrm{d}}{\mathrm{d}\mu}g_{\mu} = -\frac{g_0^3}{(4\pi)^2}\left(\frac{11}{3}N_c - \frac{2}{3}n_f\right)\,, \tag{1.17}$$

with N_c the dimension of the gauge group $SU(N_c)$ (colors) and n_f the number of fermion species (flavors). This equation demonstrates a crucial behavior of the QCD coupling—for large an increasing energy scale $\mu \gg \mu_0$ the interaction between quarks and gluons is converging until it is neglectable, which is the so-called asymptotic freedom. But the interaction-strength is increasing if μ becomes smaller. Accordingly below a momentum scale μ_{QCD} it is not possible to compute quantities using regular perturbation theory.

2 Chiral perturbation theory

> *If one writes down the most general possible Lagrangian, including all terms consistent with assumed symmetry principles, and then calculates matrix elements with this Lagrangian to any given order of perturbation theory, the result will simply be the most general possible S-matrix consistent with analyticity, perturbative unitarity, cluster decomposition and the assumed symmetry principles.*
>
> — S. Weinberg, 1979

Effective field theories as the chiral perturbation theory aim to describe a more fundamental theory in an energy regime below a certain scale Λ. For example the nucleon masses in the chiral perturbation theory (χPT) of light up and down quarks. Since the effective theory approximates the underlying theory only in this regime, knowledge of the high energy behavior can be excluded.

As demonstrated in the previous section, in the case of QCD it was not possible to start a perturbation in terms of the gluon coupling g_A for a low-energy regime because the QCD gauge group, the color $SU(3)$, caused the coupling to increase. Since the color quantum numbers are an internal parameter of the theory—only quarks and gluons carry color, while external states as hadrons are color neutral—a theory not using color as a quantum number might allow computations in a low-energy regime. However, it is essential that the symmetries of external QCD states are conserved in the effective theory as well. Thus, the only possible choice for realizing such a theory is to change the degrees of freedom such that the symmetries are preserved. E.g. the quarks and gluons are replaced by hadrons in χPT. While quarks transform as the fundamental representation of $SU(3)$, the hadrons and mesons transform under higher representations of $SU(3)$ (see figure 2.1).

Since the replacement of degrees of freedom effectively changes the interaction of the theory, one has to start with the most general effective Lagrangian respecting all symmetries. Thus one has an infinite amount of couplings (low energy constants: LECs) describing the strength of all possible interactions. Since it is not useful to compute an infinite number of diagrams when computing observable, one restricts the analysis to only relevant terms: instead of a perturbation in terms of the LECs, one perturbates in energies or momenta small compared to the associated hard scale Q/Λ. The relevance of terms will be identified by a so-called power counting.

Nevertheless a theory with an infinite amount of interactions may pose another problem: strictly speaking such a theory is non-renormalizable. But, as an important fact, those infinities still can be absorbed when one introduces and redefines LECs at each order.

In this section, basic facts about the chiral perturbation theory are mentioned to finally derive the leading order pion nucleon interactions. These quantities are needed to compute the nuclear forces which allow to compare chiral perturbation theory with QCD using the large-N_c symmetries.

As an introduction to chiral perturbation theory [Scherer and Schindler, 2012] and [Epelbaum, 2010] can be mentioned.

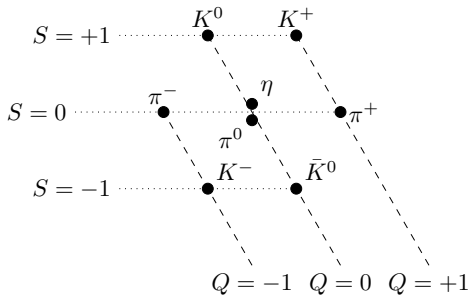

(a) Baryon octet including singlet state.

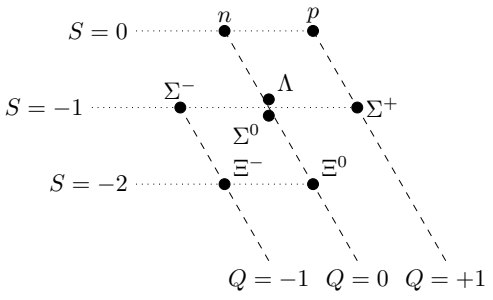

(b) Meson octet including singlet state.

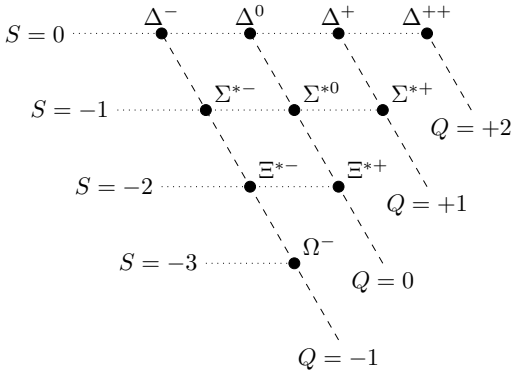

(c) Baryon decouplet.

Figure 2.1: Hadronic particles arranged according to strangeness and charge such that they fit the pattern of $SU(3)$ weight diagrams—the so-called flavor multiplets.

In the following, the analysis is restricted to the light up and down quarks. Therefore the $SU(3)$ flavor symmetry becomes the $SU(2)$ isospin symmetry. Considering that strange quark bound states are much heavier than states consisting only out of the light up and down quarks, this is a good approximation for the low-energy regime. In general one can also describe strange quark states using the chiral perturbation theory.

2.1 Chiral symmetry of QCD

As described in section 1.1, the QCD-Lagrangian is of the form

$$\mathscr{L}_{QCD} = \bar{q}\left(i\not{D} - m\right) q - \frac{1}{4}\mathrm{Tr}\left[\mathcal{G}_{\mu\nu}\mathcal{G}^{\mu\nu}\right] , \tag{2.1}$$

where the quark fields are vectors and the mass $m = \mathrm{diag}(m_u, m_d)$ is a matrix in isospin space. When introducing projection operators

$$P_R := \frac{\mathbb{1} + \gamma^5}{2} \qquad\qquad P_L := \frac{\mathbb{1} - \gamma^5}{2} , \tag{2.2}$$

where $\gamma^5 = i\gamma^0\gamma^1\gamma^2\gamma^3 = \gamma^{5\,\dagger}$, the quark fields can be expressed as right- and left-handed fields

$$q = q_R + q_L = P_R\, q + P_L\, q\,. \tag{2.3}$$

Using this, the Hamiltonian takes the following form

$$\mathscr{L}_{QCD} = \bar{q}_L\left(i\not{D}\right) q_L + \bar{q}_L\left(i\not{D}\right) q_L - \bar{q}_R m q_L - \bar{q}_L m q_R - \frac{1}{4}\mathrm{Tr}\left[\mathcal{G}_{\mu\nu}\mathcal{G}^{\mu\nu}\right] . \tag{2.4}$$

Considering that the quark masses are way smaller than the actual hadronic masses $m_u/m_N \sim 1/1000$, it is a good approximation to let the quark masses vanish:

$$m_u, m_d \to 0\,. \tag{2.5}$$

This limit is called the chiral limit. Thus, since the covariant derivative $\not{D}$ has no isospin dependence, the Lagrangian is invariant under $SU(2)_L \times SU(2)_R$ with

$$q \overset{SU(2)_L}{\longmapsto} q' = U_L\, q = \exp\left(-\frac{i}{2}\theta_L^a \tau^a\right) q \qquad q \overset{SU(2)_R}{\longmapsto} q' = U_R\, q = \exp\left(-\frac{i}{2}\theta_R^a \tau^a\right) q\,. \tag{2.6}$$

The infinitesimal variation of the Lagrangian under both transformations is given by

$$\delta\mathscr{L}_{QCD} = \mathscr{L}'_{QCD} - \mathscr{L}_{QCD} = \frac{1}{2}\bar{q}_R \left(\partial_\mu \theta_R^a \tau^a\right) \gamma^\mu q_R + \frac{1}{2}\bar{q}_L \left(\partial_\mu \theta_L^a \tau^a\right) \gamma^\mu q_L\,. \tag{2.7}$$

According to Noethers theorem, a symmetry corresponds to a conserved current

$$J_i^\mu = \frac{\partial\, \delta\mathscr{L}_{QCD}}{\partial\, \partial_\mu \epsilon_i} \qquad\qquad \partial_\mu J_i^\mu = 0\,, \tag{2.8}$$

and thus one obtains the six currents given by

$$L_\mu^a = \bar{q}_L \gamma_\mu \frac{\tau^a}{2} q_L \qquad\qquad R_\mu^a = \bar{q}_R \gamma_\mu \frac{\tau^a}{2} q_R\,. \tag{2.9}$$

Also important are the vector current and the axial current defined by

$$V_\mu^a = R_\mu^a + L_\mu^a = \bar{q}\gamma_\mu \frac{\tau^a}{2} q \qquad\qquad A_\mu^a = R_\mu^a - L_\mu^a = \bar{q}\gamma_\mu\gamma_5 \frac{\tau^a}{2} q\,. \tag{2.10}$$

Furthermore one can compute the conserved charges

$$Q_J^a = \int \mathrm{d}^3x\; J_0^a(x) \tag{2.11}$$

which generate the chiral group

$$\begin{aligned} &\left[Q_R^a\,,\, Q_R^b\right] = i\epsilon^{abc} Q_R^c \qquad \left[Q_L^a\,,\, Q_L^b\right] = i\epsilon^{abc} Q_L^c \qquad \left[Q_L^a\,,\, Q_R^b\right] = 0 \\ &\left[Q_V^a\,,\, Q_V^b\right] = i\epsilon^{abc} Q_V^c \qquad \left[Q_A^a\,,\, Q_A^b\right] = i\epsilon^{abc} Q_V^c \qquad \left[Q_V^a\,,\, Q_A^b\right] = i\epsilon^{abc} Q_A^c\,. \end{aligned} \tag{2.12}$$

These additional generators of $SU(2)$ play a crucial role for the chiral perturbation theory. As experiments have indicated, the axial current does not annihilate the vacuum, only the vector current does

$$Q_V^a\,|0\rangle = 0 \qquad\qquad Q_A^a\,|0\rangle \neq 0\,. \tag{2.13}$$

This indicates that the larger symmetry $G = SU(2)_R \times SU(2)_L$ is spontaneously broken down to only the subgroup $H = SU(2)_V \subset G$. According to the Goldstone theorem the other $n_G - n_H = 3$ generators, the generators of the subgroup $SU(2)_A$, correspond to massless[1] Goldstone-bosons—the pions (π^-,π^0,π^+).

[1] As experiments indicate, pions are not massless. This fact arises in theory if one considers that the chiral symmetry is just an approximation. If one includes the symmetry breaking mass term of the quarks, the pions become massive with mass $m_\pi \sim 140 MeV$.

2.2 Chiral pionic Lagrangian

The goal of this section is to create the most general Lagrangian containing the symmetries of the chiral QCD:

- the degrees of freedom should transform under $SU(2)_R \times SU(2)_L$ such that the Lagrangian is invariant under such transformations.
- Pionic degrees of freedom should transform linearly under $SU(2)_V$ as a three dimensional (adjoint) representation.

The idea for creating such a Lagrangian will be the following: Find a unitary parameterization U_π of the pionic fields π^a such that U transforms as

$$U_\pi \longmapsto U'_\pi = L U_\pi R^\dagger \,, \tag{2.14}$$

and respects the linear transformation behavior of π under $SU(2)_V$. If one has found this parametrization, the Lagrangian can be constructed out of derivatives of traces of combinations of multiples of $U_\pi^\dagger U_\pi$

$$\mathscr{L}_\pi = c_0 \mathrm{Tr}(U_\pi^\dagger U_\pi) + c_2 \mathrm{Tr}(\partial_\mu U_\pi^\dagger \partial^\mu U_\pi) + \cdots \,, \tag{2.15}$$

since

$$U_\pi^\dagger U_\pi \mapsto R U_\pi^\dagger L^\dagger L U_\pi R^\dagger = \mathbb{1} \,, \tag{2.16}$$

and for global rotations U_R and U_L also the derivatives commute with the rotations $\partial_\mu R = R \partial_\mu$.

However, there is a subtle difficulty when creating this Lagrangian out of parameterizations U_π. In regular QCD one has used linear representations to describe the transformation behavior of states. As pointed out before, one has three pions transforming as a linear representation under $SU(2)_V$. The group of left-handed and right-handed transformation $SU(2)_L \times SU(2)_R$ contains $3+3=6$ generators—similarly to $SO(4)$ which has also $4(4-1)/2 = 6$ generators. Since one can find a homomorphism between both algebras, both groups are isomorphic and thus one can express the representations of $SU(2)_L \times SU(2)_R$ as representations of $SO(4)$. But the smallest representation of $SO(4)$ is at least four dimensional and thus it is not possible to describe the transformation behavior of four dimensional states by using three linear independent vectors (the pions) in a linear way. Thus one has to drop the linear transformation property of general states and uses realizations instead of representations. In general one is looking for a operation Ψ which maps an element of the group $(L,R) = g \in G = SU(2)_L \times SU(2)_R$ and a parameterization of the pion-fields $U_\pi \in \mathscr{H}$ onto another parameterization of the pion-fields

$$\Psi : G \times \mathscr{H} \mapsto \mathscr{H} \,, \tag{2.17}$$

which has to fulfill the properties

$$\begin{aligned} \Psi(\mathbb{1}, U_\pi) &= U_\pi && \forall\, U_\pi \in \mathscr{H} \\ \Psi(g_1, \Psi(g_2, U_\pi)) &= \Psi(g_1 g_2, U_\pi) && \forall\, U_\pi \in \mathscr{H} \,,\ \forall\, g_1, g_2 \in G \,, \end{aligned} \tag{2.18}$$

which is indeed fulfilled by

$$\Psi((L,R), U_\pi) = L U_\pi R^\dagger \,. \tag{2.19}$$

Note that this operation would be a linear if U_π forms a vectorspace, however this will not be true in general. For infinitesimal transformations $R = \mathbb{1} - i\theta_R^a \tau^a/2$ and L accordingly one now obtains

$$L U_\pi R^\dagger = U_\pi + \frac{i}{2} \left(U_\pi \theta_R^a \tau^a - \theta_L^a \tau^a U_\pi \right) + \mathcal{O}(\theta^2) \,. \tag{2.20}$$

Since one requires that the pion fields π in U_π transform as the adjoint representation under $(V,V) = SU(2)_V \subset SU(2)_L \times SU(2)_R$, one has to require that $U_\pi = U_\pi(\tau^b \pi^b)$ since

$$\pi^b \theta_V^a \left(\tau^b \tau^a - \tau^a \tau^b\right) = -2i\epsilon^{abc} \pi^b \theta_V^a \tau^c \,, \tag{2.21}$$

and thus, as requested before, the pions will transform as adjoint representation of $SU(2)_V$

$$\pi^a \mapsto \pi^a + \epsilon^{abc} \theta_V^b \pi^c \,. \tag{2.22}$$

Note that axial transformations $(A, A^\dagger) \in SU(2)_A$ in general do not result in a simple transformation behavior for pions.

Possible choices for the paramerterization U_π are for example given by

$$U_\pi = \exp\left(i\frac{\pi^a \tau^a}{F}\right) \qquad \text{or} \qquad U_\pi = \frac{1}{F}\left(\sqrt{F^2 - \pi^2}\,\mathbb{1} + i\pi^a \tau^a\right) . \tag{2.23}$$

The LEC F is introduced to make the arguments dimensionless and can be identified with the pion decay constant f_π. As one can already see, the parameterization of U_π is not unique. But as it has been shown, all realizations are equivalent to each other modulo a non-linear field redefinition which does not change the S-matrix elements ([Coleman et al., 1969], [Callan et al., 1969] and [Haag, 1958]).

Using this, the leading order pionic Lagrangian (without the explicit symmetry breaking terms) is given by

$$\mathscr{L}_\pi^{(2)} = \frac{F^2}{4} \mathrm{Tr}(\partial_\mu U_\pi^\dagger \partial^\mu U_\pi) \,, \tag{2.24}$$

where $(n) = (2)$ denotes the number of derivatives.

2.3 Chiral Lagrangian containing nucleons

Similarly to the pions, the nucleons should transform linearly under $SU(2)_V$ and non-linearly under $SU(2)_L \times SU(2)_R$. In general, the pion matrix U_π and a nucleon vector $N = (p,n)$ should transform as

$$\begin{pmatrix} U_\pi \\ N \end{pmatrix} \mapsto \begin{pmatrix} L U_\pi R^\dagger \\ K(U_\pi, L, R) N \end{pmatrix} . \tag{2.25}$$

This transformation also respects the properties of a realization (2.18) if K fulfills

$$K(U_\pi, \mathbb{1}, \mathbb{1}) = \mathbb{1} \quad \text{and} \quad K(L_2 U_\pi R_2^\dagger, L_1, R_1) K(U_\pi, L_2, R_2) = K(U_\pi, L_1 L_2, R_1 R_2) \,. \tag{2.26}$$

Additionally it should transform the nucleons as the fundamental $SU(2)_V$ representation

$$K(U_\pi, V, V) N = V N \,. \tag{2.27}$$

A possible way for introducing this K is given by

$$K(U_\pi, L, R) = \sqrt{L U_\pi R^\dagger}^{-1} L \sqrt{U_\pi} \,, \tag{2.28}$$

since K at the identity element is the identity

$$K(U_\pi, \mathbb{1}, \mathbb{1}) = \sqrt{U_\pi}^{-1} \sqrt{U_\pi} = \mathbb{1} \,, \tag{2.29}$$

K is a group-homomorphism

$$\begin{aligned} K(L_2 U_\pi R_2^\dagger, L_1, R_1) K(U_\pi, L_2, R_2) &= \sqrt{L_1 L_2 U_\pi R_2^\dagger R_1^\dagger}^{-1} L_1 \sqrt{L_2 U_\pi R_2^\dagger} \sqrt{L_2 U_\pi R_2^\dagger}^{-1} L_2 \sqrt{U_\pi} \\ &= \sqrt{L_1 L_2 U_\pi R_2^\dagger R_1^\dagger}^{-1} L_1 L_2 \sqrt{U_\pi} \\ &= K(U_\pi, L_1 L_2, R_1 R_2) \end{aligned} \tag{2.30}$$

and transforms nucleons as the fundamental $SU(2)_V$ representation

$$\begin{aligned} K(U_\pi, V, V) &= \sqrt{VU_\pi V^\dagger}^{-1} V\sqrt{U_\pi} \\ &= \left(V\sqrt{U_\pi}V^\dagger\right)^{-1} V\sqrt{U_\pi} = V\,, \end{aligned} \tag{2.31}$$

where it was used that V is unitary and the square root of U_π denoted by $u_\pi := \sqrt{U_\pi}$ transforms as U_π since

$$\sqrt{VU_\pi V^\dagger} := \sum_{n=0} a_n \left(VU_\pi V^\dagger\right)^n = V\left(\sum_{n=0} a_n U_\pi^n\right) V^\dagger = V\sqrt{U_\pi}V^\dagger =: VuV^\dagger\,. \tag{2.32}$$

When creating the most general Lagrangian one has to acknowledge another thing. In the previous case, the chiral transformations were global, but in this case, the transformation is depending on the pion fields $U_\pi(x)$ which depend on the coordinates. Thus, derivatives do not commute with chiral transformations and one has to introduce a covariant derivative D_μ. In general one wants the transformation behavior

$$D_\mu\left(K(U_\pi(x),L,R)N\right) = K(U_\pi(x),L,R)D_\mu N\,. \tag{2.33}$$

This can be achieved by introducing the chiral connection Γ_μ by

$$\Gamma_\mu := D_\mu - \partial_\mu = \frac{1}{2}\left(u_\pi^\dagger\partial_\mu u_\pi + u_\pi\partial_\mu u_\pi^\dagger\right) \tag{2.34}$$

where the explicit transformation behavior of K and N where used to determine Γ. At the order of one derivative, one can also create another chiral invariant term

$$u_\mu := i\left(u_\pi^\dagger\partial_\mu u_\pi - u_\pi\partial_\mu u_\pi^\dagger\right)\,, \tag{2.35}$$

which transforms under parity like an axial vector $u_\mu \overset{P}{\mapsto} -u^\mu$. Using these building blocks, the most general Lagrangian with two interacting nucleons has to be of the form $\bar{N}\mathcal{O}N$, where the operator $\mathcal{O}$ transforms as $\mathcal{O}' = K\mathcal{O}K^\dagger$. This automatically guarantees the right chiral transformation behavior. Furthermore the Lagrangian has to be Hermitian and transforms even under charge conjugation, parity and time transformations. Therefore the most general chiral invariant Lagrangian containing one derivative is given by

$$\mathscr{L}_{\pi N}^{(1)} = \bar{N}\left(iD_\mu - M + \frac{G}{2}\gamma^\mu\gamma_5 u_\mu\right)N\,. \tag{2.36}$$

Note that the combination of $\bar{N}\gamma^\mu\gamma_5 u_\mu N$ is even under parity since axial currents $A_\mu \sim \bar{N}\gamma_\mu\gamma_5 N$ are odd under parity. The LECs M and G can be identified with the nucleon mass m_n and the axial vector coupling g_A. And therefore the Lagrangian containing the kinetic part of pions and nucleons as well as lowest order interactions is of the form

$$\mathscr{L}_\chi = \mathscr{L}_{\pi N}^{(1)} + \mathscr{L}_\pi^{(2)} + \cdots \tag{2.37}$$

2.4 Pion-nucleon vertices

To extract the Feynman rules of the interactions, one has to introduce a counting scheme to start a converging perturbation. A scheme for counting the soft scale momenta and masses Q^D of an effective pion Lagrangian was first introduced by [Weinberg, 1979]

$$D = 2 + \sum_d V_d(4-d) + 2N_L\,, \tag{2.38}$$

where V_d is the number of vertices including d derivatives and N_L is the number of loops. The counting scheme used in this work, which also includes nucleons, focuses rather on the number of vertices V_i and power of vertices κ_i than on possible loops in each diagram. For two nucleon processes the counting scheme will obey

$$\nu = -2 + \sum_i V_i \kappa_i \qquad \text{with} \qquad \kappa_i = d_i + p_i + \frac{3}{2} n_i - 4 \,. \tag{2.39}$$

This equation will be derived in the section 3.2.2.

Also one can use this equation to determine which vertices can contribute to which chiral order—the chiral dimension considered in this work is at most $\nu = 4$. Since one wants to discuss only interacting nucleons, one needs at least two vertices with two external nucleon legs—an incoming and an outgoing nucleon on both nucleon lines. Because the sum over $V_i \kappa_i$ has to be six at most, the highest vertex power is given by $\kappa_{\max} = 3$, while the smallest vertex power is $\kappa_{\min} = 1$. The only used vertices in this work are a vertex with two nucleons, one pion and one derivative $H_{21}^{(\kappa=1)}$ and a vertex with two nucleons, two pions and one derivative $H_{22}^{(2)}$. The vertex corresponding to two nucleons, three pions and one derivative is less problematic in the large-N_c case, since it will be proportional to $1/f_\pi^3$ and each power of $1/f_\pi$ increases the chance of a well behaved N_c scaling.

Vertices generated by $\mathscr{L}_\pi^{(n)}$ will have n derivatives, no nucleon lines and at least two pion lines, also the numbers of pion lines and derivatives have to be even to not violate the symmetries. Contributions with two pion lines correspond to the propagator and thus the first vertex corresponds to the vertex power $\kappa = 2 + 4 - 4 = 2$. But since one also needs four pion-nucleon vertices to include this vertex in a diagram, the contribution can be neglected at this chiral order. Therefore all vertices which are relevant for nucleon-nucleon scattering including pions at chiral order $\nu = 4$ are generated by $\mathscr{L}_{\pi N}^{(n)}$.

To identify the vertices, one has to expand the pion field matrices u_π of

$$\begin{aligned} \mathscr{H}_I^{(1)} &= -i\bar{N}\gamma^\mu \Gamma_\mu N - \frac{g_A}{2}\bar{N}\gamma^\mu\gamma_5 u_\mu N - \cdots \\ &= \frac{1}{4f_\pi^2}\epsilon^{abc}\bar{N}\gamma^\mu\pi^a\left(\partial_\mu\pi^b\right)\tau^c N + \frac{g_A}{2f_\pi}\bar{N}\gamma^\mu\gamma_5\left(\partial_\mu\pi^a\right)\tau^a N - \cdots \,. \end{aligned} \tag{2.40}$$

In the limit of large-N_c, baryons are static and can be treated non-relativistic. Accordingly one only looks at the positive frequency solutions of the Dirac equation. These solutions, in the Dirac representation for the γ-matrices, are given by

$$N \propto \begin{pmatrix} \Phi_s \\ \frac{\vec{\sigma}\cdot\vec{p}}{E_{\vec{p}}+m_N}\Phi_s \end{pmatrix}, \quad \gamma^0 = \begin{pmatrix} \mathbb{1} & 0 \\ 0 & -\mathbb{1} \end{pmatrix}, \quad \gamma^i = \begin{pmatrix} 0 & \sigma^i \\ \sigma^i & 0 \end{pmatrix}, \quad \gamma^5 = \begin{pmatrix} 0 & \mathbb{1} \\ -\mathbb{1} & 0 \end{pmatrix}. \tag{2.41}$$

The spinor components of the nucleon vectors can be reduced by using that $m_N \gg |\vec{p}|$

$$\bar{N}\gamma^\mu\partial_\mu\Gamma N = N^\dagger\partial_t\Gamma N + \mathcal{O}\left(\frac{1}{m_N}\right) \quad \text{and} \quad \bar{N}\gamma^\mu\gamma_5\partial_\mu\Gamma N = N^\dagger\sigma^i\partial_i\Gamma N + \mathcal{O}\left(\frac{1}{m_N}\right), \tag{2.42}$$

which results in the non-relativistic vertices

$$\mathscr{H}_{21}^{(1)}(x) = \frac{g_A}{2f_\pi}N^\dagger(x)\vec{\sigma}\cdot\left(\vec{\nabla}\boldsymbol{\pi}(x)\cdot\boldsymbol{\tau}\right)N(x)\,, \tag{2.43}$$

and

$$\mathscr{H}_{22}^{(2)}(x) = \frac{1}{4f_\pi^2}N^\dagger(x)\left(\boldsymbol{\pi}(x)\times\partial_t\boldsymbol{\pi}(x)\right)\cdot\boldsymbol{\tau}N(x)\,. \tag{2.44}$$

These vertices can be related to so-called time ordered Feynman rules when computing the matrix elements. Therefore one needs to introduce the pion and the nucleon fields

$$\pi^b(x) = \int \frac{\mathrm{d}^3k}{(2\pi)^{3/2}} \frac{1}{\sqrt{2\omega_{\vec{k}}}} \left[e^{-ik\cdot x} a^b_{\vec{k}} + e^{ik\cdot x} a^{b\,\dagger}_{\vec{k}} \right] , \tag{2.45}$$

and

$$N(x) = \sum_{j=1}^{3} \sum_{a=1}^{2} \int \frac{\mathrm{d}^3k}{(2\pi)^{3/2}} e^{-ik\cdot x}\, v(j)\, \epsilon(a)\, b^a_{j,\vec{k}} \,. \tag{2.46}$$

Now computing the matrix element of the first vertex one obtains

$$\begin{aligned} \left\langle N_{ck}(p') \,\middle|\, H^{(1)}_{21} \,\middle|\, N_{aj}(p), \pi^b(q) \right\rangle & \\ &= \frac{ig_A}{2f_\pi} \int \mathrm{d}^3x\; v^\dagger(k)\, \epsilon^\dagger(c)\, e^{-i\vec{p}'\cdot\vec{x}}\; \frac{\vec{\sigma}\cdot\vec{q}}{\sqrt{2\omega_{\vec{q}}}}\, \tau^b\; e^{i\vec{q}'\cdot\vec{x}}\; v(j)\, \epsilon(a)\, e^{i\vec{p}\cdot\vec{x}} \\ &= \frac{ig_A}{2f_\pi} \frac{(\vec{\sigma})_{kj}\cdot\vec{q}}{\sqrt{2\omega_{\vec{q}}}}\; \left(\tau^b\right)_{ca}\; \frac{1}{(2\pi)^{3/2}} \delta^{(3)}\left(\vec{p}\,' - \vec{p} - \vec{q}\right) . \end{aligned} \tag{2.47}$$

The Feynman rule associated with the one-pion vertex is given by figure 2.2 and corresponds to equation (2.48)

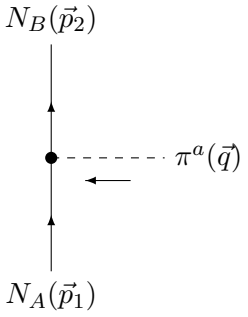

Figure 2.2: Large-N_c Feynman rules for chiral one-pion vertex.

$$\left\langle N_{j_2,i_2}(\vec{p}_2) \,\middle|\, H^{(1)}_{21} \,\middle|\, N_{j_1,i_1}(\vec{p}_1); \pi^a(\vec{q}) \right\rangle \longleftrightarrow \frac{ig_A}{2f_\pi} \frac{q^n}{\sqrt{2\omega_{\vec{q}}}} \left(\sigma^n\right)_{j_2 j_1} \left(\tau^a\right)_{i_2 i_1} . \tag{2.48}$$

Since the two-pion vertex contains a time derivative, one has to be more careful regarding the direction of the pion lines. The Feynman rule of figure 2.3a is given by equation (2.49)

$$\left\langle N_{j_2,i_2}(\vec{p}_2) \,\middle|\, H^{(2)}_{22} \,\middle|\, N_{j_1,i_1}(\vec{p}_1); \pi^a(\vec{q}_1); \pi^b(\vec{q}_2) \right\rangle \longleftrightarrow \frac{i}{f_\pi^2} \frac{\omega_{\vec{q}_1} - \omega_{\vec{q}_2}}{\sqrt{\omega_{\vec{q}_1}\omega_{\vec{q}_2}}}\; \delta_{j_2 j_1}\; \epsilon^{abc} \left(\tau^c\right)_{i_2 i_1} . \tag{2.49}$$

Note that the interchange of the pions does not change the amplitude since an interchange of the momentum labels ($1 \leftrightarrow 2$) causes a minus sign and the interchange in the levi-civita symbol indices ($a \leftrightarrow b$) generates a second minus sign. Also, the diagram with two outgoing pions (figure 2.3d) has the opposite sign compared to the previous diagram with two incoming pions.

The result for the diagram with one incoming and one outgoing pion (figure 2.3c) is minus the result for the same diagram with pions propagating in opposite direction (figure 2.3b). This can be understood as following: the inversion of pion momenta corresponds to an interchange of the nucleons, which corresponds to a transposed operator $\tau^T = -\tau^\dagger \in SU(2)_I$,

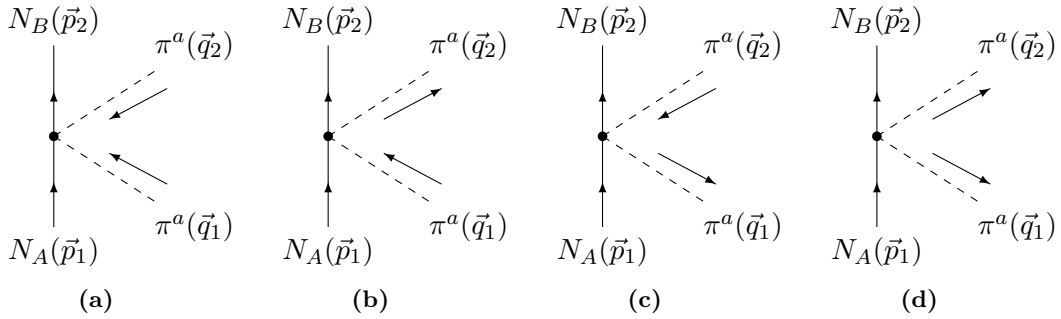

Figure 2.3: Large-N_c Feynman rules for chiral two-pion vertices.

where it was used that the complex conjugated representation has the corresponding negative eigenvalues. The Feynman rule of the corresponding diagram is given by:

$$\left\langle N_{j_2,i_2}(\vec{p}_2);\pi^b(\vec{q}_2)\,\middle|\,H_{22}^{(2)}\,\middle|\,N_{j_1,i_1}(\vec{p}_1);\pi^a(\vec{q}_1)\right\rangle \longleftrightarrow \frac{i}{f_\pi^2}\frac{\omega_{\vec{q}_1}+\omega_{\vec{q}_2}}{\sqrt{\omega_{\vec{q}_1}\omega_{\vec{q}_2}}}\;\delta_{j_2j_1}\;\epsilon^{abc}\,(\tau^c)_{i_2i_1}\;. \tag{2.50}$$

Using these rules one is now able to compute the chiral potential describing nucleon-nucleon scattering.

3 Chiral nuclear potential

When computing scattering processes in quantum physics, one is usually interested in the matrix elements of the S-operator. One possible way of approximating this operator is a perturbation in small quantities as the fermion-gluon coupling in high-energy QCD or the associated soft scale of χPT mentioned in the previous section.

Another computation scheme is directly connected to the T-operator

$$S = \mathbb{1} - iT\,. \tag{3.1}$$

The recursive Lippmann-Schwinger equation for the T-operator,

$$T = V + VGT\,, \tag{3.2}$$

makes it possible to iterate matrix-elements for a known potential V.

This also allows to invert the procedure: one could try to compute the T-matrix up to a given order, for example by computing diagrams perturbatively, to identify and extract a so-called effective potential V_{eff}. Using this potential one could furthermore iterate T up to higher orders.

In the context of large-N_c physics, [Banerjee et al., 2002] have explicitly computed an effective potential up to a given order which made it possible to compare the large-N_c scaling of an explicit computation with the predictions for general large-N_c QCD, the KSM counting rules, by [Kaplan and Savage, 1996] and [Kaplan and Manohar, 1997].

While results at leading order were trivially satisfied, the next to leading order potential also has furthermore confirmed the predictions. At this step the consistency already required non trivial cancellations of box and cross-box diagrams. At NNLO it was yet not possible to confirm the KSM counting rules (large-N_c nuclear potential puzzle, [Belitsky and Cohen, 2002]). Later on [Cohen, 2002] suggested that it is essential to use an energy-independent formalism for deriving the potential to confirm the KSM counting rules.

The goal of this section is to derive a systematic, energy-independent approach for computing the nucleon-nucleon potential by using unitary transformations in Fock-space. A general introduction to the nucleon-forces can be found in [Epelbaum, 2010]. A more complete description of the formalism can be found in [Epelbaum et al., 1998] and [Epelbaum, 2007], which also builds the foundation for the next section.

3.1 Properties of the nucleon-nucleon potential

The non-relativistic nucleon-nucleon potential is defined as the matrix element

$$V_{NN} = \left\langle N_1\left(\vec{p}_1\,', s_1', i_1'\right), N_2\left(\vec{p}_2\,', s_2', i_2'\right) \,\middle|\, V \,\middle|\, N_1\left(\vec{p}_1, s_1, i_1\right), N_2\left(\vec{p}_2, s_2, i_2\right)\right\rangle\,, \tag{3.3}$$

where $\vec{p}_n$ denotes the momentum, s_n the spin and i_n the isospin of the nucleons.

Since the potential is defined by the scattering process of those particles, knowing these

particle quantum numbers totally determines[1] the potential. Requiring specific symmetries as

(1) isospin invariance

(2) rotational invariance

(3) translation and Galilean invariance

(4) parity invariance

(5) time reversal invariance

(6) invariance under exchange of nucleon labels and

(7) hermicity

fixes the most general form of the potential (see also [Okubo and Marshak, 1958]):

$$V_{NN} \propto \left\{ \mathbb{1}_{\text{spin}} \, , \vec{\sigma}_1 \cdot \vec{\sigma}_2 \, , S_{12}\left(\vec{q}\right) \, , S_{12}\left(\vec{k}\right) , \vec{L} \cdot \vec{S} \, , \left(\vec{L} \cdot \vec{S}\right)^2 \right\} \times \left(\mathbb{1}_{\text{isospin}} \, , \boldsymbol{\tau}_1 \cdot \boldsymbol{\tau}_2 \right) , \tag{3.4}$$

where the momenta are given in relative coordinates: the relative incoming momenta is given by $\vec{p} = (\vec{p}_1 - \vec{p}_2)/2$, while the outgoing momenta are labeled with a prime. Momenta corresponding to a specific scattering channel are thus given by $\vec{q} = \vec{p}\,' - \vec{p}$ and $\vec{k} = \left(\vec{p}\,' + \vec{p}\right)/2$. The vectors $\vec{\sigma}_n$ and $\boldsymbol{\tau}_n$ denote the spin and isospin of the nucleon n. The other quantities are defined by

$$S_{12}\left(\vec{l}\right) = 3 \left(\vec{\sigma}_1 \cdot \vec{l}\right) \left(\vec{\sigma}_2 \cdot \vec{l}\right) - \vec{\sigma}_1 \cdot \vec{\sigma}_2 \, , \qquad \vec{L} = \vec{r} \times \vec{p} , \qquad \vec{S} = \frac{\vec{\sigma}_1 + \vec{\sigma}_2}{2} \, . \tag{3.5}$$

According to $\vec{p}$ the vector $\vec{r}$ corresponds to the relative center of mass coordinate. Also the potential might be multiplied by scalar functions of $\vec{p}^{\,2}$, $\vec{p} \cdot \vec{p}\,'$ and $\vec{p}\,'^{\,2}$.

The general form of the potential is thus given by the following term

$$\begin{aligned} V_{NN} = V_0^0 + V_\sigma^0 \, \vec{\sigma}_1 \cdot \vec{\sigma}_2 + V_S^0 \, \left(3 \left(\vec{\sigma}_1 \cdot \vec{q}\right) \left(\vec{\sigma}_2 \cdot \vec{q}\right) - \vec{\sigma}_1 \cdot \vec{\sigma}_2\right) + V_{\text{Spin-Orbit}}^0 \\ \left(V_0^1 + V_\sigma^1 \, \vec{\sigma}_1 \cdot \vec{\sigma}_2 + V_S^1 \, \left(3 \left(\vec{\sigma}_1 \cdot \vec{q}\right) \left(\vec{\sigma}_2 \cdot \vec{q}\right) - \vec{\sigma}_1 \cdot \vec{\sigma}_2\right) + V_{\text{Spin-Orbit}}^1\right) \boldsymbol{\tau}_1 \cdot \boldsymbol{\tau}_2 \, . \end{aligned} \tag{3.6}$$

It is also possible to compute the potential from a large-N_c QCD point of view. To identify corresponding structures, the spin and isospin depending amplitudes will be compared with the large-N_c predictions (see section 4.4).

3.2 Method of unitary transformations

As pointed out in section 2.4, the for this work relevant Hamiltonian describing the nucleon-nucleon interaction will be given by

$$H = H_0 + H_I = H_0 + H_{21} + H_{22} \, , \tag{3.7}$$

where H_0 corresponds to the kinetic part, H_{21} to two-nucleon one-pion vertices and H_{22} to two-nucleon two-pion vertices. Higher terms are suppressed by powers of the soft scale in χPT and also powers in N_c in large-N_c χPT (see also 4.2.2). The Schrödinger equation for such a Hamiltonian,

$$H \left|\Psi\right\rangle = E \left|\Psi\right\rangle \, , \tag{3.8}$$

[1] It might be the case that one expresses states of the momentum vector $\vec{p}$ as states of the absolute of the momentum p, the angular momentum l and the magnetic quantum number m_l. Since l and s are both quantum numbers of $SO(3)$ representations, their tensor product forms the higher dimensional total angular momentum representation with quantum numbers j and m_j.

can be rewritten for pure nucleonic states $|\Psi_\eta\rangle$ using projection operators η and $\lambda = \mathbb{1} - \eta$, which satisfy $\eta^2 = \eta$, $\lambda^2 = \lambda$ and $\eta\lambda = \lambda\eta = 0$. The states $|\Psi_\lambda\rangle$ therefore correspond to the remaining part of the Fock-space containing mesonic and nucleonic-mesonic states.

In this case, the Schrödinger equation is reformulated by

$$\begin{pmatrix} \eta H \eta & \eta H \lambda \\ \lambda H \eta & \lambda H \lambda \end{pmatrix} \begin{pmatrix} |\Psi_\eta\rangle \\ |\Psi_\lambda\rangle \end{pmatrix} = E \begin{pmatrix} |\Psi_\eta\rangle \\ |\Psi_\lambda\rangle \end{pmatrix} = E\,|\Psi\rangle\ . \tag{3.9}$$

Solving this equation for an effective nucleon potential

$$V_{\text{eff}}(E)\,|\Psi_\eta\rangle = (E - H_0)\,|\Psi_\eta\rangle\ , \tag{3.10}$$

will result in an expansion in powers of the interaction Hamiltonian:

$$V_{\text{eff}}(E) = \eta H_I \eta + \sum_{n=0} \eta H_I \lambda \frac{1}{E - H_0} \left(\lambda H_I \lambda \frac{1}{E - H_0} \right)^n \lambda H_I \eta\,. \tag{3.11}$$

Obviously this result is still depending on the energy E of the nucleons. To resolve this, one can apply further unitary transformations which effectively block-diagonalize the Hamiltonian and thus eliminate the energy dependence.

The states to be analyzed are defined by

$$\begin{pmatrix} |\eta\rangle \\ |\lambda\rangle \end{pmatrix} := U^\dagger \begin{pmatrix} |\Psi_\eta\rangle \\ |\Psi_\lambda\rangle \end{pmatrix}\ . \tag{3.12}$$

This leads to the modified Schrödinger equation

$$U^\dagger H U \begin{pmatrix} |\eta\rangle \\ |\lambda\rangle \end{pmatrix} = E \begin{pmatrix} |\eta\rangle \\ |\lambda\rangle \end{pmatrix}\ . \tag{3.13}$$

Using the ansatz (see also [Okubo, 1954])

$$U = \begin{pmatrix} \left(\mathbb{1} + A^\dagger A\right)^{-1/2} & -A^\dagger \left(\mathbb{1} + A^\dagger A\right)^{-1/2} \\ A \left(\mathbb{1} + A^\dagger A\right)^{-1/2} & \left(\mathbb{1} + A^\dagger A\right)^{-1/2} \end{pmatrix}\ , \tag{3.14}$$

where $A = \lambda A \eta$, one obtains the equation

$$\lambda \left(H - [\,A\,,\,H\,] - AHA\right) \eta = 0\,, \tag{3.15}$$

when requiring that $U^\dagger H U$ is block-diagonal.

Once one has solved equation (3.15) for A, one can compute the effective unitary potential for the nucleons by inserting A in

$$V_{\text{eff}}^{\text{UT}} = H_{\text{eff}}^{\text{UT}} - H_0 = \eta \left(\mathbb{1} + A^\dagger A\right)^{-1/2} \left(H + A^\dagger H + HA + A^\dagger H A\right) \left(\mathbb{1} + A^\dagger A\right)^{-1/2} \eta - H_0\,. \tag{3.16}$$

3.2.1 Perturbative ansatz for unitary potential

Starting with equation (3.15), one can obtain a recursive equation for A by using $\lambda A \eta = A$

$$\lambda \left(H_I - [\,A\,,\,H_I\,] - AH_IA\right) \eta = \lambda A \eta H_0 \eta - \lambda H_0 \lambda A \eta\,. \tag{3.17}$$

The only surviving matrix elements are of the form $\langle\lambda|\,\mathcal{O}\,|\eta\rangle$ and thus the left-hand side can be interpreted as $\lambda A\eta(E_\eta - E_\lambda)$ where the Es denote the kinetic energy of the states the operator is acting on.

A possible way for computing the effective potential is a perturbative ansatz for example in a coupling. For a Hamiltonian of the form

$$H_I = \sum_{n=1} H^{(n)}\,, \tag{3.18}$$

where terms like $H^{(n_1)}H^{(n_2)}$ should be of the same order as $H^{(n_1+n_2)}$. One can also express the operator A as

$$A = \sum_{n=1} A^{(n)}\,. \tag{3.19}$$

At the end of this section, the chiral power κ of each vertex will be used as the perturbation parameter of the expansion. This effectively transforms (3.15) to

$$\lambda A^{(n)}\eta = \frac{1}{E_\eta - E_\lambda}\lambda\left(H^{(n)} - \sum_{i=1}^{n-1}\left[\,A^{(n-i)}\,,\,H^{(i)}\,\right] - \sum_{i=1}^{n-2}\sum_{j=1}^{n-1-i} A^{(i)}H^{(j)}A^{(n-i-j)}\right)\eta\,. \tag{3.20}$$

At first, to derive the chiral power counting, the Hamiltonian is chosen to be

$$H_I \equiv H_{21}^{(1)}\,, \tag{3.21}$$

where $H_{N_N N_\pi}$ denotes the Hamiltonian with N_N nucleon lines and N_π pion lines and thus $H_{21}^{(1)}$ is proportional to the axial coupling g_A which will be the perturbation parameter in this case. At this step one can directly read off $A^{(1)}$—since $H_{21}^{(1)}$ starts at order one in the coupling and each term in equation (3.20) contains $H_{21}^{(1)}$, it is impossible to have an operator at order zero:

$$A_{21}^{(1)} = -\frac{\lambda}{E_\lambda - E_\eta}H_{21}^{(1)}\eta =: -\frac{\lambda}{\omega_\pi}H_{21}^{(1)}\eta\,, \tag{3.22}$$

where $\omega_\pi = E_\lambda - E_\eta$ corresponds to the energy of the internal pion.

Accordingly the first non-vanishing component of the effective potential starts at order g_A^2 and is given by

$$\begin{aligned} V_{\text{eff}}^{(g^2)} &= \eta\left(A_{21}^{(1)\,\dagger}H_{21}^{(1)} + H_{21}^{(1)}A_{21}^{(1)} + A_{21}^{(1)\,\dagger}H_0A_{21}^{(1)}\right)\eta \\ &\qquad - \frac{1}{2}\left(\eta\,H_0\,\eta\,A_{21}^{(1)\,\dagger}A_{21}^{(1)}\,\eta + \eta\,A_{21}^{(1)\,\dagger}A_{21}^{(1)}\,\eta\,H_0\,\eta\right) \\ &= -\eta\,H_{21}^{(1)}\frac{\lambda}{\omega_\pi}H_{21}^{(1)}\,\eta\,. \end{aligned} \tag{3.23}$$

Furthermore it was used that the nucleons are static and have nearly the same energy at each step[2].

3.2.2 Chiral power counting

To simplify the procedure of computing the effective potential for nucleonic states, it is useful to introduce another perturbation scheme—the chiral power counting. This is necessary since one would like to include several interactions corresponding to different couplings. To do so, one should associate the to be analyzed operator with a (time-ordered) diagram

$$\left\langle\Psi'\,\middle|\,\mathcal{O}\,\middle|\,\Psi\right\rangle \sim Q^\nu\,. \tag{3.24}$$

[2]In large-N_c χPT this ansatz is satisfied because the nucleon mass is at order N_c while momenta are at order 1.

Hereby ν denotes the chiral dimension of soft scale parameters as the pion mass m_π, scattering momenta $\vec{q}$ and other quantities which are smaller than the hard scale $\Lambda \sim m_N$.

To demonstrate the procedure of identifying the power counting, the diagram corresponding to the effective potential at order g_A^2 (equation (3.23)) is evaluated as a nucleon-nucleon matrix element

$$V_{\text{eff}}^{(g_A^2)}(N_1', N_2'; N_1, N_2) = -\left\langle N_1', N_2' \left| H_{21}^{(1)} \frac{\lambda}{\omega} H_{21}^{(1)} \right| N_1, N_2 \right\rangle . \tag{3.25}$$

At this step one has two different possibilities for computing the diagram: one could connect the two nucleon lines via a pion or generate a pion loop (see also figure 3.1):

$$\begin{aligned}\left\langle N_1', N_2' \left| H_{21}^{(1)} \frac{\lambda}{\omega} H_{21}^{(1)} \right| N_1, N_2 \right\rangle = & \\ & \sum_{N,\pi}\!\!\!\!\!\!\int \left\langle N_1' \,|\, N_1 \right\rangle \left\langle N_2' \left| H_{21}^{(1)} \right| N, \pi \right\rangle \frac{1}{\omega_\pi} \left\langle N, \pi \left| H_{21}^{(1)} \right| N_2 \right\rangle \\ & + \sum_{\pi}\!\!\!\!\!\!\int \left\langle N_1' \left| H_{21}^{(1)} \right| N_1, \pi \right\rangle \frac{1}{\omega_\pi} \left\langle N_2', \pi \left| H_{21}^{(1)} \right| N_2 \right\rangle + \cdots ,\end{aligned}$$

where the summation goes over all quantum numbers of the internal states and the integration over the momentum of the internal states.

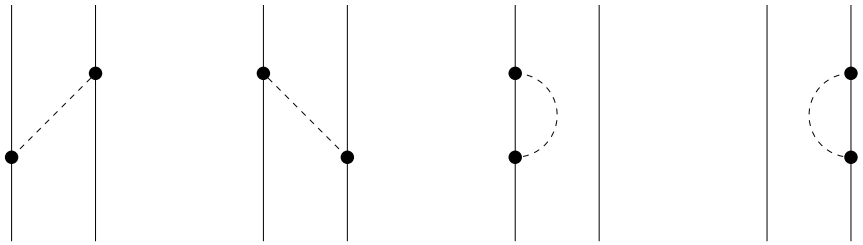

Figure 3.1: Time-ordered diagrams contributing to the nucleon-nucleon potential at order g_A^2. Time is directed upwards.

To compute the chiral scaling of diagrams one should insert the explicit form of the Hamiltonian (2.47). The connected diagrams are both given by

$$\frac{g_A^2}{4f_\pi^2} \frac{\vec{\sigma}_1 \cdot \vec{q}}{\sqrt{2\omega_{\vec{q}}}} \frac{1}{\omega_{\vec{q}}} \frac{\vec{\sigma}_2 \cdot \vec{q}}{\sqrt{2\omega_{\vec{q}}}} \, \boldsymbol{\tau}_1 \cdot \boldsymbol{\tau}_2 \, \frac{1}{(2\pi)^3} \delta^{(3)} \left(\vec{p}_1 + \vec{p}_2 - \vec{p}_1' - \vec{p}_2' \right) . \tag{3.26}$$

If one neglects the overall delta function, the terms generating the chiral dimensions can be identified according to the following rules

- Each vertex scales as $d_i - p_i/2$, where d_i is the number of derivatives or insertions of the pion mass ($d_{21} = 1$) and p_i is the number of pions at the vertex (corresponding to phase space factors $1/\sqrt{2\omega_\pi}$). This factor needs to be multiplied with the total number of each vertex V_i.
- In between each vertex the internal pion lines are responsible for a factor $1/\omega_\pi$, which decreases the chiral dimension by one. The number of those factors is given by $\sum V_i - 1$.

Thus the scaling of the loopless connected diagrams are given by

$$\nu = -\left(\sum V_i - 1 \right) + \sum V_i \left(d_i - \frac{p_i}{2} \right) . \tag{3.27}$$

To find the dimension of the pion-loop diagram one has to evaluate the integral

$$\frac{g_A^2}{4f_\pi^2} \int \frac{\mathrm{d}^3 q}{(2\pi)^{3/2}} \frac{\vec{\sigma}_1 \cdot \vec{q}}{\sqrt{2\omega_{\vec{q}}}} \frac{1}{\omega_{\vec{q}}} \frac{\vec{\sigma}_1 \cdot \vec{q}}{\sqrt{2\omega_{\vec{q}}}} \, \boldsymbol{\tau}_1 \cdot \boldsymbol{\tau}_1 \, \delta^{(3)} \left(\vec{p}_2 - \vec{p}_2' \right) \, \frac{1}{(2\pi)^3} \delta^{(3)} \left(\vec{p}_1 + \vec{p}_2 - \vec{p}_1' - \vec{p}_2' \right) . \tag{3.28}$$

This extends the set of rules to

- For each loop L the chiral dimension is increased by three.
- For each separately connected piece of nucleon lines C a delta function is generated decreasing the chiral dimension by three. Note that also single nucleon lines count as one separately connected piece.

Thus the chiral dimension of a general diagram with no external pions is given by

$$\nu = 3L + 1 + \sum V_i \left(d_i - \frac{p_i}{2} - 1 \right) - 3(C - 1) \,. \tag{3.29}$$

As stated before, one is interested to use the chiral power of a vertex as an expansion parameter for the unitary potential—the chiral dimension should only depend on the external states as well as the information about the internal vertex structure. Therefore it is useful to reformulate the chiral dimension according to this requirement.

At first one can express the number of loops L by the number of internal pion lines I_p and internal nucleon lines I_n combined with the number of vertices V_i, the number of separately connected pieces C and the number of nucleons $\tilde{N}$ which are not involved in scattering processes

$$L = I_p + I_n - \sum V_i + (C - \tilde{N}) \,. \tag{3.30}$$

Assuming that one has just one separately "active" piece ($C - \tilde{N} = 1$), for a fixed number of vertices, adding another internal line simply creates an additional loop (see figure 3.2b and 3.2d). To construct a single loop, the number of internal lines has to be equal to the number of vertices. Thus one needs to add one to form equation (3.30).

If one introduces another vertex for a fixed number of internal lines, one has to link an existing connection to the new vertex. If the new vertex connects to a disconnected nucleon line, the number of internal lines stays the same and thus the number of loops is reduced by one. If the vertex connects to an already occupied line, one creates two new internal lines and thus the number of loops stays constant.

For more separately connected "active" pieces ($C - \tilde{N} > 1$), each of those pieces needs the additional plus one to contribute to the correct loop counting (figure (3.2e)).

Furthermore one can express the total number of lines by the number of vertices (no external pions when evaluating the potential matrix elements)

$$\begin{aligned} 2I_p &= \sum V_i p_i \\ 2I_n + E_n &= \sum V_i n_i + 2\tilde{N} \,. \end{aligned} \tag{3.31}$$

For a vertex containing a single pion line, one needs two vertices to create an internal line, four vertices for two lines and so on. Note that since one is looking at the nucleonic potential, the number of external pion lines is automatically zero. Since the number of external lines is increased by two for each non-interacting nucleon, one also has to include $\tilde{N}$ for the nucleonic lines. Rewriting the number of external nucleon lines E_n as the total number of nucleons $E_n = 2N$ and combining equations (3.29), (3.30) and (3.31), one finally gets

$$\nu = 4 - 3N + \sum V_i \kappa_i \qquad \text{with} \qquad \kappa_i = d_i + p_i + \frac{3}{2} n_i - 4 \,. \tag{3.32}$$

Using equation (3.32) one can finally start a perturbative expansion for the effective nucleon-nucleon potential by just considering the external line and the vertex scaling of the corresponding operators. As an example: the chiral vertex-dimension of the operator $H_{21}^{(\kappa)}$ is

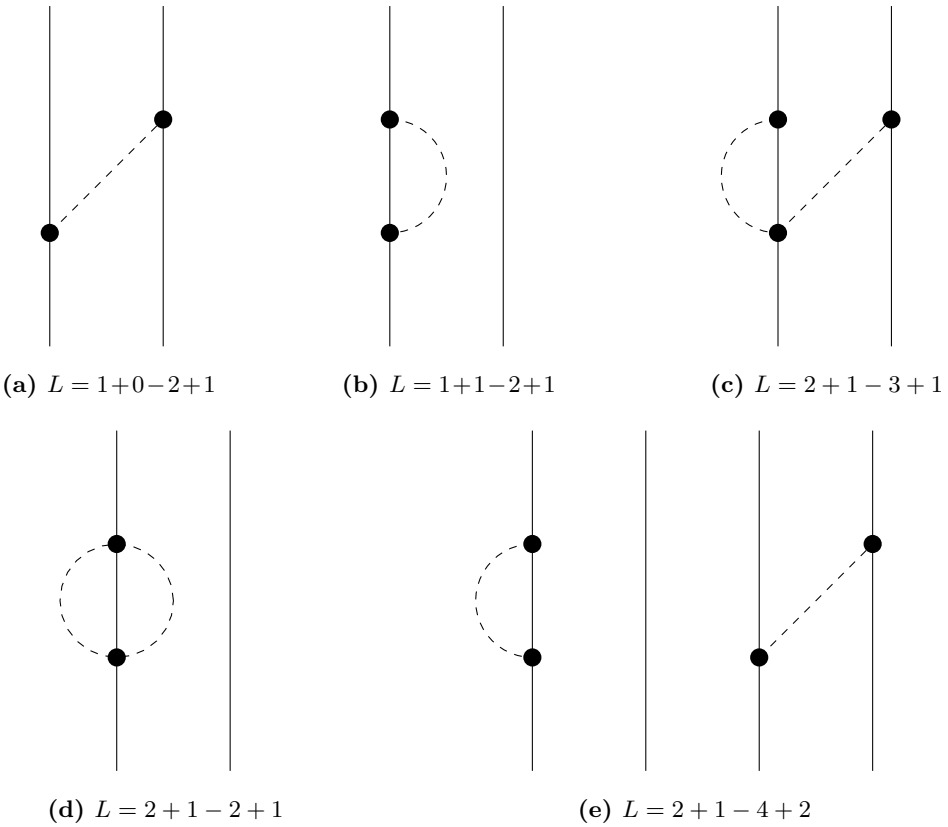

(a) $L = 1+0-2+1$ **(b)** $L = 1+1-2+1$ **(c)** $L = 2+1-3+1$

(d) $L = 2+1-2+1$ **(e)** $L = 2+1-4+2$

Figure 3.2: Example diagrams with number of loops given by equation (3.30).

given by $\kappa = 1+1+3-4 = 1$ and thus the nucleon-nucleon potential at chiral leading order is given as the contraction of two operators $H_{21}^{(1)}$ and accordingly scales as

$$V_{\text{eff}}^{(\nu)} \sim Q^{4-6+2\cdot 1} = Q^0 \,, \tag{3.33}$$

which is confirmed by the previous computation.

Also, as requested before, if one wants to compute more complex operators, the chiral vertex power of the new operator is simply the sum over all single vertex powers.

Note that one is just able to compute the chiral dimension when applying the operators to states. This defines the contraction of lines at each vertex. Before doing so the product of two operators is just a number of not contracted external lines.

4 Large-N_c Quantum Chromodynamics

> *Because of the complexity of phenomena which this theory describes [...] we cannot even dream of solving SU(3) gauge theory exactly. Therefore it is necessary to find some sort of approximation scheme.*
>
> — E. Witten, 1979

A possible approximation scheme for QCD was introduced by ['t Hooft, 1974]: instead of treating QCD as a $SU(3)$ gauge theory, one requires $SU(N_c)$ to be the gauge group of the theory. Accordingly the number of colors N_c is assumed to be large, which allows a perturbation in $1/N_c$. Still the mesons are represented as a quark-antiquark and baryons as N_c-quark bound states at leading order in N_c.

Though the Standard Model assumes that the number of colors $N_c = 3$, one still uses the large-N_c approximation to form qualitative statements. Furthermore, if it turns out that a $1/N_c$ perturbation is effectively a $1/N_c^2$ perturbation (as it will be the case for the chiral potential), the next to leading order effects only contribute by $\simeq 10\%$. Thus making large-N_c still a useful tool for approximating QCD.

This section briefly summarizes some facts about large-N_c QCD. The final goal is to compute the N_c scaling of physical quantities which are also relevant for chiral perturbation theory—namely the axial coupling g_A, the meson decay widths f_M and hadron masses as well as the large-N_c symmetry which corresponds to the spin-isospin symmetry of light quarks.

4.1 A planar diagram Theory for strong interactions

This section basically follows the work of [Witten, 1979].

Introducing $SU(N_c)$ as the gauge group of QCD basically results in the appearance of new combinatorical factors. When computing scattering processes, a gluon can couple to one out of N_c quarks, thus one obtains factors of N_c for each gluon insertion. To have a smooth N_c limit, the coupling constant g needs to scale with negative powers of N_c. Therefore one defines the scaling of $g \propto N_c^{-n}$ and computes n by requiring that diagrams of a similar type, as for example the gluon vacuum polarization, have the same smooth N_c dependence (see figure 4.1).

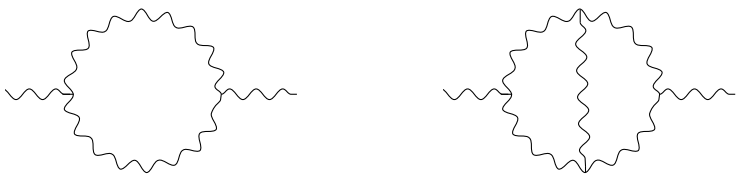

(a) Gluon loop **(b)** Double gluon loop

Figure 4.1: Diagrams contributing to gluon vacuum polarization should have the same (smooth) large-N_c scaling as $N_c \to \infty$.

The single gluon loop (figure 4.1a) contains two three-gluon vertices corresponding to N_c^{-2n}. Additionally, the sum over the internal gluon colors gives another N_c:

$$\mathcal{M}_{4.1a} \propto \sum_{b,c=1}^{N_c^2-1} f^{abc} f^{bcd} = C_2(Ad)\delta^{cd} = N_c\,\delta^{cd}\,, \tag{4.1}$$

where $C_2(Ad)$ is the quadratic Casimir invariant. Therefore the N_c scaling of figure 4.1a is given by

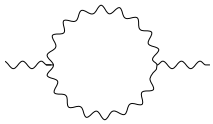 $\propto N_c^{1-2n}\,.$ (4.2)

Accordingly the two loop diagram 4.1b contains four vertices and the internal sums will result in a factor N_c^2. Thus the diagram scales with N_c^{2-4n}. For both diagrams to have the same scaling, one has to require $1-2n=0$ resulting in

$$g \mapsto \frac{g}{\sqrt{N_c}}\,. \tag{4.3}$$

To improve the understanding of large-N_c QCD it is useful to work out further scaling relations of physical quantities. The computation of diagrams in this limit can be drastically simplified by the doubleline formalism, originally introduced by t'Hooft: in color space one can represent a quark as a vector q^i, an antiquark as a covector $\bar{q}_i$ and a gluon as a matrix $\mathcal{A}^i{}_j$. As a fact from linear algebra one can express the action of a matrix on a vector as a composition of applying a covector to the initial vector and multiplying the resulting scalar with another vector. Thus, only for the purpose of counting combinatorical factors, one can represent the gluon as a combination of a quark and an antiquark: $\mathcal{A}^i{}_j \leftrightarrow q^i\bar{q}_j$.

Following this one can define diagrams in a doubleline notation. Each color index is represented by a line. Quarks flow in the opposite direction of antiquarks. Accordingly a gluon line can be expressed as a quark-antiquark doubleline (see table 4.1).

Object	QCD notation	Doubleline notation
q^i	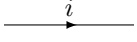	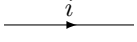
$\bar{q}_j$	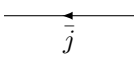	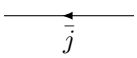
$\mathcal{A}^i{}_j$	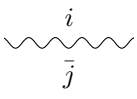	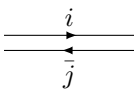

Table 4.1: Doubleline notation introduced by t'Hooft.

Using this notation for the QCD vertices (figure 4.2) one can see that each vertex has the same number of incoming and outgoing color lines: two, three and four incoming and outgoing lines for the fermion-gluon, the three-gluon and the four-gluon vertex. The fact that each incoming line is accompanied by an outgoing line represents the conservation of color.

Drawing a diagram is equivalent to contracting the indices in color space. Thus, if a color line is not constrained with a specific color number, the sum over all colors results in a factor of N_c. This effectively reassembles the freedom of a gluon to choose with which quark it is interacting. However it is important to mention that external color lines are fixed by the external particles.

Finally, to find the according N_c scaling of a diagram, one has to

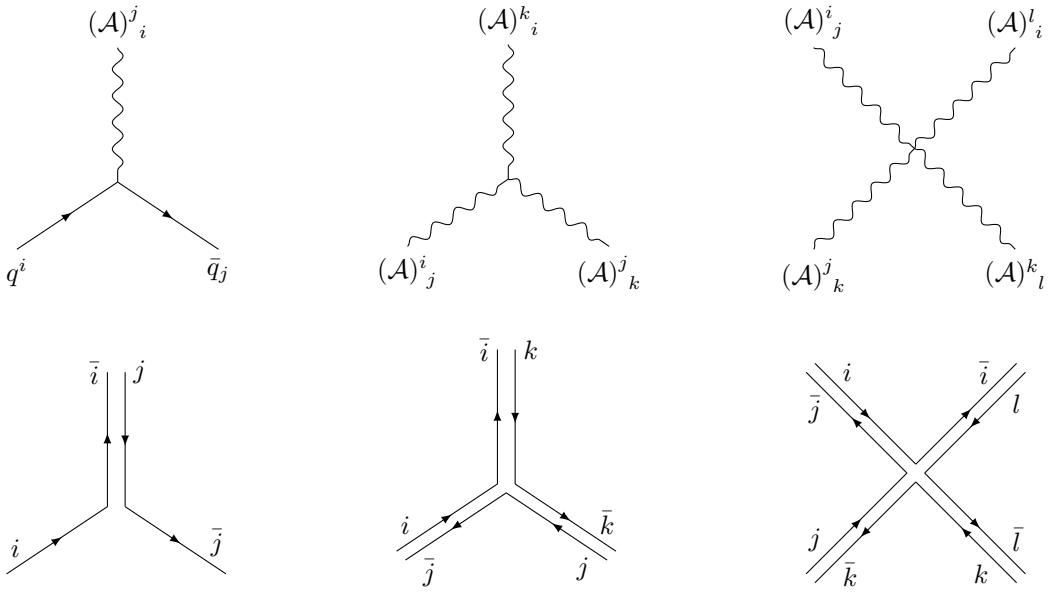

(a) Fermion-gluon vertex **(b)** Three-gluon vertex **(c)** Four-gluon vertex

Figure 4.2: QCD vertices in double line notation

- count the number V of appearing couplings g,
- contract incoming and outgoing color lines at each vertex according to the color structure,
- count the number of closed (internal) lines L
- and compute the large-N_c scaling according to

$$\mathcal{O}(N_c) = N_c^{L-V/2}\,. \tag{4.4}$$

Using the new notation the gluon vacuum polarization diagrams can be expressed as the new doubleline diagrams (figure 4.3). While figure 4.3a contains two vertices and one closed internal color line resulting in $N_c^{1-2/2} = N_c^0$, figure 4.3b contains four vertices and two closed internal lines also resulting in N_c^0.

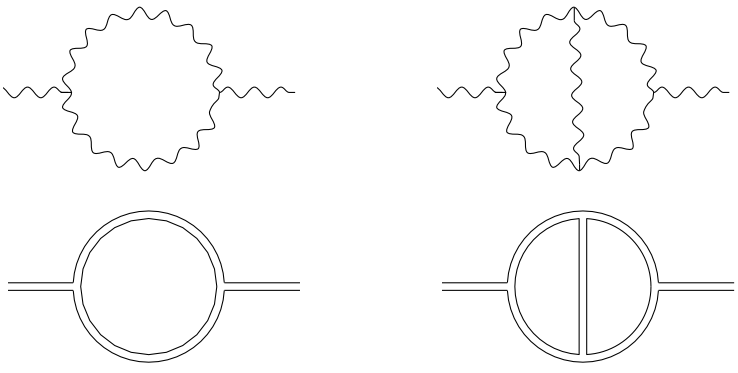

(a) Gluon loop **(b)** Double gluon loop

Figure 4.3: Gluon vacuum polarization expressed in doubleline notation.

One of the first things t'Hooft has observed was that planar diagrams are dominating non-planar diagrams. A planar diagram is a diagram drawn in a two-dimensional plane, such that the only intersections of lines correspond to vertices. One can easily verify this statement

by computing the N_c scaling of the diagrams in figure 4.4[1].

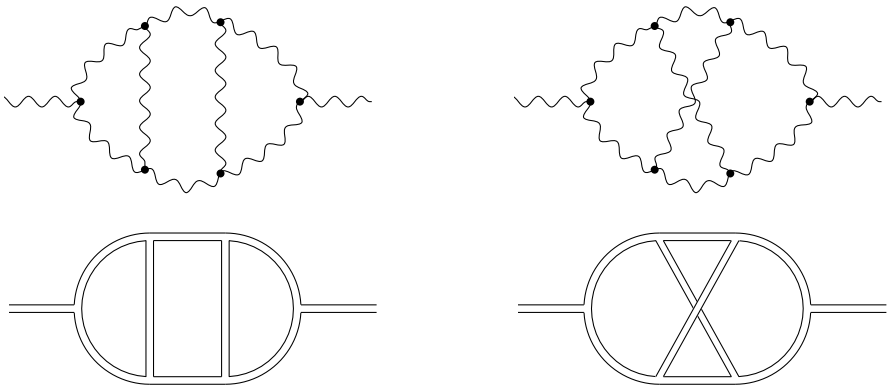

(a) Planar gluon triple loop **(b)** Non-planar gluon triple loop

Figure 4.4: Different large-N_c scaling of planar and non-planar diagrams in doubleline formalism.

While both diagrams contain six three-gluon vertices resulting in $1/N_c^3$ one has three different closed internal lines in diagram 4.4a but only one closed internal line in 4.4b. Thus one gets

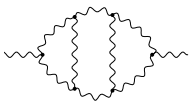 $\propto N_c^0$ and 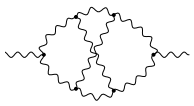 $\propto N_c^{-2}\,.$ (4.5)

Accordingly one can show that diagrams of a non-planar structure are effectively $1/N_c^2$-suppressed compared to the planar version of the diagram.

Also it is important to mention that quark loops are $1/N_c$-suppressed compared to the same diagram with a gluon loop. This is the case because the three-gluon vertex (see figure 4.2) contains an additional color line compared to the quark-gluon vertex. When contracting the lines to form a loop, the two three-gluon vertex loop has an internal closed color line while the two fermion-gluon vertex loop is just build out of an external color line. Thus the gluon loop will result in a factor of N_c^0 compared to N_c^{-1} for the quark loop.

Furthermore, when computing physical quantities, one is interested in currents in form of quarkbilinears $J = \bar{q}\,\Gamma q$, where Γ is a general tensor in Dirac spinor and or isospin space. Those current insertions $\langle 0|J^\dagger J|0\rangle$ will automatically generate at least one quark loop (the simplest contribution corresponds to a quark loop while other contributions will have some gluon or quark insertions as well).

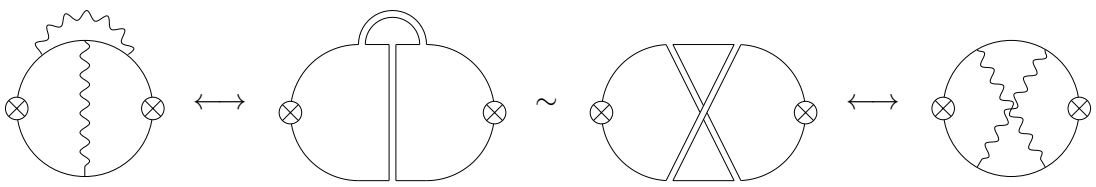

Figure 4.5: Example diagram which has a reduced N_c scaling as a penalty for not having a pure quark edge.

When quark loops appear in a diagram, the leading order diagrams are required to have the quark lines on the outer edge, as outer gluon lines could effectively reduce the N_c scaling.

[1] To underline the definition of planar diagrams, the intersection of lines only corresponds to a vertex if a dot is present at the intersection.

This is the case since diagrams avoiding this convention might be topological equivalent to a non-planar diagram. An example is presented in figure 4.5.

Summarizing the previous statements one can conclude that the leading order diagrams in large-N_c QCD are given by planar diagrams, with a minimal number of quark lines, while all the quark lines have to be on the outer edge of the diagram.

4.2 Physical quantities and Large-N_c behavior

As it was presented in the last section, introducing a group theoretical dependence on a parameter N_c effectively introduced a N_c dependence on a physical quantity—namely the gluon coupling constant g. Therefore one can furthermore expect other physical quantities to have a N_c scaling as well. In this section the N_c scaling of parameters, also present in chiral perturbation theory, is worked out. Those are the axial coupling g_A, the meson decay constants f_M and meson as well as baryon masses. All of those relations are well defined if one assumes that color confinement is still valid for large-N_c. This assumption combined with the planar diagram dominance are the starting point for the current section.

The spin and flavor dependence is suppressed in this section, thus the consistency conditions for physical quantities are just given at leading order. The results for specific spin-flavor structures, are derived in the next section.

4.2.1 Large-N_c scaling of the axial coupling

To understand the large-N_c behavior of the axial coupling one can simply analyze the matrix element of the axial current J_A

$$J_A(x) = \bar{q}(x)\Gamma_A\, q(x) \tag{4.6}$$

with Γ_A a general operator in spin and flavor space.

For working out the N_c scaling, the color representation is of further importance and to simplify the discussion, the flavor or spin dependence is suppressed. Nevertheless the flavor and spin structure have to obey further consistency conditions. Those conditions are demonstrated for the pion in section 4.3.1.

The axial coupling is defined as

$$g_A\, \mathcal{M}_A(x) =: \langle B'|J_A(x)|B\rangle \ . \tag{4.7}$$

The initial quark operator can couple to any of the N_c quarks of the first baryon, but since baryons are color neutral the second quark operator has to couple to the corresponding quark with the same color[2] of the outgoing baryon to create a non-vanishing matrix element.

$$g_A\, \mathcal{M}_A = \sum_{i=1}^{N_c} \langle B'|\bar{q}_i\Gamma_A\, q_i|B\rangle = N_c (X_A)_{B'B}\,, \tag{4.8}$$

where the matrix element $(X_A)_{B'B}$ is in general dependent on flavor and spin but independent of color[3] of the baryons. Thus, in the limit of large-N_c, the axial coupling g_A has to scale as

$$g_A \sim N_c\,. \tag{4.9}$$

[2] In principle it is also possible to create a quark and an antiquark with the same anticolor and other possibilities which do not violate the color confinement.

[3] The dependence on color is indirectly required to guarantee the right N_c scaling for further processes. Thus the commutators of this matrix will have a N_c dependence. This will be discussed in section 4.3.1.

4.2.2 Large-N_c scaling of meson decay constants and meson masses

It is also important to identify the scaling of the meson decay constants f_n, for a meson M_n, defined by

$$\langle 0|J(x)|M_n\rangle = f_n \mathcal{M}_n(x)\,. \tag{4.10}$$

To obtain the amplitude of meson decays one can look at the vacuum propagation of the current

$$\langle 0|J^\dagger(x)J(x)|0\rangle = \langle 0|J(-k)J(k)|0\rangle\ . \tag{4.11}$$

Following the discussion of Witten, one can show that the only intermediate states for the propagation, at leading order in N_c, are given by one-meson states. Thus the current matrix element would correspond to

$$\langle 0|J(-k)J(k)|0\rangle = \sum_n \frac{|\,a_n\,|^2}{k^2 - m_{M_n}^2} \qquad \text{with} \qquad a_n = \langle 0|J|M_n\rangle\ , \tag{4.12}$$

where the states $|M_n\rangle$ only correspond to one-meson (meson M_n) states.

For verifying the previous statement, one has to "cut" the diagram into two pieces and insert the identity element on the "loose ends". The non-vanishing states of the identity element are the intermediate states.

Using the statements of the previous section, the current vacuum propagation, at leading order, needs to have all quark lines on the outer edge and is a planar diagram (see figure 4.6).

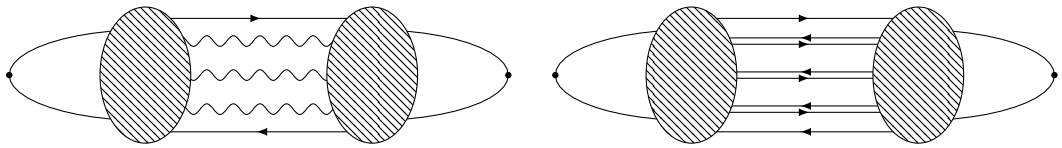

Figure 4.6: An example diagram representing the meson current propagation in regular and doubleline notation.

This fact already guarantees that it is not possible to have multi-meson states as intermediate states, since one only has one quark and one antiquark line at leading order. In principle it could still be possible to have gluon intermediate states in between. Therefore one has to show now, that it is not possible to find a linear combination of gluon and meson states as intermediate states. This is guaranteed if one furthermore requires all intermediate states to be color neutral.

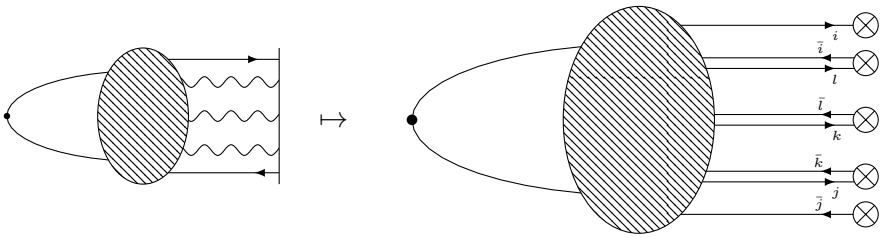

Figure 4.7: Example cut for diagram 4.6.

Cutting the diagram 4.7 in the middle generates an operator structure containing a quark corresponding to line i, three gluons corresponding to the intermediate double lines and an antiquark corresponding to line j. In general the color structure is given by the tensor

$$\mathcal{O} = \bar{q} \otimes \mathcal{A} \otimes \mathcal{A} \otimes \mathcal{A} \otimes q\,, \tag{4.13}$$

where q is one of the $N_c - 1$ fundamental representations of $SU(N_c)$ (of dimension N_c), $\bar{q}$ is in the complex conjugated representation of q and $\mathcal{A}$ is in the $N_c^2 - 1$ dimensional adjoint representation of $SU(N_c)$. Using $SU(N_c)$ group theory, this structure can be decomposed into several components

$$\mathcal{O} = \bar{q} \oplus q \oplus \mathcal{A} \oplus (\bar{q} \otimes q) \oplus (\mathcal{A} \otimes \mathcal{A}) \oplus (\bar{q} \otimes \mathcal{A} \otimes q) \cdots . \tag{4.14}$$

Since one requires the theory to be confined, only intermediate states which form a color singlet are allowed. Thus the tensor decomposes to

$$\mathcal{O} = (\bar{q} \otimes q) \oplus \bigoplus_{n=1}^{3} (\bar{q} \otimes \mathcal{A}^n \otimes q) \oplus \bigoplus_{n=2}^{3} (\mathcal{A}^n) \ . \tag{4.15}$$

Furthermore the matrix element is of form $\langle 0|\mathcal{O}|N\rangle$ which means all states in $|N\rangle$ need to be annihilated to make a contribution. therefore, the only states which are required to compute the matrix element are given by

$$\begin{aligned} |N_1\rangle &= |\bar{q}q\rangle \oplus |\mathcal{A}\mathcal{A}\mathcal{A}\rangle \\ |N_2\rangle &= |\bar{q}\mathcal{A}q\rangle \oplus |\mathcal{A}\mathcal{A}\rangle \\ |N_3\rangle &= |\bar{q}\mathcal{A}\mathcal{A}\mathcal{A}q\rangle \ . \end{aligned}$$

To finally identify if all of those states are in a color singlet for the given diagram, one has to look at the exact contractions. This can be done by using the double line formalism. Note that the cut corresponds to a Kronecker delta at each line intersection. Thus the explicit form of the tensor is given by

$$\mathcal{O} = \bar{q}_j \otimes \mathcal{A}^j{}_k \otimes \mathcal{A}^k{}_l \otimes \mathcal{A}^l{}_i \otimes q^i \, . \tag{4.16}$$

Therefore the tensor $\bar{q}_j q^i$ transforms as the adjoint representation ruling out state $|N_1\rangle$ and all possible forms of $\mathcal{A}^k{}_l \mathcal{A}^l{}_i$ transform as the adjoint representation as well ruling out states $|N_2\rangle$. Therefore the only singlet states are given by states of form $|N_3\rangle$.

States which indeed transform as the direct sum of two singlets correspond to an operator structure

$$\mathcal{O} = \bar{q}_j \otimes \mathcal{A}^j{}_i \otimes q^i \otimes \mathcal{A}^k{}_l \otimes \mathcal{A}^l{}_k \, , \tag{4.17}$$

but those operators are not of leading order, since they would require a quark line to be inside the diagram and are therefore suppressed by orders of N_c.

Thus the only intermediate states for the current propagation are indeed given by only pure mesonic states and accordingly equation (4.12) is true. Since the N_c scaling for the vacuum current propagation can be easily computed—the simplest diagram is a closed quark loop with no insertion scaling as N_c^1— the left-hand-side of (4.12) needs to have the same N_c scaling as well

$$\sum_n \frac{|\, a_n \,|^2}{k^2 - m_{M_n}^2} \propto N_c \, . \tag{4.18}$$

Since this equation should be true for all momenta, the only consistent possibility is to require m_{M_n} to be of order N_c^0 for all mesons and accordingly $a_n = \langle 0|J|M_n\rangle \propto N_c^{1/2}$. Thus the meson decay constant for all mesons[4] are given by

$$f_{M_n} \propto \sqrt{N_c} \, . \tag{4.19}$$

[4] Again it is important to underline that spin and flavor dependence pose additional consistency conditions. Therefore the here derived expressions are just given at leading order.

4.2.3 Large-N_c scaling of baryon masses

As one was able to recognize when computing baryon scattering amplitudes, inserting a gluon generates a factor of N_c for the freedom of choosing the first quark. Computing the further N_c scaling in doubleline notation, one can see that the gluon coupling just cancels the doubleline combinatorical factors. Thus baryon scattering amplitudes naturally scale as N_c and seem to be divergent for $N_c \to \infty$. This problem can be resolved by the following idea: since the Lagrangian is a functional of N_c quarks, it also has to be proportional to N_c^1. Also, when computing Feynman diagrams, one computes functional derivative of the Lagrangian, and therefore the perturbation effectively scales with N_c as well. Following this idea, the baryon masses have a N_c scaling as well.

To identify the N_c scaling of the baryon masses one could use this simplified picture: the baryon is build out of N_c quarks, thus the baryon mass is given by the constituent quark masses m_{q_n}, the kinetic quark energies T_{q_n} and the potential between quarks V_{nm}

$$m_B = \sum_{n=1}^{N_c} m_{q_n} + \sum_{n=1}^{N_c} T_{q_n} + \frac{1}{2} \sum_{n \neq m}^{N_c} V_{nm} \,. \tag{4.20}$$

The interaction between two quarks is effectively reassembled by a gluon interchange scaling with g^2/N_c, thus the average potential[5] is given by $\langle V \rangle / N_c$. Averaging over all quarks one gets

$$m_B = N_c \langle m_q \rangle + N_c \langle T_q \rangle + N_c^2 \left(\frac{\langle V \rangle}{N_c} \right) \propto N_c m_0 \,. \tag{4.21}$$

Indeed there is a more general derivation for the N_c scaling of baryon masses, but nevertheless this result of using a simple picture gives the correct N_c scaling at leading order.

One can show[6], using symmetry properties in spin and flavor space, that the masses of the baryons take the form

$$m_B = m_0 N_c \, \mathbb{1} + m_2 \frac{1}{N_c} J^2 + \mathcal{O}(N_c^{-3}) \,, \tag{4.22}$$

where J^2 is depending on the dimension of the baryon spin-representation. This basically induces the mass splitting between the nucleon and Δ-excitation

$$m_\Delta - m_N = \mathcal{O}(N_c^{-1}) \,. \tag{4.23}$$

This fact will also be used later on when explicitly computing the effective potential. Since the energy of a delta particle is equal to the nucleon mass at leading order, the propagator of a delta particle is equal to the nucleon propagator. However, to understand how a delta particle is created in large-N_c QCD, one needs to take a closer look at the flavor or isospin symmetry.

4.3 Group structure consistency conditions

4.3.1 Contracted $SU(4)$ algebra

In the previous section the N_c scaling for physical quantities where derived by requiring a consistent scaling of similar diagrams. However, the analysis did not consider the spin-flavor group structure of external states. To furthermore guarantee the convergence of specific processes, information about the spin-flavor group structure needs to be included.

[5] Using this ansatz one already recognizes that the average potential should scale as N_c at leading order.
[6] See [Jenkins, 1998].

To simplify the analysis, only the isospin $SU(2)$ symmetry of light quarks is employed in this work. Thus the spin-flavor symmetry is reduced to a spin-isospin symmetry $SU(2)_{\mathrm{J}} \times SU(2)_{\mathrm{I}}$. A more detailed instruction for creating the large-N_c spin-flavor representations was written by [Dashen et al., 1994], who also derive consistency conditions and spin-flavor representations including the strange quark. A more recent review on this topic was written by [Jenkins, 1998].

As it will be demonstrated later on, in the large-N_c limit the physical baryons, as bound states of the light up and down quarks, correspond to the generalized nucleons, Δ-resonances and higher resonances in a spin-isospin representation of dimension $I = J = n/2$. Furthermore the analysis is restricted to mesons coupled to the axial current as for example the pion.

The coupling of a pion to baryons B and B' is described by a vertex of the form

$$\frac{\partial_i \pi^a}{f_\pi} \langle B' | \bar{q} \gamma^i \gamma^5 \tau^a q | B \rangle =: \frac{g_A}{f_\pi} \partial_i \pi^a (X^{ia})_{B'B} \tag{4.24}$$

where τ^a is a isospin Pauli matrix. Using the previously made definitions, the N_c scaling of this vertex is given by $N_c/\sqrt{N_c} = \sqrt{N_c}$.

To derive consistency equations for the large-N_c spin-isospin operator X^{ia}, one could consider baryon-pion scattering processes as $\pi^a + B \to \pi^b + B'$.

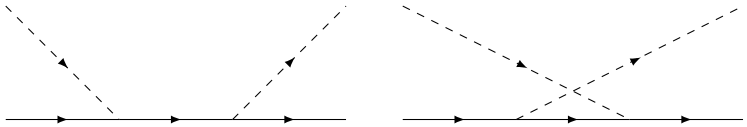

Figure 4.8: Leading diagrams contributing to $\pi^a + B \to \pi^b + B'$ process.

Combing the diagrams 4.8a and 4.8b, one obtains that the amplitude is proportional to

$$\left(\frac{g_A}{f_\pi}\right)^2 \sum_{\tilde{B}} \left[(X^{ia})_{B'\tilde{B}} (X^{jb})_{\tilde{B}B} - (X^{jb})_{B'\tilde{B}} (X^{ia})_{\tilde{B}B} \right] , \tag{4.25}$$

where the sum goes over all possible intermediate baryon states $\tilde{B}$. The relative minus sign is obtained by using that $m_B/m_\pi \propto N_c$ and thus the intermediate baryon is off-shell with an pion energy ω in diagram 4.8a while it is off-shell with $-\omega$ in diagram 4.8b.

Regarding the previously made definitions, the amplitude scales with N_c. This violates the previously discussed rules on the QCD level: the simplest diagram describing baryon meson scattering is given by a meson insertion on the same quark line. Since one inserts two mesons which are normalized by $1/f_M \propto 1/\sqrt{N_c}$ and one has N_c possibilities for choosing the coupled quark, one already starts at order N_c^0. In a similar fashion to the previously discussed scaling rules one can conclude that it is not possible to have a N_c scaling larger than N_c^0 if one requires the baryons to be color neutral. Thus, to require a consistent N_c scaling, the commutator of two X-elements has to vanish[7] at leading order in N_c

$$X^{ia} = X_0^{ia} + \mathcal{O}\left(\frac{1}{N_c}\right) \qquad \text{with} \qquad \left[X_0^{ia} \, , \, X_0^{jb} \right] = 0 \, . \tag{4.26}$$

To complete the spin-isospin algebra, one has to include the spin operator J^i and the isospin operator I^a. The operator X^{ia} should hereby transform according to $SU(2)_J$ in the spin

[7] Indeed one can show that the next to leading order term starts at order $1/N_c^2$. See [Jenkins, 1998].

component i and according to $SU(2)_I$ in the isospin component a. The complete large-N_c spin-isospin algebra has to fulfill the following commutation relations

$$\begin{aligned} \left[J^i \, , \, J^j \right] &= i \, \epsilon^{ijk} J^k \, , & \left[I^a \, , \, I^b \right] &= i \, \epsilon^{abc} I^c \, , & \left[I^a \, , \, J^i \right] &= 0 \, , \\ \left[J^i \, , \, X_0^{jb} \right] &= i \, \epsilon^{ijk} X_0^{kb} \, , & \left[I^a \, , \, X_0^{jb} \right] &= i \, \epsilon^{abc} X_0^{jc} \, , & \left[X_0^{ia} \, , \, X_0^{jb} \right] &= 0 \, , \end{aligned} \tag{4.27}$$

resulting in the so-called contracted $SU(4)$ algebra generated by the 15 generators $\{J^i\}$, $\{I^a\}$ and $\{X_0^{ia}\}$. As a matter of fact, this algebra looks similar to the embedding of $SU(2) \otimes SU(2) \to SU(4)$ generated by $\{\sigma^i\}$, $\{\tau^a\}$ via

$$\frac{\sigma^i}{2} \otimes \mathbb{1} \mapsto J^i \qquad \mathbb{1} \otimes \frac{\tau^a}{2} \mapsto I^a \qquad \frac{1}{2} \left(\sigma^i \otimes \tau^a \right) \mapsto G^{ia} \, ,$$

corresponding to the algebra

$$\begin{aligned} \left[J^i \, , \, J^j \right] &= i \, \epsilon^{ijk} J^k \, , & \left[I^a \, , \, I^b \right] &= i \, \epsilon^{abc} I^c \, , & \left[I^a \, , \, J^i \right] &= 0 \, , \\ \left[J^i \, , \, G^{jb} \right] &= i \, \epsilon^{ijk} G^{kb} \, , & \left[I^a \, , \, G^{jb} \right] &= i \, \epsilon^{abc} G^{jc} \, , & \left[G^{ia} \, , \, G^{jb} \right] &= i \, \delta^{ij} \epsilon^{abc} I^c + i \, \epsilon^{ijk} \delta^{ab} J^k \, . \end{aligned} \tag{4.28}$$

The name contracted $SU(4)$-algebra ($SU(4)_C$) is related to the fact that one is able to obtain $SU(4)_C$ by contracting $SU(4)$ by defining $X_0^{ia} := \lim_{N_c \to \infty} G^{ia}/N_c$. This also reassembles that one expects the commutator of two full spin-isospin mixing operators to be at order $1/N_c^2$:

$$\left[X^{ia} \, , \, X^{jb} \right] \sim \mathcal{O} \left(\frac{1}{N_c^2} \right) . \tag{4.29}$$

However there is a major difference between both algebras: the commutator of two spin-isospin operators G in $SU(2) \otimes SU(2) \subset SU(4)$ is not vanishing. Thus, the toral subalgebra of $SU(2) \otimes SU(2)$ is spanned by two generators resulting in two fundamental weights—the spin and isospin quantum numbers. Following the representation theory analysis this provides a physical consequence: nucleons, Δ-resonances and higher resonances all correspond to different irreducible representations and therefore it is not possible to realize mixed representation vertices like the N-Δ-vertex without explicitly breaking the group structure. This is not true for the contracted $SU(4)$-symmetry.

4.3.2 Contracted $SU(4)$ representations

The standard procedure for explicitly creating a representation of a semisimple Lie algebra—identifying simple roots and creating representations from fundamental weights—cannot be applied for the contracted $SU(4)$ algebra (denoted by $SU(4)_C$). This is the case since the subalgebra of spin-isospin mixing operators $\mathfrak{X} := \{X_0^{ia}\}$ forms an ideal of $SU(4)_C$

$$\left[X_0^{ia} \, , \, U \right] \in \mathfrak{X} \quad \forall \, X_0^{ia} \in \mathfrak{X} \quad \text{and} \quad \forall \, U \in SU(4)_C \, . \tag{4.30}$$

A possible way of generating representations is given by the method of induced representations which classifies irreducible representations of a semidirect product $G \ltimes A$ of a Lie group G and an Abelian group A. For the contracted $SU(4)$, the Lie group corresponds to $G = SU(2) \times SU(2)$ and the Abelian group is generated by the operators $\{X_0\}$. This section outlines the work of [Dashen et al., 1994] who also computed further results like the coupling strength of different baryonic vertices or the mass splitting of baryons in the limit of large-N_c by using the method of induced representations.

The goal for this section is to derive an explicit representation for the contracted $SU(4)_C$ baryons to underline that in the limit of large-N_c

- baryons B and B' of different spin J, J' and isospin I, I' representations form nonzero pion exchange matrix elements without violating the contracted $SU(4)_C$ symmetry for $|I - I'| \leq 1$ and $|J - J'| \leq 1$.
- Δ-resonances must be included for nucleon matrix elements to require that the contracted $SU(4)_C$ symmetry is valid.

Notation for representations

An element of the algebra $g \in \mathfrak{g}$ is a linear superposition of the basis of the algebra. In the case of $\mathfrak{g} = \mathfrak{su}(4)_C$ the basis is given by the generators $\{J^i, I^a, X_0^{ia}\}$ and therefore g corresponds to

$$g = \sum_{a=1}^{3} \lambda_{I,a}\, I^a + \sum_{i=1}^{3} \lambda_{J,i}\, J^i + \sum_{a,i=1}^{3} \lambda_{X,ia}\, X_0^{ia}\,. \tag{4.31}$$

Elements of the algebra generated by only spin or only isospin generators will be named $J = \sum \lambda_{J,i}\, J^i$ or I respectively. The action of an element of the algebra on a state is denoted by a "$\cdot$". The action of a group element $U(g)$ generated by a generator g is depending on the specific representation. In the case of $g \in \mathfrak{su}(4)_C$, the representations should correspond to the group of unitary operations $U(g) \in SU(4)_C$.

$$g \cdot |\Psi\rangle, \quad g \in \mathfrak{su}(4)_C \quad ; \quad U(g)\,|\Psi\rangle, \quad U(g) \in SU(4)_C$$

The operator $U(g)$ acts on the Fock-space and therefore can affect other operators as well. If one has found a set of basis vectors $\{|\Psi_i\rangle\}$, one can express the action of an operator as a matrix operation acting only on the group components of the states

$$U(g)\,|\Psi_j\rangle = \sum_i |\Psi_i\rangle\, D_{ij}^{(n)}(g)\,. \tag{4.32}$$

The representation $D_{ij}^{(n)}(g) \in GL(n,\mathbb{C}) \cap SU(4)_C$ is a matrix representation of $U(g) \in SU(4)_C$ with elements

$$\langle \Psi_i \,|\, U(g) \,|\, \Psi_j \rangle =: D_{ij}^{(n)}(g)\,. \tag{4.33}$$

A possible way for defining such representation is given by the exponential map

$$U(g) := \exp(ig)\ ,\ g \in GL(n,\mathbb{C}) \cap \mathfrak{su}(4)_C \quad \Rightarrow \quad D_{ij}^{(n)}(g) = (\exp(ig))_{ij}\ . \tag{4.34}$$

Accordingly, the transformation of an element of the algebra h under infinitesimal unitary transformation $U(g)$ is given by

$$U(g) h\, U^\dagger(g) = h + i\left(gh - hg^\dagger\right) + \mathcal{O}(g^2)\,, \tag{4.35}$$

where the bracket becomes the commutator for hermitian generators g.

Induced representations

Analogously to the idea of creating a representation for a semisimple Lie algebra, one has to identify a set of commuting operators. If one has found an eigenvector of all commuting operators, one can obtain the other states by applying all other operators to this eigenvector. In the case of $SU(4)_C$, the operators X_0^{ia} trivially form a set of commuting operators. Later on a combination of only spin and only isospin operators will be added to this set to define the large-N_c equivalent of spin and isospin.

Since all operators X_0^{ia} commute with each other, one can find an eigenvector of all operators fulfilling

$$X_0^{ia} \cdot |X\rangle = X_{ia} |X\rangle \ . \tag{4.36}$$

To underline that X_{ia} is an eigenvalue of $|\Psi\rangle$, lower indices have been used—upper indices will always express operations in the space.

A general state $|\Psi\rangle$ might have further quantum numbers which will be denoted by the quantum numbers $\{K_j\}$ corresponding to spin J^i and isospin I^a operations. These general states will be denoted by $|\Psi\rangle := \left| X\,, \vec{K} \right\rangle$, which still transforms accordingly under X_0^{ia} transformations

$$X_0^{ia} \cdot |\Psi\rangle = X_0^{ia} \cdot \left| X\,, \vec{K} \right\rangle = X_{ia} \left| X\,, \vec{K} \right\rangle \ . \tag{4.37}$$

To understand the quantum numbers $\vec{K}$, one has to understand how the state $|\Psi\rangle$ transforms under only spin and only isospin transformations. Therefore it is useful to start with the transformation behavior of the operators X_0^{ia} under such transformations

$$\begin{aligned} U(J^i) X_0^{ja} U^\dagger(J^i) &= X_0^{ja} + i \left[J^i\,,\, X_0^{ja} \right] + \mathcal{O}\left(J^2\right) \\ &= \left[(\mathbb{1})_{jk} - i (Ad_J^i)_{jk} + \mathcal{O}\left((Ad_J^i)^2 \right) \right] X_0^{ka} \qquad (4.38) \\ &= D^{(1)}_{jk}(-J^i) X_0^{ka} \qquad (4.39) \\ &= \left(D^{(1)}_{jk}(J^i) \right)^{-1} X_0^{ka}\,, \end{aligned}$$

where Ad_J^i is the three-dimensional adjoint representation of J^i. Accordingly the operator X_0^{ia} transforms as a spin one object in the i and as a isospin one object in the a component. Since a matrix element has to be a scalar under unitary transformations, one can compute the transformation law for states according to

$$\begin{aligned} X_{ia} \langle X \,|\, X \rangle &= \left\langle X \left| X_0^{ia} \right| X \right\rangle \\ &= \left\langle X \left| U^\dagger(J)\, U(J) X_0^{ia} U^\dagger(J)\, U(J) \right| X \right\rangle \\ &= \left(D^{(1)}_{ij}(J) \right)^{-1} \left\langle X' \left| X_0^{ja} \right| X' \right\rangle \qquad (4.40) \\ &= \left(D^{(1)}_{ij}(J) \right)^{-1} X'_{ja} \langle X' \,|\, X' \rangle \ . \end{aligned}$$

Thus the eigenvalues transform under the three-dimensional representation of spin $SU(2)$ which is isomorphic to the fundamental representation of rotation matrices $D^{(1)}(J) = R_J \in SO(3)$. If one understands the X label of state $|X\rangle$ to be a 3×3-matrix according to it's eigenvalues and uses that $R_I^T = R_I^{-1}$, the state transformation law is given by

$$U(J)U(I) \left| X, \vec{K} \right\rangle = \left| R_J X R_I^{-1}, \vec{K}' \right\rangle \ . \tag{4.41}$$

Note that by acting with $U(I)$ and $U(J)$ on the X-component of a state, the state in principle stays the same—just the eigenvalues are different. Different states are just generated by the action of $U(I)$ and $U(J)$ on the additional quantum numbers $\vec{K}$. Therefore, to understand the transformation behavior of the quantum numbers $\vec{K} \mapsto \vec{K}'$, one should at first find those transformations, which leave the matrix X invariant.

Since the action of spin and isospin operations transform X differently, each transformation will be expressed by an additional index

$$U_J(g) \Rightarrow g = \sum \lambda_i J^i \quad ; \quad U_I(g) \Rightarrow g = \sum \lambda_a I^a \,. \tag{4.42}$$

The set of generators which does not change X is called the *little group* or *stabilizer* of X and is defined by

$$\mathcal{G}_X := \left\{ U_J(J)U_I(I) \in SU(4)_C \,|\, X = R_J X R_I^{-1} \right\} . \tag{4.43}$$

The representation theory of the little group $\mathcal{G}_X$ will define all states for $SU(4)_C$ and since the action of $\mathcal{G}_X$ is connected to the physical spin and isospin operators, the representation theory of $\mathcal{G}_X$ will define spin and isospin for large-N_c baryons.

Obviously this seems to depend on the expectation values of the operator X_0^{ia}. Thus it is useful to analyze another quantity: the so-called *orbit* of X defined by

$$O_X := \left\{ X' \in GL(3) \,|\, X' = R_J X R_I^{-1} \quad \text{with} \quad U_J(J)U_I(I) \in SU(4)_C \right\} . \tag{4.44}$$

It can be easily shown[8] that a little group $\mathcal{G}_{X_0}$ at a point $X_0 \in O_{X_0}$ can be transferred 1-1 to the little group $\mathcal{G}_X$ at another point $X \in O_{X_0}$. Accordingly different irreducible representations of $SU(4)_C$ can be realized by picking a different initial matrix $\tilde{X}$ which is on another orbit $O_{\tilde{X}}$ with $O_{\tilde{X}} \cap O_{X_0} = \emptyset$.

This orbit identification is also making it possible to define the $\vec{K}$ quantum expectation values for a state $|\, X\,, \vec{K}\,\rangle$. The representation theory of the little group for different points on the same orbit will be defined by an arbitrary initial point X_0 on this orbit. Thus, all $\vec{K}$ expectation values are defined at this point. To measure the $\vec{K}$-value of a vector $|\, X\,, \vec{K}\,\rangle$, one has to transport $|\, X\,, \vec{K}\,\rangle$ to $|\, X_0\,, \vec{K}\,\rangle$ at first. In general this is also changing $\vec{K}$, but since this value is only measured at X_0, one can denote all quantum numbers with the X_0 expectation value of $\vec{K}$, knowing that these numbers have to be measured at X_0.

As [Dashen et al., 1994] have worked out, the reference point for physical states can be chosen to be $X_0 = \mathrm{diag}(1,1,1)$ modulo a rescaling of the coupling g_A. Thus, the little group is defined by

$$\mathcal{G}_{X_0} := \left\{ U_J(J)U_I(I) \in SU(4)_C \,\middle|\, \mathbb{1} = R_J R_I^{-1} \right\} = \left\{ U_J(g)U_I(g) \in SU(4)_C \,\middle|\, g \in \mathfrak{su}(2) \right\} \cong SU(2) . \tag{4.45}$$

Therefore the states of the contracted $SU(4)$ representations can be expressed by

$$|X_0; K, k\rangle = |X_0\rangle \otimes |K,k\rangle \ . \tag{4.46}$$

Since the initial configuration X_0 specifies the one-dimensional set of weights for the set of X_0^{ia} operators, the total number of states is given by $\dim(K) = 2K + 1$. The quantum number $|k| \leq K$ is labeling the possible states. At the reference points the normalization is chosen to be

$$\langle X_0; K,k \,|\, X_0; K, k' \rangle = \delta_{kk'} . \tag{4.47}$$

Therefore, at two different points on the orbit X_1,X_2 with $X_n = R_{J_n} X_0 R_{I_n}^{-1}$, the matrix element is only nonzero for $U_J^\dagger(J_1)U_J(J_2) = \mathbb{1}$ and for I_n accordingly. This is represented by a delta function on the group space

$$\langle X_2; K,k \,|\, X_1; K, k' \rangle = \delta_{kk'}\, \delta\left(J_2^{-1} J_1\right)\, \delta\left(I_2^{-1} I_1\right) , \tag{4.48}$$

defined by

$$\int \mathrm{d}g\ \delta(h^{-1}g) f(g) = \int \mathrm{d}g'\ \delta(g') f(hg') = f(h) , \tag{4.49}$$

where it was used that the Hurwitz integral over the group space is invariant under substitutions. Furthermore, since one now knows the group which leaves the X_0 quantum numbers

[8] See appendix A.1.

invariant, one can describe each point on the orbit by just one transformation:

$$\begin{aligned} U_J(g)\, U_I(h)\, |X_0; K, k\rangle &= U_J(g)\, U_I(h)\, U_I^\dagger(g)\, U_I(g)\, |X_0; K, k\rangle \\ &= U_I(h)\, U_I^\dagger(g)\, U_K(g)\, |X_0; K, k\rangle \\ &= \sum_{k'} U_I(h')\, |X_0; K, k'\rangle\, D^{(K)}_{k'k}(g)\,, \end{aligned} \tag{4.50}$$

where $h' = hg^{-1}$. Since one has the freedom to choose whether one transforms the states using spin or isospin transformation only, one may get different transformation properties for individual objects. Note that the final results, the vectors itself, are independent from this choice. The convention used in this work follows the convention of [Dashen et al., 1994], where the transformations to different points on the orbit are obtained by isospin transformations only.

Following the argumentation, the most general term which might represent a baryon is given by

$$|B; K\rangle = \sum_k \int \mathrm{d}g\; c_B(g,K,k) U_I(g)\, |X_0; K, k\rangle\ . \tag{4.51}$$

Note that a fixed baryon will have a non-measurable fixed quantum number K, since the matrix elements are only defined for the same little group dimensions.

It would be desirable to find a linear superposition of states such that the non-measurable quantum numbers of $SU(4)_C$-states, X_0 and k, are represented by their spin and isospin quantum numbers $(I, i; J, j)$

$$|B; K\rangle := |I, i; J, j; K\rangle\ . \tag{4.52}$$

Therefore the next goal is to find the correspondence of physical measurable states and $SU(4)_C$ weights. Thus one has to require that the states of equation (4.51) transform accordingly under spin and isospin transformations to match the coefficients c_B

$$\begin{aligned} U_J(g)\, |I, i; J, j; K\rangle &= \sum_{j'} |I, i; J, j'; K\rangle\, D^{(J)}_{j'j}(g) \\ U_I(h)\, |I, i; J, j; K\rangle &= \sum_{i'} |I, i'; J, j; K\rangle\, D^{(I)}_{i'i}(h)\,. \end{aligned} \tag{4.53}$$

A solution to this condition is given by[9]

$$|I, i; J, j; K\rangle = \sqrt{\frac{\dim(I)\dim(J)}{v}} \sum_{km} e^{i\pi k} \begin{pmatrix} I & J & K \\ m & j & -k \end{pmatrix} \int \mathrm{d}g\, D^{(I)}_{mi}\left(g^{-1}\right) U_I(g)\, |X_0\,;\, K\,, k\rangle\ . \tag{4.54}$$

The array (Wigner $3J$-Symbol) hereby represents the according Clebsch-Gordan coefficients for $SU(2)$ tensor states and $v = \int \mathrm{d}g$ is a constant representing the volume of $SU(2)$. Using the selection rules for Wigner $3J$-symbols (see A.1)

$$|\, I - J\,| \le K \le I + J\,, \qquad I + J + K \in \mathbb{Z}\,, \qquad k = m + j\,, \tag{4.55}$$

one obtains that for $K = 0$ the irreducible baryon representations are restricted to the infinite tower of states with $(I,J) = (n/2,n/2)$. These states can be identified with the nucleons for $I = J = 1/2$, the Δ-resonances for $I = J = 3/2$ and so on. And as shown before, all those states are in the same irreducible representation (depending on the orbit of X_0).

The quantum number K can be identified with a strangeness index—for $K = 0$ no strange quarks are involved, for $K > 0$ one can identify the according large-N_c baryons with $N_c = 3$ baryons containing strange quarks.

[9] See also appendix A.3 and for the Wigner $3J$-symbol appendix A.2.

Now one is finally able to compute the matrix element $\langle B'|X_0^{ia}|B\rangle$. By setting $K = 0$ one obtains[10]

$$\langle I', i'; J', j'; 0 \,|\, X_0^{na} \,|\, I, i; J, j; 0\rangle = \frac{\sqrt{\dim(J)\dim(J')}}{v} \begin{pmatrix} J' & 1 & J \\ -j' & n & j \end{pmatrix} \begin{pmatrix} I' & 1 & I \\ i' & a & -i \end{pmatrix} . \tag{4.56}$$

Here one can draw some important remarks:

- it is not possible for the pion to connect baryons of different strangeness-sectors[11] (K-sectors)
- it is possible for a pion to connect Δ-resonances and nucleons (and higher resonances with $|I' - I| \leq 1$ and $|J' - J| \leq 1$) without breaking the contracted $SU(4)$ group symmetry
- for nucleonic matrix elements, the large-N_c spin-flavor symmetry is isomorphic to the embedding $SU(2)_J \otimes SU(2)_I \to SU(4)$
- as a consequence of the previous statement, for the consistency condition (4.26) to be true for external nucleon states, intermediate Δ-states must be included.

The last points can be seen when computing nucleon matrix elements (see A.20)

$$\left\langle N' \,\middle|\, X_0^{ia} \,\middle|\, N \right\rangle \in \left\{\sigma^+, \sigma^-, \mathbb{1}\right\} \otimes \left\{\tau^+, \tau^-, \mathbb{1}\right\} , \tag{4.57}$$

and thus the commutator between pure nucleonic matrix elements is not vanishing[12].

4.4 Nucleon-nucleon potential in the limit of large-N_c

The starting point of the previous section was to look at scattering processes of hadronic objects to formulate consistency conditions on large-N_c operators. Since one has now the tools to analyze physical states, it is desirable to formulate large-N_c predictions for physical quantities—for example the nucleon-nucleon potential defined by

$$V_{NN} = V(N_1', N_2'; N_1, N_2) := \langle N_1', N_2' \,|\, H_{\text{eff}} - H_0 \,|\, N_1, N_2\rangle \ . \tag{4.58}$$

In general one is able to compute the large-N_c scaling using the quark-line formalism introduced in section 4.1. The nucleonic matrix elements of the effective potential or Hamiltonian[13] should depend on spin and isospin of the nucleons. Thus it is useful to decompose these operators as functions of the previously discussed contracted $SU(4)$ operators. After identifying the spin and isospin dependent N_c scaling in QCD, one can directly compute the nucleon-nucleon potential in χPT as a function of spin and isospin of the nucleons. Therefore this potential directly enables a comparison between QCD and χPT.

The analysis which resulted in the large-N_c predictions of the nucleon-nucleon potential was done by [Kaplan and Savage, 1996] and [Kaplan and Manohar, 1997]. One therefore refers to the KSM counting rules.

[10] More details can be found in appendix A.4.

[11] The proof can be found in A.4.

[12] In principle, since X_0 only connects $|I - J| \leq 1$ baryons, one could also use this consistency condition to compute the relative strength of the $g_{\pi NN}$ and the $g_{\pi N\Delta}$ vertex by requiring $\langle N'| \left[X_0^{ia} , X_0^{jb} \right] |N\rangle = 0$, where the sum goes over all intermediate states corresponding to Δ-resonances and nucleons. See also [Dashen et al., 1994].

[13] As Witten has shown in [Witten, 1979], physics on the hadronic regime are described by a Hartree Hamiltonian.

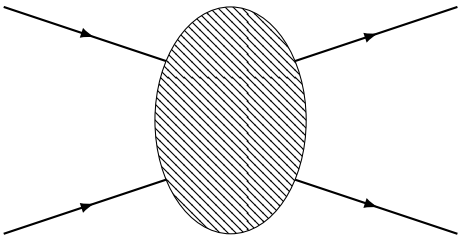

(a) Baryon-baryon scattering on hadronic level.

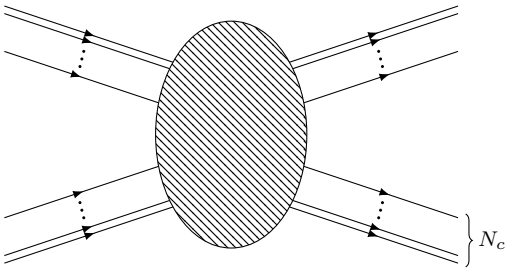

(b) Baryon-baryon scattering on quark-gluon level.

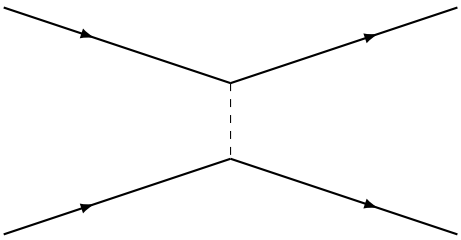

(c) Baryon-baryon scattering with mesonic exchange on hadronic level.

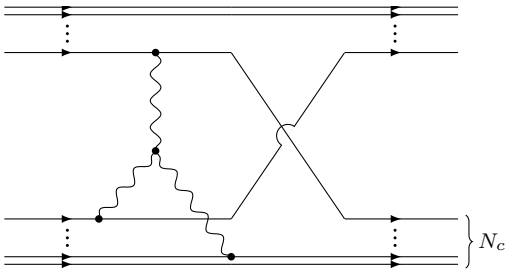

(d) Possible contribution to baryon-baryon scattering with mesonic exchange on quark-gluon level.

Figure 4.9: Though one is able to directly compare baryon-baryon scattering amplitudes on the hadronic and on the quark-gluon level, multiple diagrams on the quark-gluon level might contribute to an explicit mesonic exchange on the hadronic level.

4.4.1 Hartree Hamiltonian for QCD states

As seen before, while the quark masses are of order N_c^0, the baryon masses start at N_c. Thus for momenta at order N_c^0, the Hamiltonian containing baryons is non-relativistic at leading order in N_c. Relativistic corrections correspond next to leading order effects. Thus it is sufficient to formulate a theory for baryons by introducing the most general Hamiltonian to describe the interaction of baryons. This Hartree Hamiltonian takes the form

$$V_{NN} = \sum_{n=1}^{\infty} O^{(n)} \,, \tag{4.59}$$

where $O^{(n)}$ is a connected n-quark operator. The first step is to extract the N_c scaling of $O^{(n)}$ when applying to baryonic states. Afterwards one has to explicitly compute the leading order and extract the spin and isospin quantum numbers.

In general, when computing the baryon matrix elements of a n-quark operator $O^{(n)}$, one obtains two possible sources of N_c dependence: the combinatorical dependence and the diagrammatic dependence

$$\left\langle \{B_i'\} \middle| O^{(n)} \middle| \{B_i\} \right\rangle \sim f_{\text{Comb}}(N_c) f_{\text{Diag}}(N_c) \,. \tag{4.60}$$

$f_{\text{Comb}}(N_c)$ is computed by the possibilities of choosing the quarks on which the operator is acting on. For N_c large enough one obtains at leading order

$$f_{\text{Comb}}(N_c) \sim N_c(N_c-1)(N_c-2)\cdots(N_c-n) \sim N_c^n \,. \tag{4.61}$$

For the diagrammatic factor one can use the double line formalism introduced in section 4.1. As an example one can start with figure 4.10. To compute the N_c scaling at leading order,

one has to introduce the minimal number of vertices such that the diagram is connected. For example a three-gluon vertex, a four-gluon vertex and a direct connection scaling as g^4 and g^6 and g^2 connect all seven out of seven lines without creating a loop. Thus the diagram scales as $1/N_c^6$.

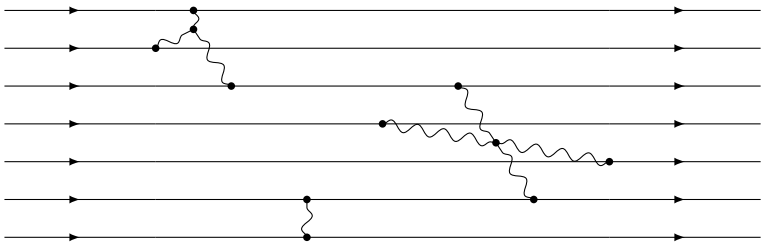

Figure 4.10: Example for a connected seven-quark diagram scaling as N_c^{-6}.

The N_c-dependence for creating a connected n-quark operator using the QCD vertices can be computed accordingly:

- The direct connection of two unconnected lines costs $1/N_c$.
- The three-gluon vertex reduces N unconnected lines to $N-2$ unconnected lines while introducing a factor of $1/N_c^2$—three gluon-quark vertices and a three-gluon vertex proportional to g^4.
- The four-gluon vertex reduces N unconnected lines to $N-3$ unconnected lines while introducing a factor of $1/N_c^3$—four gluon-quark vertices and the four-gluon vertex itself proportional to g^6.
- It is not possible to increase the N_c scaling by introducing a new vertex since the number of external lines are fixed. Thus, when introducing a new vertex, at least one line needs to connect to external line not creating a loop while the other one, two or respectively three lines for a direct connection, three- or four-gluon vertex can maximally create no, one or two loops while costing already $1/N_c$, $1/N_c^2$ or $1/N_c^3$.

Combing these rules the number of direct connections V_2, the number of three-vertices V_3 and the number of four-vertices V_4 at leading order should fulfill the following relation for a connected n-quark operator

$$n = 3V_4 + 2V_3 + V_1\,. \tag{4.62}$$

Accordingly the N_c scaling for the diagrammatic factor is given by

$$f_{\text{Diag}}(N_c) = N_c^{1-V_1-2V_3-3V_4} = N_c^{1-n}\,, \tag{4.63}$$

where the 1 requires that a connected two quark diagram scales as $1/N_c$. Following the argumentation, at leading order a n-quark operator can be expressed by

$$O^{(n)} = N_c^{1-n} O_0^{(n)}\,, \tag{4.64}$$

where the operator $O_0^{(n)}$ is at leading order $\mathcal{O}(N_c^0)$. Therefore the matrix elements are given at leading order by

$$\left\langle \{B_i'\} \middle| O^{(n)} \middle| \{B_i\} \right\rangle \sim N_c\,. \tag{4.65}$$

It is desirable to describe the Hamiltonian with operators corresponding to baryonic quantum numbers instead of quark-gluon interactions, if one wants to describe the nucleon-nucleon potential. Since one is just able to observe colorless particles in nature, physical quantities as the nucleon-nucleon potential should just depend on quantum numbers of the external nucleons—the momenta, spin and isospin.

In the previous section it was argued that one can describe the fundamental spin-isospin symmetry with the contracted $SU(4)$ group. To outline the difference between operators and matrix elements of the spin-isospin operator, the matrix elements of the operator G are given by $\langle N' \,|\, G \,|\, N \rangle = N_c X$. Thus, the Hartree Hamiltonian is given by

$$\begin{aligned} H_{\text{eff}} &= N_c \sum_{n,n_1,n_2,n_3=1}^{\infty} v_{n_1 n_2 n_3} \cdot \left(\frac{J}{N_c}\right)^{n_1} \cdot \left(\frac{I}{N_c}\right)^{n_2} \cdot \left(\frac{G}{N_c}\right)^{n_3} \delta_{n_1+n_2+n_3,n} \\ &= N_c \sum_{n,n_1,n_2} v_N \cdot \left(\frac{J}{N_c}\right)^{n_1} \cdot \left(\frac{I}{N_c}\right)^{n_2} \cdot \left(\frac{G}{N_c}\right)^{n-n_1-n_2} , \end{aligned} \tag{4.66}$$

where the "$\cdot$" denotes a contraction of the tensor-function v_N with the operators J,I and G such that the Hamiltonian fulfills all symmetries, e.g. spin, isospin, parity, time inversion etc. For matrix elements, the function v_N can just depend on momenta $\vec{p}_i$ of the baryons and relativistic corrections proportional to $\vec{p}_i/m_B$ which are $1/N_c$ corrections. Thus the coefficients v_N are at leading order N_c^0. Furthermore all operators are one body operators and therefore all matrix elements of just one operator are at most at order N_c. For nucleons which have spin and isospin at order N_c^0, the matrix elements are given by

$$\left\langle N' \,\middle|\, I \,\middle|\, N \right\rangle \sim N_c^0 \quad , \quad \left\langle N' \,\middle|\, J \,\middle|\, N \right\rangle \sim N_c^0 \quad , \quad \left\langle N' \,\middle|\, G \,\middle|\, N \right\rangle \sim N_c \,. \tag{4.67}$$

Accordingly, to find the large-N_c scaling of the nucleon-nucleon potential, one has to find the large-N_c scaling of the Hartree Hamiltonian for nucleonic matrix elements.

4.4.2 Nucleon-Nucleon matrix elements of the Hartree Hamiltonian

As discussed in chapter 3, the nucleon-nucleon potential can be separated into several components according to the spin-isospin structure of the nucleons. Analyzing the tensor structure of the Hamiltonian, one identifies the I operator as a (0,1)-tensor corresponding to isospin, the J operator as a (1,0)-tensor corresponding to spin and the G operator as a (1,1)-tensor corresponding to spin-isospin mixing numbers of the nucleons. Thus one expects the potential to have (0,0),(0,1),(1,0) and (1,1) structures

$$\begin{aligned} V_{NN} = V_0^0 + V_\sigma^0 \, \vec{J}_1 \cdot \vec{J}_2 + V_T^0 \left(3 \left(\vec{J}_1 \cdot \vec{q}\right) \left(\vec{J}_2 \cdot \vec{q}\right) - \vec{J}_1 \cdot \vec{J}_2\right) + V_{\text{Spin-Orbit}}^0 \\ V_0^1 \vec{I}_1 \cdot \vec{I}_2 + V_\sigma^1 \, X_1 \cdot X_2 + V_T^1 \left(3 \left(X_1^{ia} \cdot q^i\right) \left(X_2^{ja} \cdot q^j\right) - X_1 \cdot X_2\right) + V_{\text{Spin-Orbit}}^1 \,. \end{aligned} \tag{4.68}$$

The upper index of V_j^i expresses the rank of the isospin component, the lower index the rank of the spin component.

To extract the large-N_c scaling of the components which are scalar in the momenta V_i^j with $i = 0, 1$ and $j = 0,\sigma$, the so-called central potential, one has to require that v_N of equation (4.66) is a scalar. Thus one gets

$$V_{NN}^C = N_c \sum_{n,n_1,n_2} v_N \left(q^2, k^2\right) \left\langle N_1', N_2' \middle| \left(\frac{J}{N_c}\right)^{n_1} \cdot \left(\frac{I}{N_c}\right)^{n_2} \cdot \left(\frac{G}{N_c}\right)^{n-n_1-n_2} \middle| N_1, N_2 \right\rangle . \tag{4.69}$$

Now one has to contract the operators such that they contribute to the leading order for each of the four possible tensorial ranks. The easiest rank to extract is obviously the (0,0) rank which is at leading order given by $n_i = 0 = n$. Thus one directly gets

$$V_0^0 \sim N_c \,. \tag{4.70}$$

The spin-isospin (1,1) rank is obtained by using G operators, or contractions of $I \cdot J$ operators (or more complex contractions). Since the matrix elements of the G operators dominate the

large-N_c scaling, the central spin-isospin potential is composed only out of contractions of G operators. Furthermore, to fulfill spin and isospin conservation, one needs an even number of G operators:

$$V_\sigma^1 \sim N_c \sum_{n=1} v_n \left(q^2,k^2\right) \left\langle N_1',N_2' \middle| \left(\frac{G\cdot G}{N_c^2}\right)^n \middle| N_1,N_2 \right\rangle . \tag{4.71}$$

For the leading order one could directly choose $n = 1$. The leading order scaling of this contraction is given by

$$\left\langle N_1',N_2' \middle| \frac{G^{ia}G^{ia}}{N_c^2} \middle| N_1,N_2 \right\rangle = X_1^{ia}X_2^{ia} + \mathcal{O}(N_c^{-1}) , \tag{4.72}$$

since a term where both operators act on one nucleon can effectively be reduced to one operator using commutation and anti-commutation relations of the operators:

$$\left\langle N_i' \middle| \hat{G}\cdot\hat{G} \middle| N_i \right\rangle \sim N_c(\mathbb{1} + X_i) + \mathcal{O}(1) . \tag{4.73}$$

Thus, at leading order, the central rank (1,1) potential is given by

$$V_\sigma^1 \sim N_c . \tag{4.74}$$

To compute the (1,0) or the (0,1) component, one needs to include contractions of kind $J\cdot J$ or $(G\cdot J)\cdot(G\cdot J)$ for spin and $(J \mapsto I)$ respectively for the isospin. In both cases this effectively reduces the leading order by N_c^{-2} resulting in

$$V_\sigma^0 \sim \frac{1}{N_c} \sim V_0^1 . \tag{4.75}$$

This also indicates the dominance of the $I_t = J_t$ rule of the Skyrme model as shown by [Kaplan and Savage, 1996]

$$V_J^I \sim \frac{1}{N_c^{|I-J|}} . \tag{4.76}$$

Following the same analysis, [Kaplan and Manohar, 1997] has proven further relations including the tensor potential V_T and the spin-orbit potentials.

Isospin	V_0	V_σ	V_T
$\mathbb{1}\cdot\mathbb{1}$	N_c	$1/N_c$	$1/N_c$
$\vec{\tau}_1\cdot\vec{\tau}_2$	$1/N_c$	N_c	N_c

Table 4.2: KSM counting rules: Large-N_c scaling of the nucleon-nucleon potential (without spin-orbit contributions).

4.5 Chiral perturbation theory in the limit of large-N_c

As demonstrated in chapter 2, χPT makes it possible to explicitly compute the nucleon-nucleon potential while possessing the same symmetry as the more fundamental theory: the QCD. In the limit of large-N_c the color $SU(3)$ becomes the color $SU(N_c)$ which has no direct consequences for χPT—the degrees of freedoms in QCD which carry the quantum number color, the quarks and gluons, do not appear in χPT. But, as shown in the previous sections, many consequences for physical quantities and symmetries arise from consistency conditions of large-N_c QCD. Therefore one can compare the quantities which describe the same object in large-N_c QCD and large-N_c χPT.

Since the spin and the approximate isospin symmetry of large-N_c QCD becomes the contracted $SU(4)$ symmetry, also the corresponding effective theory, large-N_c χPT should posses this symmetry

$$\begin{aligned} \sigma^i &\mapsto J^i & \left\langle N' \middle| J^i \middle| N \right\rangle &= \left(J^i\right)_{N'N} \\ \tau^a &\mapsto I^a & \left\langle N' \middle| I^a \middle| N \right\rangle &= \left(I^a\right)_{N'N} \\ \sigma^i\tau^a &\mapsto G^{ia} & \left\langle N' \middle| G^{ia} \middle| N \right\rangle &= g_A \left(X^{ia}\right)_{N'N} . \end{aligned} \tag{4.77}$$

Furthermore the commutators of two spin-isospin mixing operators X^{ia} is at order $1/N_c^2$. The leading order scaling of large-N_c objects which affect χPT are summarized in table 4.3.

Quantity	m_N	$m_N - m_\Delta$	m_π	$\vec{q}$	g_A	f_π
Large-N_c scaling	N_c	$1/N_c$	1	1	N_c	$\sqrt{N_c}$

Table 4.3: Large-N_c objects and leading order scaling affecting chiral perturbation theory.

Accordingly the large-N_c version of the χPT Feynman-rules (equations (2.48), (2.49) and (2.50)) have to be changed. The spin and isospin quantum numbers of a nucleon (j,i) which correspond to $SU(2) \times SU(2)$ now become a spin-isospin quantum number A corresponding to $SU(4)_C$. Thus the matrix elements of the one- and two-pion vertices are given by

$$\left\langle N_B(\vec{p}_2) \middle| H_{21}^{(1)} \middle| N_A(\vec{p}_1); \pi^a(\vec{q}) \right\rangle \longleftrightarrow \frac{i g_A}{2 f_\pi} \frac{q^i}{\sqrt{2\omega_{\vec{q}}}} \left(X^{ia}\right)_{BA} \sim \sqrt{N_c}\, q^i \left(X^{ia}\right)_{BA} , \tag{4.78}$$

and

$$\begin{aligned} \left\langle N_B(\vec{p}_2) \middle| H_{21}^{(1)} \middle| N_A(\vec{p}_1); \pi^a(\vec{q}_1); \pi^b(\vec{q}_2) \right\rangle &\longleftrightarrow \frac{i}{f_\pi^2} \frac{\omega_{\vec{q}_1} - \omega_{\vec{q}_2}}{\sqrt{\omega_{\vec{q}_1}\omega_{\vec{q}_2}}} \epsilon^{abc} \left(I^c\right)_{BA} \sim \frac{1}{N_c} \epsilon^{abc} \left(I^c\right)_{BA} \\ \left\langle \pi^b(\vec{q}_2); N_B(\vec{p}_2) \middle| H_{21}^{(1)} \middle| N_A(\vec{p}_1); \pi^a(\vec{q}_1) \right\rangle &\longleftrightarrow \frac{i}{f_\pi^2} \frac{\omega_{\vec{q}_1} + \omega_{\vec{q}_2}}{\omega_{\vec{q}_1}\omega_{\vec{q}_2}} \epsilon^{abc} \left(I^c\right)_{BA} \sim \frac{1}{N_c} \epsilon^{abc} \left(I^c\right)_{BA} . \end{aligned} \tag{4.79}$$

According to this, the leading large-N_c scaling in χPT can directly be computed by counting the number of one-pion vertices N_1, the number of two pion vertices N_2 and the commutators of one-pion vertices C appearing in the amplitude

$$\mathcal{O}_{N_c}\left(V_{NN}\right) = \frac{N_1}{2} - N_2 - 2C . \tag{4.80}$$

Also using the chiral dimension for the two nucleon potential (3.32), one finally gets

$$\mathcal{O}_{N_c}\left(V_{NN}^{(\nu)}\right) = \frac{\nu}{2} + 1 - 2N_2 - 2C . \tag{4.81}$$

Though one would like to proof that the matrix elements of the QCD Hartree potential posses the same N_c scaling as the χPT potential (see figure 4.9), it is not guaranteed that partial amplitudes corresponding to the same operator structure have the same N_c scaling, e.g.

$$\langle N_1; N_2 \,|\, I \cdot G \cdot J \,|\, N_1; N_2 \rangle_{\chi\mathrm{PT}} \neq \langle N_1; N_2 \,|\, I \cdot G \cdot J \,|\, N_1; N_2 \rangle_{QCD} . \tag{4.82}$$

This is the case since the QCD operators act on quarks, while the χPT versions act on baryons. The N_c dependence in the QCD case is heavily depending on the number of interacting quarks, however, the χPT version does not acknowledge this.

While the upper N_c bound of the QCD potential is given by N_c^1 and in general decreasing with the number of different quark interactions, the χPT potential is only limited by the chiral order. One can only demand the same N_c scaling for both potentials, if they are computed non-perturbatively—one takes the sum over the maximal number of quark operators in the QCD case or the sum up to all chiral orders in the χPT case.

Fortunately one is able to compute the leading N_c scaling of the amplitude in the QCD case, since one can take the sum over all quarks inhibited in the interacting nucleons. One is even able to split the potential into different spin and isospin depending amplitudes and predict their scaling, as demonstrated in the previous section. Thus the leading order scaling of the spin and isospin depending amplitudes are predicted by large-N_c QCD. If large-N_c χPT posses the same scaling, all partial chiral amplitudes, corresponding to specific spin and isospin amplitudes of the potential, are not allowed to violate the leading order scaling predicted by QCD.

To confirm the consistency of large-N_c potentials, one has to explicitly compute the chiral amplitude, identify the tensor structure to evaluate the leading order QCD prediction and compute the chiral N_c scaling depending on the couplings and commutator structure of the amplitude.

Part II

Nucleon-nucleon potential

5 Operator structure of effective unitary potential

In this chapter, the nucleon-nucleon potential will be explicitly computed up to NNLO ($\nu = 4$). This will be done by following the instructions of the previous section 3.2. As mentioned before, one starts a perturbation in the chiral vertex-dimension of associated operators.

The interacting part of the Hamiltonian has vertices corresponding to the vertex-dimension $\kappa_i = d_i + p_i + 3/2\, n_i - 4$

$$H_I = H_{21}^{(1)} + H_{22}^{(2)} \,. \tag{5.1}$$

The procedure of perturbatively computing the order of sub terms of the effective potential inhabits products of kind $H_I \lambda A \eta$. To simplify the counting of those terms, it is useful to furthermore separate the projection operator λ in several subspaces corresponding to the number of intermediate pions

$$\lambda = \sum_{i=1} \lambda^i \quad , \quad \lambda^i \lambda^j = \delta^{ij} \lambda^i \,. \tag{5.2}$$

Using this equation, equation (3.20) becomes

$$\lambda^i A^{(\kappa)} \eta = \frac{\lambda^i}{\omega_i} \left(H_I^{(\kappa)} - \sum_{n=1}^{2} \lambda^i A^{(\kappa-n)} \eta H_I^{(n)} + \sum_{n=1}^{2} \sum_{j=i-2}^{i+2} \lambda^i H_I^{(n)} \lambda^j A^{(\kappa-n)} \right. \tag{5.3}$$

$$\left. - \sum_{n=1}^{\kappa-2} \sum_{j=1}^{2} \lambda^i A^{(n)} \eta\, H_I^{(j)} \lambda^j A^{(\kappa-n-j)} \right) \eta \,. \tag{5.4}$$

Note that the second operator contains the expression $\eta H_I \eta$ and thus only $H_{22}^{(2)}$ can make contributions which corresponds to a closed pion loop (tadpole). One can show that after renormalization this loop can directly be absorbed in the redefinition of the physical nucleon mass (see [Epelbaum et al., 2003]) and thus this term will be neglected in this analysis.

Terms like $\lambda^i H_{22}^{(2)} \lambda^i$ can behave differently, since they are able to absorb and emit a pion which is in general not creating a tadpole directly.

Analogously one can start to compute the terms which contribute to the effective potential given by equation (3.16) by expanding in the chiral dimension. The result for the effective unitary potential at order $\nu = 0$, $\nu = 2$ and $\nu = 4$ are given below. A more complete derivation can be found in [Epelbaum et al., 1998] up to order $\nu = 2$ or [Epelbaum, 2007] including order $\nu = 4$.

5.1 Unitary potential at leading order

At leading order the effective unitary nucleon-nucleon potential is given by one term (when neglecting the tadpole diagrams)

$$V_{NN}^{(0)} = -\eta\, H_{21}^{(1)} \frac{\lambda^1}{\omega_1} H_{21}^{(1)}\, \eta \,. \tag{5.5}$$

Neglecting the diagrams which can be absorbed during renormalization, the diagrams contributing to the potential are given by the first two diagrams in figure 3.1 and effectively correspond to the potential

$$V_{NN}^{(0)} = -\frac{g_A^2}{4f_\pi^2}\frac{X_1^{ia}\,q^i\;X_2^{ja}\,q^j}{\vec{q}^{\,2}+m_\pi^2}\,. \tag{5.6}$$

5.2 Unitary potential at next to leading order

The unitary potential at next to leading order—or at the two pion exchange level—can be separated in three different types: the potential without $H_{22}^{(2)}$ vertices (seagull vertices)

$$V_{NN_0}^{(2)} = \frac{1}{2}\left(\eta\,H_{21}^{(1)}\frac{\lambda^1}{\omega_1}H_{21}^{(1)}\,\eta\,H_{21}^{(1)}\frac{\lambda^1}{\omega_1^2}H_{21}^{(1)}\,\eta - \eta\,H_{21}^{(1)}\frac{\lambda^1}{\omega_1}H_{21}^{(1)}\frac{\lambda^2}{\omega_1+\omega_2}H_{21}^{(1)}\frac{\lambda^1}{\omega_1}H_{21}^{(1)}\,\eta\right)$$
$$+\,\text{hermetean conjugation}\,. \tag{5.7}$$

The potential containing one seagull vertex

$$V_{NN_1}^{(2)} = \frac{1}{2}\left(2\eta\,H_{22}^{(2)}\frac{\lambda^2}{\omega_1+\omega_2}H_{21}^{(1)}\frac{\lambda^1}{\omega_1}H_{21}^{(1)}\,\eta + \eta\,H_{21}^{(1)}\frac{\lambda^1}{\omega_1}H_{22}^{(2)}\frac{\lambda^1}{\omega_1}H_{21}^{(1)}\,\eta\right) + h.c.\,. \tag{5.8}$$

And finally the part corresponding to two seagull vertices

$$V_{NN_2}^{(2)} = -\eta\,H_{22}^{(2)}\frac{\lambda^2}{\omega_1+\omega_2}H_{22}^{(2)}\,\eta\,. \tag{5.9}$$

The time-ordered topologies describing the potential are given in figure 5.1. The potential $V_{NN_0}^{(2)}$ contains six box diagrams (figure 5.1a) and six cross-box diagrams (figure 5.1b). The potential $V_{NN_1}^{(2)}$ is build out of six seagull diagrams (figure 5.1c), while the potential $V_{NN_2}^{(2)}$ corresponds to two football diagrams (figure 5.1d). All individual possibilities can also be found in appendix B.1.

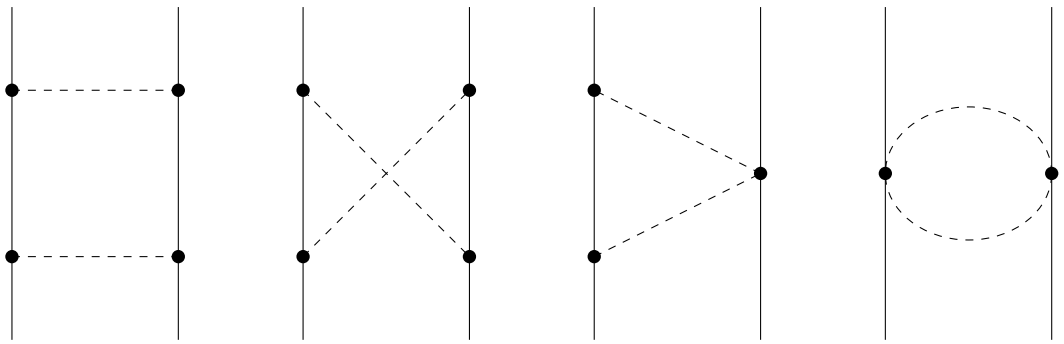

(a) Box diagram **(b)** Cross-box diagram **(c)** Seagull diagram **(d)** Football diagram

Figure 5.1: Diagrams contributing to the effective unitary nucleon-nucleon potential at order chiral order $\nu = 2$.

5.3 Unitary potential at next to next to leading order

Due to the number of new operator structures at NNLO, it is useful to organize the effective unitary potential. In the following content the potential is separated in the part without seagull vertices, with one seagull vertex, with two seagull vertices and with three seagull vertices.

5.3.1 Potential without seagull vertices

At chiral order $\nu = 4$, it is furthermore useful to separate the effective unitary potential according to six different operator structure types generating 120 diagrams which can be summarized as the six topologies of figure 5.2.

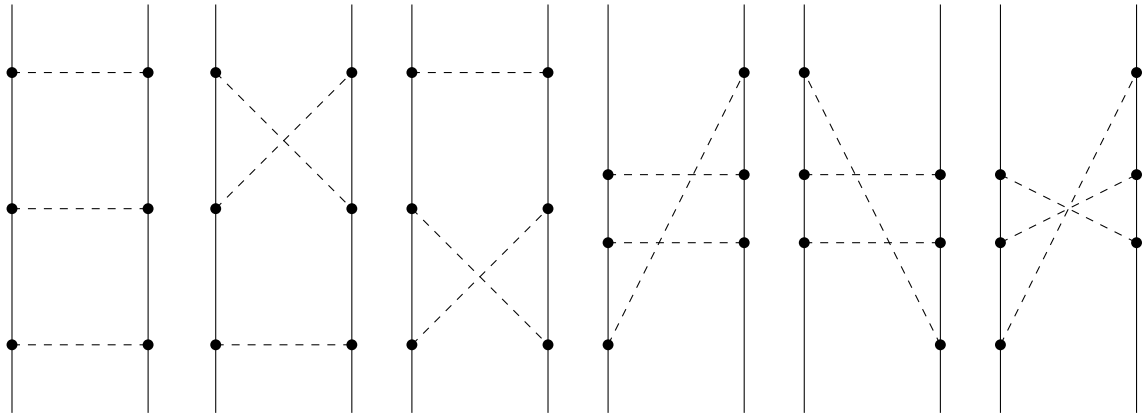

(a) Double-box diagram **(b)** Upper cross-box diagram **(c)** Lower cross-box diagram **(d)** Left to right slashed box diagram **(e)** Right to left slashed box diagram **(f)** Slashed cross-box diagram

Figure 5.2: Diagrams without seagull vertex contributing to the effective unitary nucleon-nucleon potential at chiral order $\nu = 4$.

The following operator structure contributes to diagrams with three intermediate only nucleon states corresponding to eight of twenty double-box topologies (see figure 5.2a).

$$\begin{aligned} V^{(4)}_{NN_{0,1}} = -\frac{1}{8}\Bigg(& 4\eta\, H^{(1)}_{21}\frac{\lambda^1}{\omega_1^3} H^{(1)}_{21}\,\eta\, H^{(1)}_{21}\frac{\lambda^1}{\omega_1} H^{(1)}_{21}\,\eta\, H^{(1)}_{21}\frac{\lambda^1}{\omega_1} H^{(1)}_{21}\,\eta \\ & + 3\eta\, H^{(1)}_{21}\frac{\lambda^1}{\omega_1^2} H^{(1)}_{21}\,\eta\, H^{(1)}_{21}\frac{\lambda^1}{\omega_1^2} H^{(1)}_{21}\,\eta\, H^{(1)}_{21}\frac{\lambda^1}{\omega_1} H^{(1)}_{21}\,\eta \\ & + \eta\, H^{(1)}_{21}\frac{\lambda^1}{\omega_1^2} H^{(1)}_{21}\,\eta\, H^{(1)}_{21}\frac{\lambda^1}{\omega_1} H^{(1)}_{21}\,\eta\, H^{(1)}_{21}\frac{\lambda^1}{\omega_1^2} H^{(1)}_{21}\,\eta\Bigg) + h.c.\,. \end{aligned} \tag{5.10}$$

The next structure corresponds to diagrams in which each intermediate state has at least one pion

$$\begin{aligned} V^{(4)}_{NN_{0,2}} = & -\eta\, H^{(1)}_{21}\frac{\lambda^1}{\omega_1} H^{(1)}_{21}\frac{\lambda^2}{\omega_1+\omega_2} H^{(1)}_{21}\frac{\lambda^1}{\omega_1} H^{(1)}_{21}\frac{\lambda^2}{\omega_1+\omega_2} H^{(1)}_{21}\frac{\lambda^1}{\omega_1} H^{(1)}_{21}\,\eta \\ & -\eta\, H^{(1)}_{21}\frac{\lambda^1}{\omega_1} H^{(1)}_{21}\frac{\lambda^2}{\omega_1+\omega_2} H^{(1)}_{21}\frac{\lambda^3}{\omega_1+\omega_2+\omega_3} H^{(1)}_{21}\frac{\lambda^2}{\omega_1+\omega_2} H^{(1)}_{21}\frac{\lambda^1}{\omega_1} H^{(1)}_{21}\,\eta\,. \end{aligned} \tag{5.11}$$

The first structure is responsible for four double-box structures (figure B.3), 16 of 40 slashed box structures (figure B.5), six of 20 lower cross-box and six of 20 upper cross-box diagrams (figure B.6), while the second structure generates all 20 slashed cross-box diagrams (figure B.4), 24 of 40 slashed box diagrams and two of each cross-box diagrams.

The last structure, diagrams with exactly one intermediate only nucleon state, mainly contributes to the cross-box structure (each 12 of 20) and also to the double-box structure (eight

of 20).

$$
\begin{aligned}
V^{(4)}_{NN_{0,3}} =& \frac{1}{2}\left(\eta\, H^{(1)}_{21}\,\frac{\lambda^1}{\omega_1^2}\,H^{(1)}_{21}\,\eta\, H^{(1)}_{21}\,\frac{\lambda^1}{\omega_1}\,H^{(1)}_{21}\,\frac{\lambda^2}{\omega_1+\omega_2}\,H^{(1)}_{21}\,\frac{\lambda^1}{\omega_1}\,H^{(1)}_{21}\,\eta\right. \\
&+\eta\, H^{(1)}_{21}\,\frac{\lambda^1}{\omega_1}\,H^{(1)}_{21}\,\eta\, H^{(1)}_{21}\,\frac{\lambda^1}{\omega_1^2}\,H^{(1)}_{21}\,\frac{\lambda^2}{\omega_1+\omega_2}\,H^{(1)}_{21}\,\frac{\lambda^1}{\omega_1}\,H^{(1)}_{21}\,\eta \\
&+\eta\, H^{(1)}_{21}\,\frac{\lambda^1}{\omega_1}\,H^{(1)}_{21}\,\eta\, H^{(1)}_{21}\,\frac{\lambda^1}{\omega_1}\,H^{(1)}_{21}\,\frac{\lambda^2}{(\omega_1+\omega_2)^2}\,H^{(1)}_{21}\,\frac{\lambda^1}{\omega_1}\,H^{(1)}_{21}\,\eta \\
&\left.+\eta\, H^{(1)}_{21}\,\frac{\lambda^1}{\omega_1}\,H^{(1)}_{21}\,\eta\, H^{(1)}_{21}\,\frac{\lambda^1}{\omega_1}\,H^{(1)}_{21}\,\frac{\lambda^2}{\omega_1+\omega_2}\,H^{(1)}_{21}\,\frac{\lambda^1}{\omega_1^2}\,H^{(1)}_{21}\,\eta\right) + h.c.\,.
\end{aligned}
\tag{5.12}
$$

5.3.2 Potential with one seagull vertex

The potential corresponding to the terms with explicitly one seagull vertex are generated by all possible permutation of the three topologies in figure 5.3.

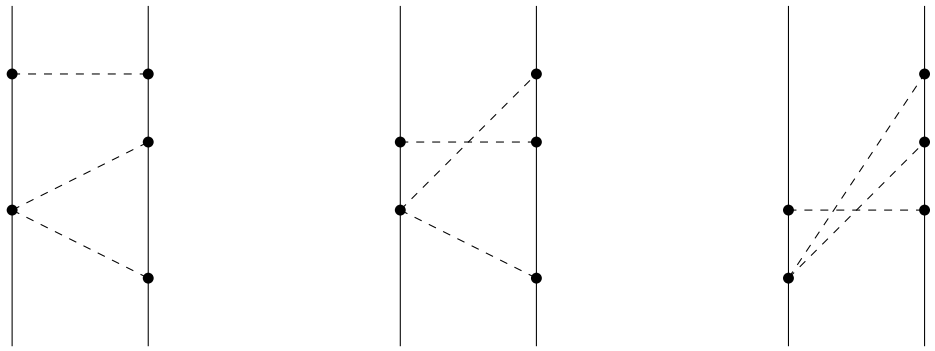

(a) Diagrams with no crossed pion lines

(b) Diagrams with a crossed pion line

(c) Diagrams with two crossed pion lines

Figure 5.3: Diagrams with explicitly one seagull vertex contributing to the effective unitary nucleon-nucleon potential at chiral order $\nu = 4$. To be complete, hermitian conjugated diagrams and diagrams with exchanged nucleon lines correspond to a similar but different structure.

The operator structure and the diagrams are organized such that the seagull vertex is at the first, second, ..., fifth position. Combining all three topologies one finds five times 24 diagrams (see section B.2.2).

For the seagull vertex at the initial position one finds

$$
\begin{aligned}
V^{(4)}_{NN_{1,1}} =& -\frac{1}{2}\left(\eta\, H^{(1)}_{21}\,\frac{\lambda^1}{\omega_1^2}\,H^{(1)}_{21}\,\eta\, H^{(1)}_{21}\,\frac{\lambda^1}{\omega_1}\,H^{(1)}_{21}\,\frac{\lambda^2}{\omega_1+\omega_2}\,H^{(2)}_{22}\,\eta\right. \\
&+\eta\, H^{(1)}_{21}\,\frac{\lambda^1}{\omega_1}\,H^{(1)}_{21}\,\eta\, H^{(1)}_{21}\,\frac{\lambda^1}{\omega_1^2}\,H^{(1)}_{21}\,\frac{\lambda^2}{\omega_1+\omega_2}\,H^{(2)}_{22}\,\eta \\
&\left.+\eta\, H^{(1)}_{21}\,\frac{\lambda^1}{\omega_1}\,H^{(1)}_{21}\,\eta\, H^{(1)}_{21}\,\frac{\lambda^1}{\omega_1}\,H^{(1)}_{21}\,\frac{\lambda^2}{(\omega_1+\omega_2)^2}\,H^{(2)}_{22}\,\eta\right) \\
&+\eta\, H^{(1)}_{21}\,\frac{\lambda^1}{\omega_1}\,H^{(1)}_{21}\,\frac{\lambda^2}{\omega_1+\omega_2}\,H^{(1)}_{21}\,\frac{\lambda^1}{\omega_1}\,H^{(1)}_{21}\,\frac{\lambda^2}{\omega_1+\omega_2}\,H^{(2)}_{22}\,\eta \\
&+\eta\, H^{(1)}_{21}\,\frac{\lambda^1}{\omega_1}\,H^{(1)}_{21}\,\frac{\lambda^2}{\omega_1+\omega_2}\,H^{(1)}_{21}\,\frac{\lambda^3}{\omega_1+\omega_2+\omega_3}\,H^{(1)}_{21}\,\frac{\lambda^2}{\omega_1+\omega_2}\,H^{(2)}_{22}\,\eta\,,
\end{aligned}
\tag{5.13}
$$

for the seagull at second position the result is

$$
\begin{aligned}
V^{(4)}_{NN_{1,2}} = -\frac{1}{2}\Bigg(& \eta\, H^{(1)}_{21}\, \frac{\lambda^1}{\omega_1^2}\, H^{(1)}_{21}\, \eta\, H^{(1)}_{21}\, \frac{\lambda^1}{\omega_1}\, H^{(2)}_{22}\, \frac{\lambda^1}{\omega_1}\, H^{(1)}_{21}\, \eta \\
& + \eta\, H^{(1)}_{21}\, \frac{\lambda^1}{\omega_1}\, H^{(1)}_{21}\, \eta\, H^{(1)}_{21}\, \frac{\lambda^1}{\omega_1^2}\, H^{(2)}_{22}\, \frac{\lambda^1}{\omega_1}\, H^{(1)}_{21}\, \eta \\
& + \eta\, H^{(1)}_{21}\, \frac{\lambda^1}{\omega_1}\, H^{(1)}_{21}\, \eta\, H^{(1)}_{21}\, \frac{\lambda^1}{\omega_1}\, H^{(2)}_{22}\, \frac{\lambda^1}{\omega_1^2}\, H^{(1)}_{21}\, \eta \Bigg) \\
& + \eta\, H^{(1)}_{21}\, \frac{\lambda^1}{\omega_1}\, H^{(1)}_{21}\, \frac{\lambda^2}{\omega_1+\omega_2}\, H^{(1)}_{21}\, \frac{\lambda^1}{\omega_1}\, H^{(2)}_{22}\, \frac{\lambda^1}{\omega_1}\, H^{(1)}_{21}\, \eta \\
& + \eta\, H^{(1)}_{21}\, \frac{\lambda^1}{\omega_1}\, H^{(1)}_{21}\, \frac{\lambda^2}{\omega_1+\omega_2}\, H^{(1)}_{21}\, \frac{\lambda^3}{\omega_1+\omega_2+\omega_3}\, H^{(2)}_{22}\, \frac{\lambda^1}{\omega_1}\, H^{(1)}_{21}\, \eta\,,
\end{aligned}
\tag{5.14}
$$

for the seagull at the middle position one obtains

$$
\begin{aligned}
V^{(4)}_{NN_{1,3}} = \frac{1}{2}\Bigg(& \eta\, H^{(1)}_{21}\, \frac{\lambda^1}{\omega_1}\, H^{(1)}_{21}\, \frac{\lambda^2}{\omega_1+\omega_2}\, H^{(2)}_{22}\, \frac{\lambda^2}{\omega_1+\omega_2}\, H^{(1)}_{21}\, \frac{\lambda^1}{\omega_1}\, H^{(1)}_{21}\, \eta \\
& - \eta\, H^{(1)}_{21}\, \frac{\lambda^1}{\omega_1^2}\, H^{(1)}_{21}\, \frac{\lambda^2}{\omega_1+\omega_2}\, H^{(2)}_{22}\, \eta\, H^{(1)}_{21}\, \frac{\lambda^1}{\omega_1}\, H^{(1)}_{21}\, \eta \\
& - \eta\, H^{(1)}_{21}\, \frac{\lambda^1}{\omega_1}\, H^{(1)}_{21}\, \frac{\lambda^2}{(\omega_1+\omega_2)^2}\, H^{(2)}_{22}\, \eta\, H^{(1)}_{21}\, \frac{\lambda^1}{\omega_1}\, H^{(1)}_{21}\, \eta \\
& - \eta\, H^{(1)}_{21}\, \frac{\lambda^1}{\omega_1}\, H^{(1)}_{21}\, \frac{\lambda^2}{\omega_1+\omega_2}\, H^{(2)}_{22}\, \eta\, H^{(1)}_{21}\, \frac{\lambda^1}{\omega_1^2}\, H^{(1)}_{21}\, \eta \Bigg) + h.c.\,,
\end{aligned}
\tag{5.15}
$$

and last but not least for the seagull vertex at fourth and fifth position one gets

$$
\begin{aligned}
V^{(4)}_{NN_{1,4}} &= V^{(4)\,\dagger}_{NN_{1,2}} \\
V^{(4)}_{NN_{1,1}} &= V^{(4)\,\dagger}_{NN_{1,5}}\,.
\end{aligned}
\tag{5.16}
$$

At this point one could observe that structures containing at least one pion in each intermediate step are positive and all other structures are multiplied by $-1/2$.

5.3.3 Potential with two seagull vertices

The operator structure containing two seagull vertices at order $\nu = 4$ causes two different topologies (figure 5.4).

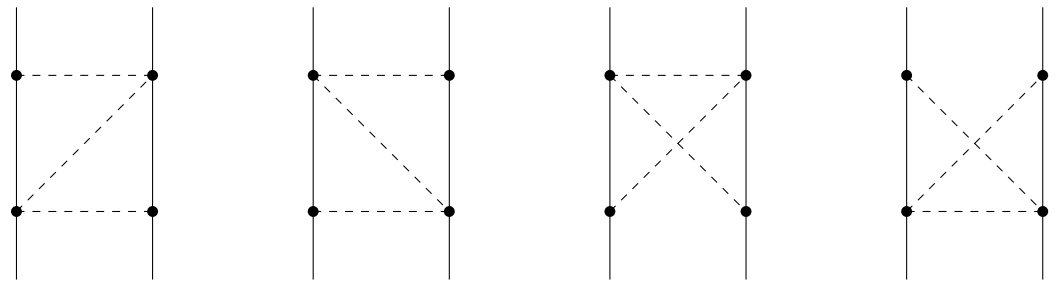

(a) Z diagram **(b)** Mirrored Z diagram **(c)** X-bar diagram **(d)** Conjugated X-bar diagram

Figure 5.4: Diagrams with two seagull vertices contributing to the effective unitary nucleon-nucleon potential at chiral order $\nu = 4$.

At this order one obtains 24 diagrams (figure B.12) corresponding to the following structure:

$$
\begin{aligned}
V^{(4)}_{NN_3} = \frac{1}{2}\Bigg(&\eta\, H^{(1)}_{21}\,\frac{\lambda^1}{\omega_1^2}\,H^{(1)}_{21}\,\eta\, H^{(2)}_{22}\,\frac{\lambda^2}{\omega_1+\omega_2}\,H^{(2)}_{22}\,\eta + \eta\, H^{(1)}_{21}\,\frac{\lambda^1}{\omega_1}\,H^{(1)}_{21}\,\eta\, H^{(2)}_{22}\,\frac{\lambda^2}{(\omega_1+\omega_2)^2}\,H^{(2)}_{22}\,\eta \\
&- \eta\, H^{(1)}_{21}\,\frac{\lambda^1}{\omega_1}\,H^{(2)}_{22}\,\frac{\lambda^1}{\omega_1}\,H^{(2)}_{22}\,\frac{\lambda^1}{\omega_1}\,H^{(1)}_{21}\,\eta \\
&- \eta\, H^{(1)}_{21}\,\frac{\lambda^1}{\omega_1}\,H^{(2)}_{22}\,\frac{\lambda^3}{\omega_1+\omega_2+\omega_3}\,H^{(2)}_{22}\,\frac{\lambda^1}{\omega_1}\,H^{(1)}_{21}\,\eta \\
&- \eta\, H^{(2)}_{22}\,\frac{\lambda^2}{\omega_1+\omega_2}\,H^{(1)}_{21}\,\frac{\lambda^1}{\omega_1}\,H^{(1)}_{21}\,\frac{\lambda^2}{\omega_1+\omega_2}\,H^{(2)}_{22}\,\eta \\
&-\eta\, H^{(2)}_{22}\,\frac{\lambda^2}{\omega_1+\omega_2}\,H^{(1)}_{21}\,\frac{\lambda^3}{\omega_1+\omega_2+\omega_3}\,H^{(1)}_{21}\,\frac{\lambda^2}{\omega_1+\omega_2}\,H^{(2)}_{22}\,\eta\Bigg) \\
&- \eta\, H^{(1)}_{21}\,\frac{\lambda^1}{\omega_1}\,H^{(1)}_{21}\,\frac{\lambda^2}{\omega_1+\omega_2}\,H^{(2)}_{22}\,\frac{\lambda^2}{\omega_1+\omega_2}\,H^{(2)}_{22}\,\eta \\
&- \eta\, H^{(1)}_{21}\,\frac{\lambda^1}{\omega_1}\,H^{(2)}_{22}\,\frac{\lambda^1}{\omega_1}\,H^{(1)}_{21}\,\frac{\lambda^2}{\omega_1+\omega_2}\,H^{(2)}_{22}\,\eta \\
&- \eta\, H^{(1)}_{21}\,\frac{\lambda^1}{\omega_1}\,H^{(2)}_{22}\,\frac{\lambda^3}{\omega_1+\omega_2+\omega_3}\,H^{(1)}_{21}\,\frac{\lambda^2}{\omega_1+\omega_2}\,H^{(2)}_{22}\,\eta + h.c.\,.
\end{aligned}
\tag{5.17}
$$

6 Consistency of nuclear potential in the limit of large-N_c

As mentioned before, to verify the consistency of the nuclear potential in the limit of large-N_c, one has to compute the potential using the Hartree Hamiltonian from a QCD point of view and compare this potential with the corresponding χPT result. Since the QCD predictions inhibit the leading order N_c scaling, one can say that the predictions are consistent, if the large-N_c scaling of the chiral potential is equal or smaller than the QCD prediction at leading order.

The main difference in both formalism is the following: while the large-N_c scaling of QCD potential is directly computed by the symmetries, e.g. the spin, isospin and spin-isospin operators J, I and G, the large-N_c scaling of the χPT potential is dictated by the physical quantities like the axial coupling g_A, the pion decay constant f_π and the commutator structure of spin-isospin operators X. This is the case since for the effective unitary chiral potential, one has to explicitly insert states to overcome the nucleonic and mesonic projection operators at each step. Therefore commutators of spin-isospin operators will be essential to guarantee the consistency of both predictions.

6.1 Consistency at leading chiral order

At leading chiral order the potential is proportional to two one-pion vertices (equation (5.5)). Since the one-pion vertex is proportional to X^{ia}, the most general potential corresponds to

$$V_{NN}^{(0)} \propto v^{i_1,i_2}\, X_1^{i_1 a} X_2^{i_2 a} \leftrightarrow V_\sigma^1\, X_1 \cdot X_2 + V_T^1 \left(3 \left(X_1^{ia} \cdot q^i\right) \left(X_2^{ja} \cdot q^j\right) - X_1 \cdot X_2\right) . \tag{6.1}$$

Thus, this amplitude contributes to either the central potential with $I = 1 = J$ or the tensor potential also with $I = 1 = J$, both scaling as N_c.

The direct computation in large-N_c results in

$$V_{NN}^{(0)} = -\frac{g_A^2}{4 f_\pi^2} \frac{X_1^{ia} X_2^{ja}}{\vec{q}^{\,2} + m_\pi^2} q^i q^j \sim \frac{N_c^2}{N_c} , \tag{6.2}$$

which directly proofs that the chiral version and the according QCD version of the nucleon-nucleon potential have the same large-N_c scaling at leading chiral order.

6.2 Consistency at next to leading order

To organize the NLO corresponding to two pion exchanges ($\nu = 2$), the analysis is organized in three sections corresponding to the according operator structure (section 5.2).

6.2.1 Potential without seagull vertices

Checking the dimension of the couplings, this potential scales as $g_A^4/f_\pi^4 \sim N_c^2$, which is obviously a contradiction. To resolve this problem, the amplitude computed by the unitary

transformation ansatz has to generate a commutator of spin-isospin operators. By summing over all box and cross-box diagrams one obtains

$$V^{(2)}_{NN_0} \propto \frac{g_A^4}{f_\pi^4} \int \mathrm{d}q_1^3 \int \mathrm{d}q_2^3 \, \frac{\omega_1^2+\omega_1\omega_2+\omega_2^2}{\omega_1^3\omega_2^3(\omega_1+\omega_2)} \, q_1^{i_1} q_1^{j_1} q_2^{i_2} q_2^{j_2} \, X_1^{i_2 b} X_1^{i_1 a} \left[X_2^{j_1 a} \, , \, X_2^{j_2 b} \right] \delta^{(3)}\left(\vec{q}-\vec{q}_1-\vec{q}_2\right) . \tag{6.3}$$

The ω_i are the energies of corresponding pions $\omega_i := \sqrt{q_i^2+m_\pi^2}$.

The appearing commutator is a non-trivial result obtained by cancellations of box and cross-box diagrams. Also, for commutators to vanish in large-N_c QCD, one has to explicitly allow Δ-resonances as intermediate states (see 4.3.1). This was already observed by [Banerjee et al., 2002].

Since the energy prefactor is symmetric in the momenta q_1 and q_2 one can interchange the momenta (substitution), relabel the spin components ($i_1 \leftrightarrow i_2$,$j_1 \leftrightarrow j_2$) and finally relabel the isospin components (a,b) to obtain

$$\begin{aligned} q_1^{i_1} q_1^{j_1} q_2^{i_2} q_2^{j_2} X_1^{i_2 b} X_1^{i_1 a} \left[X_2^{j_1 a} \, , \, X_2^{j_2 b} \right] &= q_2^{i_1} q_2^{j_1} q_1^{i_2} q_1^{j_2} X_1^{i_2 a} X_1^{i_1 b} \left[X_2^{j_1 b} \, , \, X_2^{j_2 a} \right] \\ &= q_1^{i_1} q_1^{j_1} q_2^{i_2} q_2^{j_2} X_1^{i_1 b} X_1^{i_2 a} \left[X_2^{j_2 a} \, , \, X_2^{j_2 b} \right] \\ &= -q_1^{i_1} q_1^{j_1} q_2^{i_2} q_2^{j_2} X_1^{i_1 a} X_1^{i_2 b} \left[X_2^{j_1 a} \, , \, X_2^{j_2 b} \right] . \end{aligned} \tag{6.4}$$

Therefore the potential effectively scales as

$$V^{(2)}_{NN_0} \propto \frac{g_A^4}{f_\pi^4} \left[X_1^{i_2 b} \, , \, X_1^{i_1 a} \right] \left[X_2^{j_1 a} \, , \, X_2^{j_2 b} \right] \sim \frac{1}{N_c^2} \, . \tag{6.5}$$

Because the spin-isospin nucleonic matrix elements of contracted $SU(4)$ operators correspond to the ordinary $SU(4)$ commutation relations at leading order in N_c (see (4.57))

$$\left[G^{ia} \, , \, G^{jb} \right] = \frac{i}{4} \left(\delta^{ab} \epsilon^{ijk} J^k + \delta^{ij} \epsilon^{abc} I^c \right) , \tag{6.6}$$

the above potential amplitude (for nucleons only) should correspond to

$$V^{(2)}_{NN_0} \propto f^{i_1 i_2 j_1 j_2} \left(3\epsilon^{i_1 i_2 i} \epsilon^{j_1 j_2 j} J_1^i J_2^j + 2\delta^{i_1 i_2} \delta^{j_1 j_2} I_1 \cdot I_2 \right) \propto I_1 \cdot I_2 \, , \tag{6.7}$$

since the coefficients are symmetric in ($i_1 \leftrightarrow i_2$,$j_1 \leftrightarrow j_2$). Thus the leading order QCD prediction $1/N_c$ (for V_0^1) gets confirmed by the actual χPT-scaling $1/N_c^2$.

6.2.2 Potential with a seagull vertex

The amplitude for this part of the potential is given by

$$V^{(2)}_{NN_1} \propto \frac{g_A^2}{f_\pi^4} \int \mathrm{d}q_1^3 \int \mathrm{d}q_2^3 \, \frac{1}{\omega_1\omega_2(\omega_1+\omega_2)} \, q_1^i q_2^j \, \epsilon^{abc} \left(X_1^{bj} X_1^{ai} I_2^c + I_1^c X_2^{bj} X_2^{ai} \right) \delta^{(3)}\left(\vec{q}-\vec{q}_1-\vec{q}_2\right) . \tag{6.8}$$

Again, since the momenta structure is symmetric, the spin components (i,j) are symmetric as well. Because the isospin structure is anti-symmetric in (a,b), the spin-isospin operators are effectively expressed by a commutator

$$\begin{aligned} V^{(2)}_{NN_1} &\propto \frac{g_A^2}{f_\pi^4} \epsilon^{abc} v^{ij} \left(\left[X_1^{bj} \, , \, X_1^{ai} \right] I_2^c + I_1^c \left[X_2^{bj} \, , \, X_2^{ai} \right] \right) \overset{\chi_{\mathrm{PT}}}{\sim} \frac{1}{N_c^2} \\ &\propto v^{ij} \delta^{ij} I_1 \cdot I_2 \overset{\mathrm{QCD}}{\lesssim} \frac{1}{N_c} \, , \end{aligned} \tag{6.9}$$

which is consistent with the QCD prediction.

6.2.3 Potential with two seagull vertices

The potential with two seagull vertices, the football diagrams, are trivially consistent.

In the chiral case, the couplings scale as $1/f_\pi^4 \sim 1/N_c^2$ and makes its only contribution to V_0^1 which is predicted to be at $1/N_c$ at leading order.

Thus, the large-N_c predictions by KSM are consistent with the explicit computations in χPT at chiral order $\nu = 2$ for pionic exchanges.

Note that the chiral potential at order $\nu = 2$ scales as $1/N_c^2$ in total. Thus the chiral leading order dominates the NLO by N_c^3.

6.3 General consistency conditions

Analogously to the previous order, it is useful to separate the diagrams by the number of seagull vertices. At a specific number of seagull vertices N_2, the large-N_c scaling is trivially consistent.

An amplitude generated by N_1 one-pion vertices and N_2 two-pion vertices scales at leading order in N_c as following

$$\begin{aligned} V_{NN}^{(\nu)} &= v \cdot \left\langle N'; N \left| \left(\frac{g_A}{f_\pi} X\right)^{N_1} \cdot \left(\frac{1}{f_\pi^2} I\right)^{N_2} \right| N'; N \right\rangle \\ &\sim N_c^{N_1/2-N_2} \left(v_1 \cdot \langle N \,|\, G \,|\, N\rangle \cdot \langle N' \,|\, G \,|\, N'\rangle\right)^{n_1} \\ &\quad \times \left(v_2 \cdot \langle N \,|\, I \,|\, N\rangle \cdot \langle N' \,|\, I \,|\, N'\rangle\right)^{n_2} \\ &\quad \times \prod_{i=1}^{n_3} \left(v_{3,i} \cdot \langle N \,|\, G \cdot I^{a_i} \cdot G \,|\, N\rangle \cdot \left\langle N' \left| I^{a_i+1} \right| N' \right\rangle\right) \\ &\quad \times \prod_{j=1}^{n_4} \left(v_{3,j} \cdot \left\langle N \left| G \cdot I^{b_j} \right| N \right\rangle \cdot \left\langle N' \left| I^{b_j} \cdot G \right| N' \right\rangle\right) + (N' \leftrightarrow N)\,. \end{aligned}$$

The first possible contraction corresponds to one-pion exchanges. The second contraction corresponds to pion loops, the third structure forms M-like diagrams while the last structure corresponds to N-like pion shapes (see figure 6.1).

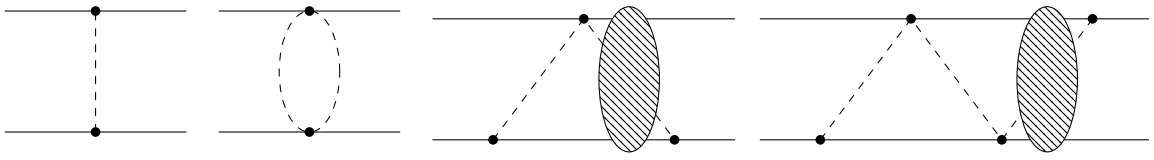

(a) One-pion exchange **(b)** Pion loop **(c)** M-like structure **(d)** N-like structure

Figure 6.1: Possible structures corresponding to topological different operator contractions. The blob in figure 6.1c and 6.1d denotes insertions of multiple two-seagull vertices contracted such that the pion line is not interrupted.

As discussed before, a combination of those structures may correspond to commutators of spin-isospin operators. At this point it is useful to take a closer look at the diagrams which can generate such commutators. This far, the commutator structure generated by the potential where caused by two different processes:

(1) when computing the full amplitude, the energy-denominator structure results in an effective minus sign between two pairs of commuted operators and

(2) the anti-symmetric tensor structure in isospin space combined with a symmetric structure in spin space of just one diagram directly reduces the product of two operators to a commutator.

Note that the first effect can also result in a double commutator structure if sufficiently enough spin-isospin operators are available. This was demonstrated for the chiral order $\nu = 2$ without seagull vertices (equation (6.5)).

The second effect can only be caused by the M-like vertex structure (see figure 6.1c). If the isospin contraction of both spin-isospin operators is anti-symmetrically, one generates a commutator, since the partial amplitude is of the following form

$$\begin{aligned} V_{NN_M}^{(N)} &\propto \left(\prod_{n=1}\int \mathrm{d}^3 q_n\right) f\left(\left\{\vec{q}_n^{\,2}\right\}\right)\ \delta^{(3)}\left(\vec{q}-\sum_{n=1}\vec{q}_n\right)\ q_1^i q_2^j\ X_1^{ia}\, X_1^{jb} \\ &= \left(\prod_{n=2}\int \mathrm{d}^3 q_n\right) f\left(\left\{\vec{q}_n^{\,2}\right\}, \tilde{\vec{q}}^{\,2}, \vec{q}_2^{\,2}, \tilde{\vec{q}}\cdot\vec{q}_2\right)\ (\tilde{q}-q_2)^i q_2^j\ X_1^{ia}\, X_1^{jb}\,, \end{aligned} \tag{6.10}$$

where $\tilde{\vec{q}} = \vec{q} - \sum_{n=3}\vec{q}_n$. Since $\tilde{\vec{q}}$ is the only momentum effectively affecting $\vec{q}_2$ in this integral, the result has to be of the following form

$$V_{NN_M}^{(N)} \propto \left(\prod_{n=3}\int \mathrm{d}^3 q_n\right)\left(f_1\left(\left\{\vec{q}_n^{\,2}\right\}, \tilde{\vec{q}}^{\,2}\right)\ \tilde{q}^i\tilde{q}^j + f_2\left(\left\{\vec{q}_n^{\,2}\right\}, \tilde{\vec{q}}^{\,2}\right)\ \tilde{q}^2\delta^{ij}\right)\ X_1^{ia}\, X_1^{jb}\,, \tag{6.11}$$

which is obviously symmetric in the spin components. Thus, each M-like structure, which is anti-symmetric in the isospin components, directly generates a commutator of spin-isospin mixing operators. Note that not all M-like structures are anti-symmetric in isospin space—in general this is depending on the number of inserted seagull vertices.

6.4 Potential at next to next to leading order

Using equation (4.81) and the diagram structure shown in section 5.3.1 one can directly identify the structure with a possible violation of the KSM counting rules.

The two-seagull structures correspond to the N-like pion-line structure. Thus one gets

$$V_{NN_N}^{(4)} \sim N_c^{\frac{4}{2}+1-2\cdot 2-2C} \lesssim \frac{1}{N_c}\,, \tag{6.12}$$

which automatically fulfills the KSM predictions, independent of the explicit contribution to the spin-isospin structure of the potential[1].

The potential with only one seagull vertex corresponds to diagrams with one one-pion exchange and a M-like structure which is anti-symmetric in isospin space. The according consistency condition demands

$$V_{NN_M}^{(4)} \sim N_c^{\frac{4}{2}+1-2\cdot 1-2C} \lesssim \frac{N_c}{N_c^{2C}}\,, \tag{6.13}$$

which is automatically fulfilled only if the amplitude is proportional to at least one commutator structure. The first commutator is directly generated by the anti-symmetric seagull structure as discussed in the previous section. Thus, also the potential with just one seagull vertex at chiral order $\nu = 4$ satisfies the KSM counting rules.

[1] For the same reasons also the potential with three seagull vertices, which is not shown because it is used for renormalizing the two-pion amplitudes, scales as $1/N_c^3$.

Last but not least one has to analyze the consistency of the potential structure without seagull vertices which demands at least one commutator if it makes contributions with $I = J$ or two commutators if it contributes to exchanges with $I \neq J$ at leading order.

$$N_c^{3-2C} \lesssim \begin{cases} N_c & , \quad I = J \\ \frac{1}{N_c} & , \quad I \neq J \end{cases} \tag{6.14}$$

6.4.1 Potential without seagull vertices

As mentioned before, for the effective potential at NNLO to be consistent with the KSM counting rules, the structure without seagull vertices needs at least one commutator of spin-isospin mixing operators X. Since a single diagram in general has no anti-symmetrical tensor structures as in the previous case, the only way for obtaining commutators is given by summing up the whole amplitude and obtaining a relative minus signs caused by the energy structure.

Because one has to compute several diagrams, it is again useful to gather terms corresponding to a similar operator structure. To systematically compute the amplitudes, the following procedure is used: the first vertex on the first nucleon line (left line) will emit or absorb the pion with isospin label a and momentum component $q_1^{i_1}$. Accordingly, since only one-pion operators are involved, the corresponding vertex is proportional to $X_1^{i_1 a} q_1^{i_1}$. Since this pion has to be absorbed by another vertex on the second nucleon line, the corresponding operator will be denoted by $X_2^{j_1 a} q_1^{j_1}$, which is in general not on the first position of the second nucleon line. This procedure is repeated until all vertices are labeled. An example amplitude is given by figure 6.2.

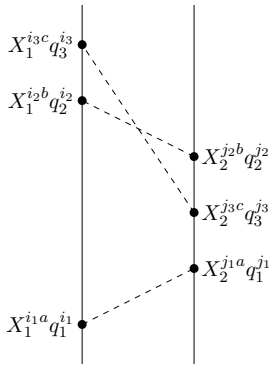

$$\propto \frac{1}{2}\left(\frac{1}{\omega_1^2\omega_2\omega_3^3(\omega_2+\omega_3)^2} + \frac{2}{\omega_1^2\omega_2\omega_3^4(\omega_2+\omega_3)} + \frac{1}{\omega_1^3\omega_2\omega_3^3(\omega_2+\omega_3)}\right) \times X_1^{i_3 c} X_1^{i_2 b} X_1^{i_1 a} X_2^{j_2 b} X_2^{j_3 c} X_2^{j_1 a} q_1^{i_1} q_2^{i_2} q_3^{i_3} q_1^{j_1} q_2^{j_2} q_3^{j_3} \,.$$

Figure 6.2: An example contribution to the upper cross-box topology.

Using this formalism, the three operators of the first nucleon will always be in the same order, while the operators for the second nucleon will be ordered differently for each different diagram structure. Note that the energy structure can vary even if the spin-isospin structure stays the same.

To identify the spin-isospin dependence of the overall amplitude at leading order in N_c, one can concentrate on the spin-isospin structure generated by the double-box diagrams (figure 5.2a)

$$V^{(4)}_{NN_{\text{Double-box}}} \propto q_1^{i_1} q_2^{i_2} q_3^{i_3} q_1^{j_1} q_2^{j_2} q_3^{j_3} X_1^{i_3 c} X_1^{i_2 b} X_1^{i_1 a} X_2^{j_3 c} X_2^{j_2 b} X_2^{j_1 a} \,, \tag{6.15}$$

because any other diagram can be expressed by this structure plus corrections at order $1/N_c^2$. One can verify this statement by commuting each structure until it corresponds to the double-box structure. The commutators of spin-isospin operators are at order $1/N_c^2$ and

therefore do not contribute to the leading order

$$X_1^{i_3c}X_1^{i_2b}X_1^{i_1a}X_2^{j_2b}X_2^{j_3c}X_2^{j_1a} = X_1^{i_3c}X_1^{i_2b}X_1^{i_1a}\left(X_2^{j_3c}X_2^{j_2b}X_2^{j_1a} + \left[X_2^{j_2b}, X_2^{j_3c}\right]X_2^{j_1a}\right)$$
$$= X_1^{i_3c}X_1^{i_2b}X_1^{i_1a}X_2^{j_3c}X_2^{j_2b}X_2^{j_1a} + \mathcal{O}\left(\frac{1}{N_c^2}\right). \tag{6.16}$$

Thus, for the $1/N_c^2$ corrections, one also has to look at other operator structures. This is important since the overall potential scales as N_c^3 and therefore the corrections are effectively at order N_c.

To identify the spin-isospin dependence of each term, one has to reduce the six operator structure to one operator at each nucleon line. Hereby the correspondence of the contracted $SU(4)$ to the regular $SU(4)$ symmetry can be used to compute the contractions (see equation (4.28))

$$G^{ia}G^{jb} = \frac{1}{2}\left(\left\{G^{ia}, G^{jb}\right\} + \left[G^{ia}, G^{jb}\right]\right) \tag{6.17}$$
$$= \left(\frac{1}{4}\delta^{ij}\delta^{ab}\mathbb{1} - \frac{1}{2}\epsilon^{ijk}\epsilon^{abc}G^{kc}\right) + \frac{i}{2}\left(\epsilon^{ijk}\delta^{ab}J^k + \delta^{ij}\epsilon^{abc}I^c\right).$$

Therefore one also needs the reduction relations for spin and isospin operators

$$J^iG^{bj} = \frac{1}{2}\left(\delta^{ij}I^b + i\epsilon^{ijk}G^k\right) \qquad J^iJ^j = \frac{1}{4}\delta^{ij}\mathbb{1} + \frac{i}{2}\epsilon^{ijk}J^k \tag{6.18}$$
$$I^aG^{bj} = \frac{1}{2}\left(\delta^{ab}J^j + i\epsilon^{abc}G^c\right) \qquad I^aI^b = \frac{1}{4}\delta^{ab}\mathbb{1} + \frac{i}{2}\epsilon^{abc}I^c. \tag{6.19}$$

Relating this back to the contracted $SU(4)$ operators, one knows that the commutator of two X will be at order $1/N_c^2$. All other commutators should remain at the same order since they are well defined for the contracted $SU(4)$. Because there are no conditions on the anticommutators of spin-isospin operators X, one can use that they are at the same order as the operators themselves. Using this one can reduce the previous structure (6.15) to a sum of single operators

$$X_1^{i_3c}X_1^{i_2b}X_1^{i_1a} = \frac{1}{2}\left(\left\{X_1^{i_3c}, X_1^{i_2b}\right\} + \frac{1}{N_c^2}\left[X_1^{i_3c}, X_1^{i_2b}\right]\right)X_1^{i_1a} \tag{6.20}$$
$$= \frac{1}{4}\delta^{i_2i_3}\delta^{bc}X_1^{i_1a} - \frac{1}{2}\epsilon^{i_2i_3k}\epsilon^{bcd}X_1^{kd}X_1^{i_1a} + \frac{i}{2N_c^2}\left(\epsilon^{i_3i_2k}\delta^{bc}J^k + \delta^{i_2i_3}\epsilon^{cbd}I^d\right)X_1^{i_1a}$$
$$= \frac{1}{4}\left(\delta^{i_2i_3}\delta^{bc}X_1^{i_1a} + \epsilon^{i_2i_3k}\epsilon^{ki_1l}\epsilon^{bcd}\epsilon^{dae}X_1^{le}\right)$$
$$- \frac{1}{8}\epsilon^{i_1i_2i_3}\epsilon^{abc}\mathbb{1}_1 - \frac{i}{4N_c^2}\epsilon^{abc}\left(\delta^{i_1i_2}J_1^{i_3} - \delta^{i_1i_3}J_1^{i_2} + \delta^{i_2i_3}J_1^{i_1}\right)$$
$$- \frac{i}{4N_c^2}\epsilon^{i_1i_2i_3}\left(\delta^{ab}I_1^c - \delta^{ac}I_1^b + \delta^{bc}I_1^a\right)$$
$$- \frac{i}{4N_c^2}\left(\epsilon^{i_2i_3k}\delta^{bc}\epsilon^{ki_1l}X_1^{la} + \delta^{i_2i_3}\epsilon^{bcd}\epsilon^{dae}X_1^{i_1e}\right).$$

This directly helps to identify the structure of (6.15): as one can directly notice, each term corresponding to a spin-isospin operator is completely symmetric in two of three spin and isospin components (two Kronecker deltas), which is verified by the identity

$$\epsilon^{i_2i_3k}\epsilon^{ki_1l} = \delta^{i_1i_2}\delta^{l\,i_3} - \delta^{i_1i_3}\delta^{l\,i_2}. \tag{6.21}$$

Each term corresponding to an identity is completely anti-symmetric in its structure (two Levi-Civita symbols), each term corresponding to a spin operator contains a delta in its spin components but an epsilon in its isospin components and accordingly each isospin term a delta in isospin and an epsilon in spin.

When one wants to compute the full tensor structure for both nucleons, one has to contract the tensor components for both nucleon lines. The isospin indices are directly the same, while one has to use the symmetry of the momentum structure in spin components: the structure is independent in the three interchanges $(i_n \leftrightarrow j_n)$ individually. Thus, for contracting the lines, one can assume that $i_n = j_n$. Therefore it is only possible to contract operators of one kind with each other and accordingly one just gets operators with $I \neq J$ at order $1/N_c^4$:

$$X_1^{i_1 a} X_1^{i_2 b} X_1^{i_3 c} X_2^{j_1 a} X_2^{j_2 b} X_2^{j_3 c} \sim A_0 \left(\mathbb{1}_1 \mathbb{1}_2 + X_1 X_2\right) + \frac{A_4}{N_c^4} \left(X_1 X_2 + J_1 J_2 + I_1 I_2\right) . \tag{6.22}$$

Note that for this ordering of operators, it is not possible to get terms at order $1/N_c^2$.

From this computation one can conclude several facts:

(1) Even if one computes an operator structure which is not ordered according to (6.15) in the second nucleon operator structure, the only possible contribution to order $1/N_c^2$ is given by pairs of $X_1 \cdot X_2$. The other terms get canceled according to their prefactors.

(2) Commuting a six operator structure before reducing it is equal to dropping one of the anticommutators and thus also upholds the structure.

(3) Since commuting operators before reducing them directly reduces the order by $1/N_c^2$, the leading order amplitude can be brought to the form such that it corresponds to all energy denominators times the structure defined by equation (6.15).

Thus, if the leading order is vanishing ($A_0 = 0$), the leading order spin-isospin structure of the full potential amplitude has $I = J$ and scales as N_c which confirms the KSM counting at chiral order $\nu = 4$

$$V^{(4)}_{NN_{\text{Double Box}}} \sim A_0 \, N_c^3 \, \left(\mathbb{1}_1 \mathbb{1}_2 + X_1 X_2\right) + A_2 \, N_c \, X_1 \cdot X_2 + \frac{A_4}{N_c} \left(X_1 X_2 + J_1 J_2 + I_1 I_2\right) + \mathcal{O}\left(\frac{1}{N_c^3}\right) . \tag{6.23}$$

The amplitudes before ordering are given in the next paragraphs.

Double box diagrams

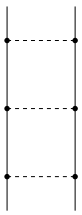

$$\begin{aligned}
\propto \quad & - X_1^{c i_3} X_1^{b i_2} X_1^{a i_1} X_2^{c j_3} X_2^{b j_2} X_2^{a j_1} \frac{q_1^{i_1} q_1^{j_1} q_2^{i_2} q_2^{j_2} q_3^{i_3} q_3^{j_3}}{\omega_1^4 \omega_2^3 \left(\omega_1 + \omega_2\right)^2 \omega_3^4 \left(\omega_2 + \omega_3\right)^2 \left(\omega_1 + \omega_2 + \omega_3\right)} \\
& \times \Big(\omega_1^5 \left(4\omega_2^3 + 9\omega_3\omega_2^2 + 4\omega_3^2\omega_2 + \omega_3^3\right) \\
& \quad + \omega_1^4 \left(12\omega_2^4 + 31\omega_3\omega_2^3 + 22\omega_3^2\omega_2^2 + 9\omega_3^3\omega_2 + 2\omega_3^4\right) \\
& \quad + \omega_1^3 \left(12\omega_2^5 + 37\omega_3\omega_2^4 + 39\omega_3^2\omega_2^3 + 24\omega_3^3\omega_2^2 + 9\omega_3^4\omega_2 + \omega_3^5\right) \\
& \quad + \omega_2\omega_1^2 \left(4\omega_2^5 + 17\omega_3\omega_2^4 + 34\omega_3^2\omega_2^3 + 39\omega_3^3\omega_2^2 + 22\omega_3^4\omega_2 + 4\omega_3^5\right) \\
& \quad + \omega_2^2\omega_3 \left(\omega_2 + \omega_3\right)^2 \omega_1 \left(2\omega_2^2 + 13\omega_3\omega_2 + 9\omega_3^2\right) \\
& \quad + 4\omega_2^3\omega_3^2 \left(\omega_2 + \omega_3\right)^3\Big) .
\end{aligned} \tag{6.24}$$

Crossed box diagrams

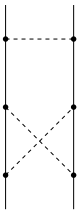

$$\propto \; 2X^{ci_3}X^{bi_2}X^{ai_1}X^{cj_3}X^{aj_1}X^{bj_2}\frac{q_1^{i_1}q_1^{j_1}q_2^{i_2}q_2^{j_2}q_3^{i_3}q_3^{j_3}}{\omega_1^4\omega_2^4\left(\omega_1+\omega_2\right)^2\omega_3^3\left(\omega_1+\omega_3\right)\left(\omega_2+\omega_3\right)^2\left(\omega_1+\omega_2+\omega_3\right)}$$

$$\begin{aligned}
&\times\left(\omega_1^6\left(\omega_2^3+3\omega_3\omega_2^2+4\omega_3^2\omega_2+2\omega_3^3\right)\right.\\
&\quad+\omega_1^5\left(3\omega_2^4+11\omega_3\omega_2^3+18\omega_3^2\omega_2^2+14\omega_3^3\omega_2+4\omega_3^4\right)\\
&\quad+\omega_1^4\left(4\omega_2^5+17\omega_3\omega_2^4+31\omega_3^2\omega_2^3+30\omega_3^3\omega_2^2+14\omega_3^4\omega_2+2\omega_3^5\right)\\
&\quad+\omega_2\omega_1^3\left(3\omega_2^5+16\omega_3\omega_2^4+32\omega_3^2\omega_2^3+33\omega_3^3\omega_2^2+18\omega_3^4\omega_2+4\omega_3^5\right)\\
&\quad+\omega_2^2\left(\omega_2+\omega_3\right)^2\omega_1^2\left(\omega_2^3+7\omega_3\omega_2^2+11\omega_3^2\omega_2+3\omega_3^3\right)\\
&\quad+2\omega_2^3\omega_3\left(\omega_2+\omega_3\right)^2\omega_1\left(\omega_2^2+4\omega_3\omega_2+2\omega_3^2\right)\\
&\quad\left.+2\omega_2^4\omega_3^2\left(\omega_2+\omega_3\right)^3\right)\,.
\end{aligned}\tag{6.25}$$

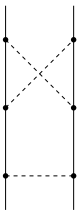

$$\propto \; 2X^{ci_3}X^{bi_2}X^{ai_1}X^{bj_2}X^{cj_3}X^{aj_1}\frac{q_1^{i_1}q_1^{j_1}q_2^{i_2}q_2^{j_2}q_3^{i_3}q_3^{j_3}}{\omega_1^3\omega_2^4\left(\omega_1+\omega_2\right)^2\omega_3^4\left(\omega_1+\omega_3\right)\left(\omega_2+\omega_3\right)^2\left(\omega_1+\omega_2+\omega_3\right)}$$

$$\begin{aligned}
&\times\left(\omega_1^5\left(2\omega_2^4+4\omega_3\omega_2^3+3\omega_3^2\omega_2^2+4\omega_3^3\omega_2+2\omega_3^4\right)\right.\\
&\quad+\omega_1^4\left(6\omega_2^5+16\omega_3\omega_2^4+17\omega_3^2\omega_2^3+18\omega_3^3\omega_2^2+14\omega_3^4\omega_2+4\omega_3^5\right)\\
&\quad+\omega_1^3\left(6\omega_2^6+22\omega_3\omega_2^5+32\omega_3^2\omega_2^4+33\omega_3^3\omega_2^3+30\omega_3^4\omega_2^2+14\omega_3^5\omega_2+2\omega_3^6\right)\\
&\quad+\omega_2\omega_1^2\left(2\omega_2^6+12\omega_3\omega_2^5+26\omega_3^2\omega_2^4+32\omega_3^3\omega_2^3+31\omega_3^4\omega_2^2+18\omega_3^5\omega_2+4\omega_3^6\right)\\
&\quad+\omega_2^2\omega_3\omega_1\left(2\omega_2^5+9\omega_3\omega_2^4+16\omega_3^2\omega_2^3+17\omega_3^3\omega_2^2+11\omega_3^4\omega_2+3\omega_3^5\right)\\
&\quad\left.+\omega_2^3\omega_3^2\left(\omega_2+\omega_3\right)^2\left(\omega_2^2+\omega_3\omega_2+\omega_3^2\right)\right)
\end{aligned}\tag{6.26}$$

Slashed box diagrams

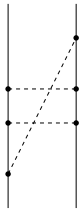

$$\propto \; -2X^{ci_3}X^{bi_2}X^{ai_1}X^{aj_1}X^{cj_3}X^{bj_2}\frac{q_1^{i_1}q_1^{j_1}q_2^{i_2}q_2^{j_2}q_3^{i_3}q_3^{j_3}}{\omega_1^4\omega_2^2\left(\omega_1+\omega_2\right)\omega_3^2\left(\omega_1+\omega_3\right)\left(\omega_2+\omega_3\right)^2\left(\omega_1+\omega_2+\omega_3\right)}$$

$$\begin{aligned}
&\times\left(\omega_1^3\left(2\omega_2^2+5\omega_3\omega_2+2\omega_3^2\right)\right.\\
&\quad+\omega_1^2\left(2\omega_2^3+7\omega_3\omega_2^2+7\omega_3^2\omega_2+2\omega_3^3\right)\\
&\quad+\left(\omega_2+\omega_3\right)^2\omega_1\left(\omega_2^2+5\omega_3\omega_2+\omega_3^2\right)\\
&\quad\left.+\omega_1^5+2\left(\omega_2+\omega_3\right)\omega_1^4+2\omega_2\omega_3\left(\omega_2+\omega_3\right)^3\right)\,.
\end{aligned}\tag{6.27}$$

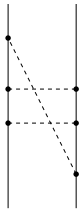

$$\propto \; -2X^{ci_3}X^{bi_2}X^{ai_1}X^{bj_2}X^{aj_1}X^{cj_3}\frac{q_1^{i_1}q_1^{j_1}q_2^{i_2}q_2^{j_2}q_3^{i_3}q_3^{j_3}}{\omega_1^2\omega_2^2\left(\omega_1+\omega_2\right)^2\omega_3^4\left(\omega_1+\omega_3\right)\left(\omega_2+\omega_3\right)\left(\omega_1+\omega_2+\omega_3\right)}$$

$$\begin{aligned}
&\times\left(+\omega_1^3\left(6\omega_2^2+7\omega_3\omega_2+2\omega_3^2\right)\right.\\
&\quad+\omega_1^2\left(6\omega_2^3+12\omega_3\omega_2^2+7\omega_3^2\omega_2+2\omega_3^3\right)\\
&\quad+\omega_1\left(2\omega_2^4+7\omega_3\omega_2^3+7\omega_3^2\omega_2^2+5\omega_3^3\omega_2+2\omega_3^4\right)\\
&\quad+\omega_3\left(\omega_2+\omega_3\right)^2\left(\omega_2^2+\omega_3^2\right)\\
&\quad\left.+\left(2\omega_2+\omega_3\right)\omega_1^4\right)\,.
\end{aligned}\tag{6.28}$$

Slashed cross-box diagrams

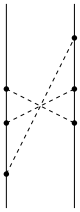

$$\propto \quad -2X^{ci_3}X^{bi_2}X^{ai_1}X^{aj_1}X^{bj_2}X^{cj_3}\frac{q_1^{i_1}q_1^{j_1}q_2^{i_2}q_2^{j_2}q_3^{i_3}q_3^{j_3}}{\omega_1^3\omega_2\left(\omega_1+\omega_2\right)^2\omega_3^3\left(\omega_2+\omega_3\right)^2\left(\omega_1+\omega_2+\omega_3\right)}$$
$$\times\left(\omega_1\left(3\omega_2^3+6\omega_3\omega_2^2+4\omega_3^2\omega_2+\omega_3^3\right)\right.$$
$$+\left(\omega_2+\omega_3\right)^2\left(\omega_2^2+\omega_3\omega_2+\omega_3^2\right)$$
$$\left.+\omega_1^4+\left(3\omega_2+\omega_3\right)\omega_1^3+\left(2\omega_2+\omega_3\right)^2\omega_1^2\right)\,. \tag{6.29}$$

Finding the commutators

From a naive point of view, if the KSM predicted N_c scaling was satisfied, after ordering each amplitude to the same operator structure, the factor corresponding to the sum over all energy denominators should be zero. However this is yet not the case.

Since the diagrams have been arranged to fit into a specific pattern, the amplitude is not completely symmetric in its momentum structure. In general, a difference of two specific energy structures times an operator structure might also correspond to a commutator of both operators. The following computation will be used later on to generate further commutators.

As an example, if the amplitude looks like the following structure times a function which is completely symmetric in $(q_1 \leftrightarrow q_2 \leftrightarrow q_3)$

$$X_1^{ci_3}X_1^{bi_2}X_1^{ai_1}X_2^{cj_3}X_2^{bj_2}X_2^{aj_1}q_1^{i_1}q_1^{j_1}q_2^{i_2}q_2^{j_2}q_3^{i_3}q_3^{j_3}\left(\omega_1^{n_1}\omega_2^{n_2}\omega_3^{n_3}-\omega_1^{n_2}\omega_2^{n_1}\omega_3^{n_3}\right)\,, \tag{6.30}$$

the structure can be brought to a form corresponding to a commutator. Relabeling the momenta $q_1 \leftrightarrow q_2$ for the left term is effectively equal to interchanging the spin indices of the momentum structure $(i_1 \leftrightarrow i_2)$ and $(j_1 \leftrightarrow j_2)$

$$=X_1^{ci_3}X_1^{bi_2}X_1^{ai_1}X_2^{cj_3}X_2^{bj_2}X_2^{aj_1}\left(q_1^{i_1}q_1^{j_1}q_2^{i_2}q_2^{j_2}-q_2^{i_1}q_2^{j_1}q_1^{i_2}q_1^{j_2}\right)q_3^{i_3}q_3^{j_3}\omega_1^{n_1}\omega_2^{n_2}\omega_3^{n_3}\,. \tag{6.31}$$

Since one sums over all indices, one can now relabel the indices $(i_1 \leftrightarrow i_2)$, $(j_1 \leftrightarrow j_2)$ and $(a \leftrightarrow b)$ for the second structure resulting in

$$=\left(X_1^{ci_3}X_1^{bi_2}X_1^{ai_1}X_2^{cj_3}X_2^{bj_2}X_2^{aj_1}-X_1^{ci_3}X_1^{ai_1}X_1^{bi_2}X_2^{cj_3}X_2^{aj_1}X_2^{bj_2}\right)q_1^{i_1}q_1^{j_1}q_2^{i_2}q_2^{j_2}q_3^{i_3}q_3^{j_3}\omega_1^{n_1}\omega_2^{n_2}\omega_3^{n_3}\,, \tag{6.32}$$

which, as discussed before, is proportional to a structure with at least one commutator and therefore scaling as $1/N_c^2$.

To use the relabeling of momenta to symmeterize the full amplitude, the full amplitude has to be brought to the form

$$\mathcal{M}\propto\sum_{n_1,n_2,n_3}q_1^{i_1}q_1^{j_1}q_2^{i_2}q_2^{j_2}q_3^{i_3}q_3^{j_3}\omega_1^{n_1}\omega_2^{n_2}\omega_3^{n_3}f(\omega_1,\omega_2,\omega_3)(X_1X_1X_1X_2X_2X_2)^{I_{n_1n_2n_3}}\,, \tag{6.33}$$

where f is completely symmetric in the interchange of each ω_i. The full amplitude is proportional to a delta function which inhibits those momenta but may differ in the sign, but since the full amplitude is also quadratic in each momentum, one can simply interchange the sign of the momenta without changing the amplitude. Finally Multiplying the amplitude with the full denominator

$$\omega_1^4\omega_2^4\left(\omega_1+\omega_2\right)^2\omega_3^4\left(\omega_1+\omega_3\right)^2\left(\omega_2+\omega_3\right)^2\left(\omega_1+\omega_2+\omega_3\right)\,, \tag{6.34}$$

brings the amplitude on the desired form (6.33) ($f \propto 1$).

Since the full potential is at order $[\omega]^{-8}$ and the previous denominator is at order $[\omega]^{19}$, the sum over all n_i has to be

$$n_1 + n_2 + n_3 = 11\,. \tag{6.35}$$

In the following section all terms which are permutations of (n_1, n_2, n_3) are substituted such that $n_3 \geq n_2 \geq n_1$ according to this section. The completely symmeterized operator structure has to be proportional to at least one commutator to satisfy the large-N_c consistency conditions. Since one is able to order such terms by introducing commutators (equation (6.16)), for $X \mapsto \mathbb{1}$, the structure has to vanish.

From direct computations one can see that one is not able to get non-trivial contributions for $n_i > 7$. Thus all possible contributions are respected by the following ten structures.

Operator structure for terms (0,4,7)

$$\begin{aligned}
&8X^{ci_3}X^{ai_1}X^{bi_2}X^{cj_3}X^{bj_2}X^{aj_1} + 8X^{ai_1}X^{bi_2}X^{ci_3}X^{bj_2}X^{aj_1}X^{cj_3}\\
&+ 4X^{bi_2}X^{ci_3}X^{ai_1}X^{cj_3}X^{bj_2}X^{aj_1} + 4X^{ai_1}X^{ci_3}X^{bi_2}X^{aj_1}X^{bj_2}X^{cj_3}\\
&+ 4X^{ai_1}X^{ci_3}X^{bi_2}X^{cj_3}X^{aj_1}X^{bj_2} + 4X^{bi_2}X^{ci_3}X^{ai_1}X^{bj_2}X^{aj_1}X^{cj_3}\\
&- 8X^{ai_1}X^{bi_2}X^{ci_3}X^{bj_2}X^{cj_3}X^{aj_1} - 8X^{ci_3}X^{ai_1}X^{bi_2}X^{bj_2}X^{cj_3}X^{aj_1}\\
&- 8X^{ci_3}X^{ai_1}X^{bi_2}X^{cj_3}X^{aj_1}X^{bj_2} - 8X^{ai_1}X^{bi_2}X^{ci_3}X^{aj_1}X^{bj_2}X^{cj_3}\,.
\end{aligned} \tag{6.36}$$

Operator structure for terms (1,3,7)

$$\begin{aligned}
&16X^{ai_1}X^{bi_2}X^{ci_3}X^{bj_2}X^{aj_1}X^{cj_3} + 16X^{ci_3}X^{ai_1}X^{bi_2}X^{cj_3}X^{bj_2}X^{aj_1}\\
&+ 8X^{bi_2}X^{ci_3}X^{ai_1}X^{bj_2}X^{aj_1}X^{cj_3} + 8X^{ai_1}X^{ci_3}X^{bi_2}X^{aj_1}X^{bj_2}X^{cj_3}\\
&+ 8X^{bi_2}X^{ci_3}X^{ai_1}X^{cj_3}X^{bj_2}X^{aj_1} + 8X^{ai_1}X^{ci_3}X^{bi_2}X^{cj_3}X^{aj_1}X^{bj_2}\\
&+ 4X^{ai_1}X^{bi_2}X^{ci_3}X^{aj_1}X^{cj_3}X^{bj_2} + 4X^{ci_3}X^{ai_1}X^{bi_2}X^{aj_1}X^{cj_3}X^{bj_2}\\
&- X^{ai_1}X^{ci_3}X^{bi_2}X^{aj_1}X^{cj_3}X^{bj_2} - X^{bi_2}X^{ci_3}X^{ai_1}X^{bj_2}X^{cj_3}X^{aj_1}\\
&- 4X^{ci_3}X^{ai_1}X^{bi_2}X^{bj_2}X^{aj_1}X^{cj_3} - 4X^{ai_1}X^{bi_2}X^{ci_3}X^{cj_3}X^{bj_2}X^{aj_1}\\
&- 12X^{ci_3}X^{ai_1}X^{bi_2}X^{bj_2}X^{cj_3}X^{aj_1} - 12X^{ai_1}X^{bi_2}X^{ci_3}X^{bj_2}X^{cj_3}X^{aj_1}\\
&- 19X^{ai_1}X^{bi_2}X^{ci_3}X^{aj_1}X^{bj_2}X^{cj_3} - 19X^{ci_3}X^{ai_1}X^{bi_2}X^{cj_3}X^{aj_1}X^{bj_2}\,.
\end{aligned} \tag{6.37}$$

Operator structure for terms (2,2,7)

$$\begin{aligned}
&12X^{ai_1}X^{bi_2}X^{ci_3}X^{bj_2}X^{aj_1}X^{cj_3} + 12X^{ai_1}X^{bi_2}X^{ci_3}X^{aj_1}X^{cj_3}X^{bj_2}\\
&+ 6X^{bi_2}X^{ai_1}X^{ci_3}X^{aj_1}X^{bj_2}X^{cj_3} + 6X^{bi_2}X^{ai_1}X^{ci_3}X^{bj_2}X^{cj_3}X^{aj_1}\\
&- 4X^{ai_1}X^{bi_2}X^{ci_3}X^{cj_3}X^{aj_1}X^{bj_2} - 4X^{ai_1}X^{bi_2}X^{ci_3}X^{cj_3}X^{bj_2}X^{aj_1}\\
&- 2X^{bi_2}X^{ai_1}X^{ci_3}X^{cj_3}X^{bj_2}X^{aj_1} - 2X^{bi_2}X^{ai_1}X^{ci_3}X^{aj_1}X^{cj_3}X^{bj_2}\\
&- 4X^{bi_2}X^{ai_1}X^{ci_3}X^{bj_2}X^{aj_1}X^{cj_3} - 4X^{ai_1}X^{bi_2}X^{ci_3}X^{bj_2}X^{cj_3}X^{aj_1}\\
&- 16X^{ai_1}X^{bi_2}X^{ci_3}X^{aj_1}X^{bj_2}X^{cj_3}\,.
\end{aligned} \tag{6.38}$$

Operator structure for terms (0,5,6)

$$
\begin{aligned}
&24X^{ci_3}X^{ai_1}X^{bi_2}X^{cj_3}X^{bj_2}X^{aj_1} + 24X^{ai_1}X^{bi_2}X^{ci_3}X^{bj_2}X^{aj_1}X^{cj_3} \\
&+ 12X^{bi_2}X^{ci_3}X^{ai_1}X^{cj_3}X^{bj_2}X^{aj_1} + 12X^{ai_1}X^{ci_3}X^{bi_2}X^{aj_1}X^{bj_2}X^{cj_3} \\
&+ 12X^{ai_1}X^{ci_3}X^{bi_2}X^{cj_3}X^{aj_1}X^{bj_2} + 12X^{bi_2}X^{ci_3}X^{ai_1}X^{bj_2}X^{aj_1}X^{cj_3} \\
&- 24X^{ai_1}X^{bi_2}X^{ci_3}X^{bj_2}X^{cj_3}X^{aj_1} - 24X^{ci_3}X^{ai_1}X^{bi_2}X^{bj_2}X^{cj_3}X^{aj_1} \\
&- 24X^{ci_3}X^{ai_1}X^{bi_2}X^{cj_3}X^{aj_1}X^{bj_2} - 24X^{ai_1}X^{bi_2}X^{ci_3}X^{aj_1}X^{bj_2}X^{cj_3} .
\end{aligned}
$$

Operator structure for terms (1,4,6)

$$
\begin{aligned}
&72X^{ai_1}X^{bi_2}X^{ci_3}X^{bj_2}X^{aj_1}X^{cj_3} + 72X^{ci_3}X^{ai_1}X^{bi_2}X^{cj_3}X^{bj_2}X^{aj_1} \\
&+ 36X^{ai_1}X^{ci_3}X^{bi_2}X^{cj_3}X^{aj_1}X^{bj_2} + 36X^{bi_2}X^{ci_3}X^{ai_1}X^{cj_3}X^{bj_2}X^{aj_1} \\
&+ 36X^{bi_2}X^{ci_3}X^{ai_1}X^{bj_2}X^{aj_1}X^{cj_3} + 36X^{ai_1}X^{ci_3}X^{bi_2}X^{aj_1}X^{bj_2}X^{cj_3} \\
&+ 12X^{ai_1}X^{bi_2}X^{ci_3}X^{aj_1}X^{cj_3}X^{bj_2} + 12X^{ci_3}X^{ai_1}X^{bi_2}X^{aj_1}X^{cj_3}X^{bj_2} \\
&- 4X^{ai_1}X^{ci_3}X^{bi_2}X^{aj_1}X^{cj_3}X^{bj_2} - 4X^{bi_2}X^{ci_3}X^{ai_1}X^{bj_2}X^{cj_3}X^{aj_1} \\
&- 12X^{ai_1}X^{bi_2}X^{ci_3}X^{cj_3}X^{bj_2}X^{aj_1} - 12X^{ci_3}X^{ai_1}X^{bi_2}X^{bj_2}X^{aj_1}X^{cj_3} \\
&- 60X^{ai_1}X^{bi_2}X^{ci_3}X^{bj_2}X^{cj_3}X^{aj_1} - 60X^{ci_3}X^{ai_1}X^{bi_2}X^{bj_2}X^{cj_3}X^{aj_1} \\
&- 80X^{ai_1}X^{bi_2}X^{ci_3}X^{aj_1}X^{bj_2}X^{cj_3} - 80X^{ci_3}X^{ai_1}X^{bi_2}X^{cj_3}X^{aj_1}X^{bj_2} .
\end{aligned} \tag{6.39}
$$

Operator structure for terms (2,3,6)

$$
\begin{aligned}
&84X^{ci_3}X^{ai_1}X^{bi_2}X^{cj_3}X^{bj_2}X^{aj_1} + 84X^{ai_1}X^{bi_2}X^{ci_3}X^{bj_2}X^{aj_1}X^{cj_3} \\
&+ 48X^{ci_3}X^{ai_1}X^{bi_2}X^{aj_1}X^{cj_3}X^{bj_2} + 48X^{ai_1}X^{bi_2}X^{ci_3}X^{aj_1}X^{cj_3}X^{bj_2} \\
&+ 42X^{bi_2}X^{ci_3}X^{ai_1}X^{bj_2}X^{aj_1}X^{cj_3} + 42X^{bi_2}X^{ci_3}X^{ai_1}X^{cj_3}X^{bj_2}X^{aj_1} \\
&+ 42X^{ai_1}X^{ci_3}X^{bi_2}X^{aj_1}X^{bj_2}X^{cj_3} + 42X^{ai_1}X^{ci_3}X^{bi_2}X^{cj_3}X^{aj_1}X^{bj_2} \\
&- 6X^{ai_1}X^{ci_3}X^{bi_2}X^{bj_2}X^{aj_1}X^{cj_3} - 6X^{bi_2}X^{ci_3}X^{ai_1}X^{cj_3}X^{aj_1}X^{bj_2} \\
&- 6X^{ai_1}X^{ci_3}X^{bi_2}X^{cj_3}X^{bj_2}X^{aj_1} - 6X^{bi_2}X^{ci_3}X^{ai_1}X^{aj_1}X^{bj_2}X^{cj_3} \\
&- 12X^{ci_3}X^{ai_1}X^{bi_2}X^{aj_1}X^{bj_2}X^{cj_3} - 12X^{ai_1}X^{bi_2}X^{ci_3}X^{cj_3}X^{aj_1}X^{bj_2} \\
&- 17X^{bi_2}X^{ci_3}X^{ai_1}X^{bj_2}X^{cj_3}X^{aj_1} - 17X^{ai_1}X^{ci_3}X^{bi_2}X^{aj_1}X^{cj_3}X^{bj_2} \\
&- 24X^{ai_1}X^{bi_2}X^{ci_3}X^{cj_3}X^{bj_2}X^{aj_1} - 24X^{ci_3}X^{ai_1}X^{bi_2}X^{bj_2}X^{aj_1}X^{cj_3} \\
&- 48X^{ai_1}X^{bi_2}X^{ci_3}X^{bj_2}X^{cj_3}X^{aj_1} - 48X^{ci_3}X^{ai_1}X^{bi_2}X^{bj_2}X^{cj_3}X^{aj_1} \\
&- 103X^{ai_1}X^{bi_2}X^{ci_3}X^{aj_1}X^{bj_2}X^{cj_3} - 103X^{ci_3}X^{ai_1}X^{bi_2}X^{cj_3}X^{aj_1}X^{bj_2} .
\end{aligned} \tag{6.40}
$$

Operator structure for terms (1,5,5)

$$
\begin{aligned}
&112X^{ai_1}X^{bi_2}X^{ci_3}X^{aj_1}X^{cj_3}X^{bj_2} + 64X^{ai_1}X^{bi_2}X^{ci_3}X^{bj_2}X^{aj_1}X^{cj_3} \\
&+ 56X^{ai_1}X^{ci_3}X^{bi_2}X^{cj_3}X^{aj_1}X^{bj_2} + 8X^{ai_1}X^{ci_3}X^{bi_2}X^{aj_1}X^{bj_2}X^{cj_3} \\
&- 8X^{ai_1}X^{bi_2}X^{ci_3}X^{cj_3}X^{bj_2}X^{aj_1} - 8X^{ai_1}X^{ci_3}X^{bi_2}X^{bj_2}X^{cj_3}X^{aj_1} \\
&- 48X^{ai_1}X^{bi_2}X^{ci_3}X^{cj_3}X^{aj_1}X^{bj_2} - 48X^{ai_1}X^{ci_3}X^{bi_2}X^{cj_3}X^{bj_2}X^{aj_1} \\
&- 61X^{ai_1}X^{ci_3}X^{bi_2}X^{aj_1}X^{cj_3}X^{bj_2} - 67X^{ai_1}X^{bi_2}X^{ci_3}X^{aj_1}X^{bj_2}X^{cj_3} .
\end{aligned} \tag{6.41}
$$

Operator structure for terms (2,4,5)

$$
\begin{aligned}
&192X^{ai_1}X^{bi_2}X^{ci_3}X^{bj_2}X^{aj_1}X^{cj_3} + 192X^{ci_3}X^{ai_1}X^{bi_2}X^{cj_3}X^{bj_2}X^{aj_1} \\
&+ 96X^{ai_1}X^{ci_3}X^{bi_2}X^{cj_3}X^{aj_1}X^{bj_2} + 96X^{bi_2}X^{ci_3}X^{ai_1}X^{bj_2}X^{aj_1}X^{cj_3} \\
&+ 96X^{ai_1}X^{ci_3}X^{bi_2}X^{aj_1}X^{bj_2}X^{cj_3} + 96X^{bi_2}X^{ci_3}X^{ai_1}X^{cj_3}X^{bj_2}X^{aj_1} \\
&+ 80X^{ci_3}X^{ai_1}X^{bi_2}X^{aj_1}X^{cj_3}X^{bj_2} + 80X^{ai_1}X^{bi_2}X^{ci_3}X^{aj_1}X^{cj_3}X^{bj_2} \\
&- 8X^{ai_1}X^{ci_3}X^{bi_2}X^{cj_3}X^{bj_2}X^{aj_1} - 8X^{bi_2}X^{ci_3}X^{ai_1}X^{aj_1}X^{bj_2}X^{cj_3} \\
&- 8X^{bi_2}X^{ci_3}X^{ai_1}X^{cj_3}X^{aj_1}X^{bj_2} - 8X^{ai_1}X^{ci_3}X^{bi_2}X^{bj_2}X^{aj_1}X^{cj_3} \\
&- 16X^{ai_1}X^{bi_2}X^{ci_3}X^{cj_3}X^{aj_1}X^{bj_2} - 16X^{ci_3}X^{ai_1}X^{bi_2}X^{aj_1}X^{bj_2}X^{cj_3} \\
&- 31X^{ai_1}X^{ci_3}X^{bi_2}X^{aj_1}X^{cj_3}X^{bj_2} - 31X^{bi_2}X^{ci_3}X^{ai_1}X^{bj_2}X^{cj_3}X^{aj_1} \\
&- 48X^{ai_1}X^{bi_2}X^{ci_3}X^{cj_3}X^{bj_2}X^{aj_1} - 48X^{ci_3}X^{ai_1}X^{bi_2}X^{bj_2}X^{aj_1}X^{cj_3} \\
&- 128X^{ai_1}X^{bi_2}X^{ci_3}X^{bj_2}X^{cj_3}X^{aj_1} - 128X^{ci_3}X^{ai_1}X^{bi_2}X^{bj_2}X^{cj_3}X^{aj_1} \\
&- 225X^{ci_3}X^{ai_1}X^{bi_2}X^{cj_3}X^{aj_1}X^{bj_2} - 225X^{ai_1}X^{bi_2}X^{ci_3}X^{aj_1}X^{bj_2}X^{cj_3}\,. \qquad (6.42)
\end{aligned}
$$

Operator structure for terms (3,3,5)

$$
\begin{aligned}
&184X^{ai_1}X^{bi_2}X^{ci_3}X^{aj_1}X^{cj_3}X^{bj_2} + 168X^{ai_1}X^{bi_2}X^{ci_3}X^{bj_2}X^{aj_1}X^{cj_3} \\
&+ 100X^{bi_2}X^{ai_1}X^{ci_3}X^{aj_1}X^{bj_2}X^{cj_3} + 84X^{bi_2}X^{ai_1}X^{ci_3}X^{bj_2}X^{cj_3}X^{aj_1} \\
&- 8X^{bi_2}X^{ai_1}X^{ci_3}X^{cj_3}X^{aj_1}X^{bj_2} - 20X^{bi_2}X^{ai_1}X^{ci_3}X^{cj_3}X^{bj_2}X^{aj_1} \\
&- 36X^{bi_2}X^{ai_1}X^{ci_3}X^{aj_1}X^{cj_3}X^{bj_2} - 48X^{ai_1}X^{bi_2}X^{ci_3}X^{cj_3}X^{bj_2}X^{aj_1} \\
&- 56X^{ai_1}X^{bi_2}X^{ci_3}X^{bj_2}X^{cj_3}X^{aj_1} - 72X^{ai_1}X^{bi_2}X^{ci_3}X^{cj_3}X^{aj_1}X^{bj_2} \\
&- 77X^{bi_2}X^{ai_1}X^{ci_3}X^{bj_2}X^{aj_1}X^{cj_3} - 219X^{ai_1}X^{bi_2}X^{ci_3}X^{aj_1}X^{bj_2}X^{cj_3}\,. \qquad (6.43)
\end{aligned}
$$

Operator structure for terms (3,4,4)

$$
\begin{aligned}
&256X^{ai_1}X^{bi_2}X^{ci_3}X^{aj_1}X^{cj_3}X^{bj_2} + 226X^{ai_1}X^{bi_2}X^{ci_3}X^{bj_2}X^{aj_1}X^{cj_3} \\
&+ 128X^{ai_1}X^{ci_3}X^{bi_2}X^{cj_3}X^{aj_1}X^{bj_2} + 98X^{ai_1}X^{ci_3}X^{bi_2}X^{aj_1}X^{bj_2}X^{cj_3} \\
&- 30X^{ai_1}X^{ci_3}X^{bi_2}X^{bj_2}X^{cj_3}X^{aj_1} - 32X^{ai_1}X^{ci_3}X^{bi_2}X^{bj_2}X^{aj_1}X^{cj_3} \\
&- 38X^{ai_1}X^{bi_2}X^{ci_3}X^{cj_3}X^{bj_2}X^{aj_1} - 62X^{ai_1}X^{ci_3}X^{bi_2}X^{cj_3}X^{bj_2}X^{aj_1} \\
&- 64X^{ai_1}X^{bi_2}X^{ci_3}X^{bj_2}X^{cj_3}X^{aj_1} - 94X^{ai_1}X^{bi_2}X^{ci_3}X^{cj_3}X^{aj_1}X^{bj_2} \\
&- 148X^{ai_1}X^{ci_3}X^{bi_2}X^{aj_1}X^{cj_3}X^{bj_2} - 240X^{ai_1}X^{bi_2}X^{ci_3}X^{aj_1}X^{bj_2}X^{cj_3}\,. \qquad (6.44)
\end{aligned}
$$

As one can easily verify, setting $X \mapsto \mathbb{1}$ lets all of these ten amplitudes vanish.

Therefore one is able to see that the whole amplitude corresponds to at least one commutator structure, which confirms the predicted N_c scaling.

Accordingly all contributions to the chiral nucleon-nucleon potential up to order $\nu = 4$ satisfy the predicted large-N_c scaling by KSM.

6.5 General considerations

As shown in the previous section, it is possible to proof the large-N_c consistency of the effective chiral nucleon-nucleon potential up to chiral order $\nu = 4$ using the systematic

approach of unitary transformations. However, it would be desirable to proof the consistency up to all orders. Therefore it is useful to consider equation (4.81)

$$\mathcal{O}_{N_c}\left(V_{NN}^{(\nu)}\right) = \frac{\nu}{2} + 1 - 2N_2 - 2C\,, \tag{6.45}$$

since general baryon scattering amplitudes scale as N_c, while amplitudes contributing to $I \neq J$ contributions scale as $1/N_c$, one has to solve

$$\frac{\nu}{2} + 1 - 2N_2 - 2C = \begin{cases} 1 & , \quad I = J \\ -1 & , \quad I \neq J \end{cases}\,, \tag{6.46}$$

which directly demands the existence of C commutators for specific diagrams. Furthermore one can directly interfere that for each chiral order a certain number of two-pion vertices will result in a correctly scaling diagram. As pointed out before, certain operator structures (specific M-like structures) are already proportional to a commutator and thus are decreasing the N_c scaling furthermore. Nevertheless, the most critical structure is the structure containing no two-pion vertices $N_2 = 0$. As it has been done at the chiral order $\nu = 2$ and $\nu = 4$, one has to analyze the operator and energy denominator structure of each diagram to identify the large-N_c scaling—both structures are equally important.

Looking at the operator structure of only one-pion vertices, one can directly observe the following fact—if $N_1 = \nu + 2 = 2n$ is the number of one-pion vertices, the operator structure is composed out of n X_1 and n X_2 operators

$$X_1 \cdot X_1 \cdots X_1 X_2 \cdot X_2 \cdots X_2\,. \tag{6.47}$$

Explicitly computing the diagrams using the same labeling procedure as in the previous section one gets for the X_1 operators

$$X_1^{i_n a_n} X_1^{i_{n-1} a_{n-1}} \cdots X_1^{i_2 a_2} X_1^{i_1 a_1}\,. \tag{6.48}$$

By inserting at least one commutator, all possible structures for the second nucleon can be brought to the same form[2]. For $n \in 2^{\mathbb{N}}$, the leading order contribution of this structure is given by reducing the operators with anticommutator relations

$$\left\{X_1^{i_n a_n}\,,\, X_1^{i_{n-1} a_{n-1}}\right\} \cdots \left\{X_1^{i_2 a_2}\,,\, X_1^{i_1 a_1}\right\} \left\{X_2^{j_n a_n}\,,\, X_2^{j_{n-1} a_{n-1}}\right\} \cdots \left\{X_2^{j_2 a_2}\,,\, X_2^{j_1 a_1}\right\}\,. \tag{6.49}$$

Using further anticommutator reductions one finally obtains a term

$$S^{i,j,a}\mathbb{1}_1 \cdot \mathbb{1}_2 + A^{i,j,a} X_1 \cdot X_2\,, \tag{6.50}$$

where the coefficient $S^{i,j,a}$ is totally symmetric and $A^{i,j,a}$ is totally anti-symmetric in each pair

$$(i_n,i_{n-1}), \cdots, (i_2,i_1), (j_n,j_{n-1}), \cdots, (j_2,j_1), (a_n,a_{n-1}), \cdots, (a_2,a_1)\,. \tag{6.51}$$

The next to leading order term would correspond to exactly one term reduced by a commutator reduction, however this reduction has to be paired with the same anticommutator reduction from the other nucleon line which results in a zero since commutator reductions are symmetric in spin and anti-symmetric in isospin or vice versa (equation (6.17)). Thus the effective next to leading order term is of kind

$$\begin{aligned} &\left\{X_1^{i_n a_n}\,,\, X_1^{i_{n-1} a_{n-1}}\right\} \cdots \left[\, X_1^{i_m a_m}\,,\, X_1^{i_{m-1} a_{m-1}} \,\right] \cdots \left\{X_1^{i_2 a_2}\,,\, X_1^{i_1 a_1}\right\} \\ &\qquad \times \left\{X_2^{j_n a_n}\,,\, X_2^{j_{n-1} a_{n-1}}\right\} \cdots \left[\, X_2^{j_m a_m}\,,\, X_2^{j_{m-1} a_{m-1}} \,\right] \cdots \left\{X_2^{j_2 a_2}\,,\, X_2^{j_1 a_1}\right\}\,, \end{aligned} \tag{6.52}$$

[2] i_m becomes j_m in the X_2 case, while each pair is individually symmetric in the interchange of $(i_m \leftrightarrow j_m)$.

where exactly the term corresponding to the same spin-isospin components is reduced by an anticommutator at both nucleon lines. Using the same argumentation one can also order existing operator structures which differ from the ordering introduced by equation (6.16) up to order $1/N_c^4$. The only term not vanishing when introducing a commutator on the second nucleon line is given by a similar commutator on the first nucleon line. Thus one can directly acknowledge the following fact: for $N_1/2 =$ even one-pion vertices, the structure scales as

$$X_1X_1\cdots X_1X_2X_2\cdots X_2 = (\mathbb{1} + X_1\cdot X_2) + \frac{1}{N_c^4}\,(X_1\cdot X_2 + J_1\cdot J_2 + I_1\cdot I_2) + \mathcal{O}\left(\frac{1}{N_c^8}\right). \tag{6.53}$$

Thus one has an effective $1/N_c^4$ expansion. The same behavior has already been observed for $\nu = 2$. Thus, if one was able to verify that the amplitudes at leading order in N_c are vanishing, one directly reduces the order by $1/N_c^4$. Therefore the energy structure has to guarantee that the sum over all operator structures vanish at leading order.

As seen before, for $n \notin 2^{\mathbb{N}}$, the argumentation stays the same but it is in general also possible to obtain terms at $1/N_c^2$ when contracting the last pairs of operators:

$$\begin{aligned} X_1X_1\cdots X_1X_2X_2\cdots X_2 &\to \{\,X_1\,,\,X_1\,\}\cdots\{\,X_1\,,\,X_1\,\}\,X_1\,\{\,X_2\,,\,X_2\,\}\cdots\{\,X_2\,,\,X_2\,\}\,X_2 \\ &\to \cdots \to X_1X_1X_1X_2X_2X_2 \\ &\sim 1 + 1/N_c^2\,. \end{aligned} \tag{6.54}$$

In the analysis at chiral order $\nu = 4$ it has been necessary to symmeterize and collect all terms to guarantee the consistency (starting from equation (6.30)). This directly proposes a necessary condition for the potential to fulfill: if one drops the pion-dependence in spin, isospin and momentum space

$$\omega_i \mapsto \omega \qquad\qquad q_n^{i_n} \mapsto q \qquad\qquad X^{ia} \mapsto X\,, \tag{6.55}$$

the sum over all diagrams has to be zero. Note that this is just a way to test if a potential is able to vanish in leading order, it does not guarantee that its contribution is actually vanishing.

Doing so, the actual operator structure corresponding to a time-ordered diagram is not important—one just has to look at the numerical factors and count the diagrams. However, this can be realized more efficiently than the actual computation procedure.

As an example, at the chiral order $\nu = 4$ one has the following operator structures:

- the double-box structure corresponding to

$$-\frac{2}{\omega^5}\,H_{21}^{(1)}\,\lambda^1\,H_{21}^{(1)}\,\eta\,H_{21}^{(1)}\,\lambda^1\,H_{21}^{(1)}\,\eta\,H_{21}^{(1)}\,\lambda^1\,H_{21}^{(1)}\,\eta\,, \tag{6.56}$$

- the upper and lower cross-box structure corresponding to

$$\frac{7}{8\omega^5}\,H_{21}^{(1)}\,\lambda^1\,H_{21}^{(1)}\,\eta\,H_{21}^{(1)}\,\lambda^1\,H_{21}^{(1)}\,\lambda^2\,H_{21}^{(1)}\,\lambda^1\,H_{21}^{(1)}\,\eta\,, \tag{6.57}$$

  and its hermitian conjugated structure,

- the slashed box structure

$$-\frac{1}{4\omega^5}\eta\,H_{21}^{(1)}\,\lambda^1\,H_{21}^{(1)}\,\lambda^2\,H_{21}^{(1)}\,\lambda^1\,H_{21}^{(1)}\,\lambda^2\,H_{21}^{(1)}\,\lambda^1\,H_{21}^{(1)}\,\eta \tag{6.58}$$

- and the slashed cross-box structure

$$-\frac{1}{12\omega^5}\eta\,H_{21}^{(1)}\,\lambda^1\,H_{21}^{(1)}\,\lambda^2\,H_{21}^{(1)}\,\lambda^3\,H_{21}^{(1)}\,\lambda^2\,H_{21}^{(1)}\,\lambda^1\,H_{21}^{(1)}\,\eta\,. \tag{6.59}$$

Since in this limit, the operators become just bare counting operators, one finds eight double-box structures, two times 16 single cross-box structures, 32 slashed box structures and 48 slashed cross-box structures which finally result in

$$\frac{1}{\omega^5}\left(\frac{7}{8}\cdot 2\cdot 16 - 2\cdot 8 - \frac{1}{4}\cdot 32 - \frac{1}{12}\cdot 48\right) = 0\,. \tag{6.60}$$

Fortunately there is also a quick way for computing the number of diagrams corresponding to a structure: One has to read the operator structure from left to right and each time a pion is emitted or absorbed, one has to count the possibilities for drawing this diagram:

- Each time a pion is emitted, one gets a factor of two, since one is free in the choice of the nucleon line the pion is attached to.
- Each time a pion is absorbed, one gets a factor corresponding to the previous number of intermediate pions, since one is free in the choice which pion gets absorbed but cannot choose which nucleon absorbs the pion.

As an example, the slashed cross-box structure corresponds to

$$\eta\, H_{21}^{(1)}\, \lambda^1\, H_{21}^{(1)}\, \lambda^2\, H_{21}^{(1)}\, \lambda^3\, H_{21}^{(1)}\, \lambda^2\, H_{21}^{(1)}\, \lambda^1\, H_{21}^{(1)}\, \eta \leftrightarrow 1\cdot 2\cdot 3\cdot 2\cdot 2\cdot 2 = 48\,. \tag{6.61}$$

Using this one can also verify easily that the chiral potential at order $\nu = 6$ containing only one-pion vertices also fulfills the necessary requirements for being consistent with the large-N_c predictions. The operator structure, when dropping the information of a pion, is given by

$$\begin{aligned}\frac{1}{288\omega^7}\Big(&1440\,\eta\, H_{21}^{(1)}\, \lambda^1\, H_{21}^{(1)}\, \eta\, H_{21}^{(1)}\, \lambda^1\, H_{21}^{(1)}\, \eta\, H_{21}^{(1)}\, \lambda^1\, H_{21}^{(1)}\, \eta\, H_{21}^{(1)}\, \lambda^1\, H_{21}^{(1)}\, \eta \\ &+ 180\,\eta\, H_{21}^{(1)}\, \lambda^1\, H_{21}^{(1)}\, \eta\, H_{21}^{(1)}\, \lambda^1\, H_{21}^{(1)}\, \lambda^2\, H_{21}^{(1)}\, \lambda^1\, H_{21}^{(1)}\, \lambda^2\, H_{21}^{(1)}\, \lambda^1\, H_{21}^{(1)}\, \eta \\ &+ 180\,\eta\, H_{21}^{(1)}\, \lambda^1\, H_{21}^{(1)}\, \lambda^2\, H_{21}^{(1)}\, \lambda^1\, H_{21}^{(1)}\, \eta\, H_{21}^{(1)}\, \lambda^1\, H_{21}^{(1)}\, \lambda^2\, H_{21}^{(1)}\, \lambda^1\, H_{21}^{(1)}\, \eta \\ &+ 180\,\eta\, H_{21}^{(1)}\, \lambda^1\, H_{21}^{(1)}\, \lambda^2\, H_{21}^{(1)}\, \lambda^1\, H_{21}^{(1)}\, \lambda^2\, H_{21}^{(1)}\, \lambda^1\, H_{21}^{(1)}\, \eta\, H_{21}^{(1)}\, \lambda^1\, H_{21}^{(1)}\, \eta \\ &+ 52\,\eta\, H_{21}^{(1)}\, \lambda^1\, H_{21}^{(1)}\, \eta\, H_{21}^{(1)}\, \lambda^1\, H_{21}^{(1)}\, \lambda^2\, H_{21}^{(1)}\, \lambda^3\, H_{21}^{(1)}\, \lambda^2\, H_{21}^{(1)}\, \lambda^1\, H_{21}^{(1)}\, \eta \\ &+ 52\,\eta\, H_{21}^{(1)}\, \lambda^1\, H_{21}^{(1)}\, \lambda^2\, H_{21}^{(1)}\, \lambda^3\, H_{21}^{(1)}\, \lambda^2\, H_{21}^{(1)}\, \lambda^1\, H_{21}^{(1)}\, \eta\, H_{21}^{(1)}\, \lambda^1\, H_{21}^{(1)}\, \eta \\ &- 2\,\eta\, H_{21}^{(1)}\, \lambda^1\, H_{21}^{(1)}\, \lambda^2\, H_{21}^{(1)}\, \lambda^3\, H_{21}^{(1)}\, \lambda^4\, H_{21}^{(1)}\, \lambda^3\, H_{21}^{(1)}\, \lambda^2\, H_{21}^{(1)}\, \lambda^1\, H_{21}^{(1)}\, \eta \\ &- 4\,\eta\, H_{21}^{(1)}\, \lambda^1\, H_{21}^{(1)}\, \lambda^2\, H_{21}^{(1)}\, \lambda^3\, H_{21}^{(1)}\, \lambda^2\, H_{21}^{(1)}\, \lambda^3\, H_{21}^{(1)}\, \lambda^2\, H_{21}^{(1)}\, \lambda^1\, H_{21}^{(1)}\, \eta \\ &- 12\,\eta\, H_{21}^{(1)}\, \lambda^1\, H_{21}^{(1)}\, \lambda^2\, H_{21}^{(1)}\, \lambda^3\, H_{21}^{(1)}\, \lambda^2\, H_{21}^{(1)}\, \lambda^1\, H_{21}^{(1)}\, \lambda^2\, H_{21}^{(1)}\, \lambda^1\, H_{21}^{(1)}\, \eta \\ &- 12\,\eta\, H_{21}^{(1)}\, \lambda^1\, H_{21}^{(1)}\, \lambda^2\, H_{21}^{(1)}\, \lambda^1\, H_{21}^{(1)}\, \lambda^2\, H_{21}^{(1)}\, \lambda^3\, H_{21}^{(1)}\, \lambda^2\, H_{21}^{(1)}\, \lambda^1\, H_{21}^{(1)}\, \eta \\ &- 36\,\eta\, H_{21}^{(1)}\, \lambda^1\, H_{21}^{(1)}\, \lambda^2\, H_{21}^{(1)}\, \lambda^1\, H_{21}^{(1)}\, \lambda^2\, H_{21}^{(1)}\, \lambda^1\, H_{21}^{(1)}\, \lambda^2\, H_{21}^{(1)}\, \lambda^1\, H_{21}^{(1)}\, \eta \\ &- 450\,\eta\, H_{21}^{(1)}\, \lambda^1\, H_{21}^{(1)}\, \eta\, H_{21}^{(1)}\, \lambda^1\, H_{21}^{(1)}\, \lambda^2\, H_{21}^{(1)}\, \lambda^1\, H_{21}^{(1)}\, \eta\, H_{21}^{(1)}\, \lambda^1\, H_{21}^{(1)}\, \eta \\ &- 657\,\eta\, H_{21}^{(1)}\, \lambda^1\, H_{21}^{(1)}\, \eta\, H_{21}^{(1)}\, \lambda^1\, H_{21}^{(1)}\, \eta\, H_{21}^{(1)}\, \lambda^1\, H_{21}^{(1)}\, \lambda^2\, H_{21}^{(1)}\, \lambda^1\, H_{21}^{(1)}\, \eta \\ &-657\,\eta\, H_{21}^{(1)}\, \lambda^1\, H_{21}^{(1)}\, \lambda^2\, H_{21}^{(1)}\, \lambda^1\, H_{21}^{(1)}\, \eta\, H_{21}^{(1)}\, \lambda^1\, H_{21}^{(1)}\, \eta\, H_{21}^{(1)}\, \lambda^1\, H_{21}^{(1)}\, \eta\Big)\,.\end{aligned} \tag{6.62}$$

Counting the number of diagrams with the previously mentioned method one now obtains

$$\begin{aligned}\frac{1}{288\omega^7}\,(&23040 + 11520 + 11520 + 11520 + 4992 + 4992 \\ &-768 - 1152 - 2304 - 2304 - 4608 - 14400 - 21024 - 21024) = 0\end{aligned} \tag{6.63}$$

However only explicit computations may verify that the energy structure explicitly forces the leading order contribution to vanish. If this was the case, the next to leading order term in the N_c expansion of the operator structure might be at order $1/N_c^4$ (order $\nu = 6$ contributes to $8/2 = 4 = 2^2$ operators on one nucleon line) has and thus the potential might scale as $N_c^0 \lesssim N_c$ satisfying the KSM counting rules.

7 Conclusion

7.1 Conclusion

As the main result of this work, the large-N_c scaling of the nucleon-nucleon potential directly computed in chiral perturbation theory using the method of unitary transformations up to chiral order $\nu = 4$ is consistent with predictions made on a QCD level. Even the potential at order $\nu = 6$ corresponding to only one-pion exchanges might be consistent as well. Furthermore, methods have been demonstrated to systematically extend the analysis to higher orders, while the number of diagrams possibly violating the predictions can be directly identified. Additionally it has been shown that specific chiral terms of the potential have a N_c expansions which is effectively a $1/N_c^4$ expansion.

While it would be desirable to extend the analysis to higher orders, it seems that there is a general difficulty using the method of unitary transformations. As calculations for potential consisting of only one-pion exchanges have shown, the needed cancellations resulting in a reduced N_c scaling are heavily depending on the energy structure as well as the operator structure.

While the analysis of section 6.5 has demonstrated a necessary condition for the potential to be large-N_c consistent, it is not obvious if one can formulate a sufficient condition for the potential to be large-N_c consistent. This is the case since at orders $\nu \geq 8$, the couplings scale as N_c^5. Thus, even if the first term of the N_c expansion vanishes, the next to leading order still scales as N_c^3, which violates the predictions. The only possibility for the potential to still be consistent would be a second commutator structure induced by the energy structure. However this demands a simultaneous treatment of energy and operator structure when analyzing the potential.

Though it was not possible to proof the large-N_c consistency for the nucleon-nucleon potential at all orders, one was in principle able to demonstrate that there are no puzzling difficulties when testing the consistency.

Also, if one assumes that the chiral potential is consistent with large-N_c predictions, one could pose several conditions on the potential:

- It is essential for the potential to have the unitary structure. Already small derivations from this structure lead to non-vanishing amplitudes at leading order. Thus the large-N_c consistency poses a hard condition on the potential structure, which can be used to test the completeness of a potential for a given chiral order.
- Additionally to the chiral counting one may include the N_c counting when computing processes. This can help since one can directly read of the N_c scaling of specific structures which contain two-pion vertices—some are $1/N_c^2$ suppressed compared to others while still on the same chiral level (some M-like structures).

Future works in this field could try to extend the procedure by proving that leading order amplitudes of an operator structure may vanish at each chiral order, different interactions may not violate the counting, or different scattering processes may be consistent as well.

Acknowledgments

I would like to thank my supervisor Evgeny Epelbaum for helpful ideas and insights in χPT during the creation of this work. Also I would like to thank Simone Danisch for useful comments on how to make this text more readable.

Since this master thesis also represents the end of my (master) student era, I would also like to thank several others who have helped me during this process in multiple ways. I have been fortunate for being supported by my family and friends, even though it might have been difficult at some occasions. Furthermore I am thankful for a broad range of conversations on physics and things beyond physics I have had with my fellow students, supervisors and teachers. Also I am grateful that I have been supported in an ideological and financial way which helped me to find new motivation and to improve myself. Especially I want to thank those, who have made it possible to realize my semester abroad at the North Carolina State University. And last but not least I am oblige to thank those who have pushed and have motivated me during sports which has helped me to stay focused and balanced.

Appendix

A Contracted $SU(4)$ computations

A.1 Little group orbit identification

The analysis of the contracted $SU(4)$ representation heavily relies on the symmetry properties of the little group. To be able to define quantum expectation values, it is important to identify those values along the orbit. Thus one has to show that one can also identify the little group $\mathcal{G}_X$ at one point X with a little group $\mathcal{G}_{X_0}$ at another point X_0 on the same orbit $\mathcal{O}_X = \mathcal{O}_{X_0}$.

For $X \in \mathcal{O}_{X_0}$ one finds a pair $g_0, h_0 \in \mathfrak{su}(4)_C$ such that

$$X_0 = R_J(g_0) X R_I^{-1}(h_0)\,.$$

If the little group at X_0 is given by $\mathcal{G}_{X_0}$, then one finds $U_J(g)U_I(h) \in \mathcal{G}_{X_0}$ such that

$$X_0 = R_J(g) X_0 R_I^{-1}(h)\,.$$

The members of the little group at X, $U_J(g')U_I(h') \in \mathcal{G}_X$, can now be related to $U_J(g)U_I(h)$ by $g' = g_0^{-1} g g_0$ and h accordingly since

$$\begin{aligned} R_J(g_0^{-1}gg_0) X R_I^{-1}(h_0^{-1}hh_0) &= R_J(g_0^{-1}) R_J(g) X_0 R_I^{-1}(h) R_I^{-1}(h_0^{-1}) \\ &= R_J(g_0^{-1}) X_0 R_I^{-1}(h_0) \\ &= X\,. \end{aligned}$$

This fact is making it possible to specify one reference configuration X_0 for a given orbit $\mathcal{O}_{X_0}$ and relate all quantum numbers for another configuration X to the numbers at X_0.

A.2 Wigner 3J symbols and D-matrices

The explicit construction of baryonic contracted $SU(4)$ states is relying on representation theory of the little group for a specific configuration X_0. For the physical baryons, this group is given by $SU(2)$. Thus mathematical tools of $SU(2)$ representation theory, namely the Clebsch-Gordan coefficients and as a consequence Wigner D-matrices and Wigner $3J$-symbols, play a significant role for simplifying the construction of states.

A more detailed instruction to $SU(2)$ group theory tools as Wigner D-matrices and $3J$-symbols can be found in [Wigner and Griffin, 1959], which contains most of the proofs constituted in this section. Further identities can also be found in [Messiah, 1981].

For states which transform under $SU(2)$, a tensor product can be decomposed in a direct sum of irreducible representations. These representations can be expressed by the Wigner D-matrices of dimension $\dim(j_i) = 2j_i + 1$, where each $j_i \in \mathbb{N}/2$,

$$D^{(j_1)} \otimes D^{(j_2)} = \bigoplus_{j_3 = |\,j_1 - j_2\,|}^{j_1 + j_2} D^{(j_3)}\,.$$

Accordingly a set of states transforming in one of those irreducible representations can be expressed in the tensor basis by

$$|j_3, m_3\rangle = \sum_{m_1}\sum_{m_2} c^{j_1 j_2 j_3}_{m_1 m_2 m_3}\ |j_1, m_1\rangle \otimes |j_2, m_2\rangle =: \sum_{m_1}\sum_{m_2} c^{j_1 j_2 j_3}_{m_1 m_2 m_3}\ |j_1, m_1; j_2, m_2\rangle\ ,$$

which have to fulfill the conditions

$$\begin{aligned} |\, j_1 - j_2 \,| \leq j_3 \leq j_1 + j_2 \,, \qquad & j_1 + j_2 + j_3 \in \mathbb{Z} \,, \\ 0 = m_1 + m_2 - m_3 \,, \qquad & m_i \in \{\, -j_i, \, -j_i + 1, \, \cdots \,, j_i - 1, j_i \,\} \,. \end{aligned} \tag{A.1}$$

The Clebsch-Gordon coefficients $c^{j_1 j_2 j_3}_{m_1 m_2 m_3}$ can be extracted by projecting on the specific states and are directly related to the Wigner $3J$-symbols defined by

$$\begin{pmatrix} j_1 & j_2 & j_3 \\ m_1 & m_2 & -m_3 \end{pmatrix} := \frac{(-1)^{j_1 - j_2 + m_3}}{\sqrt{\dim(j_3)}} \, \langle j_1, m_1; j_2, m_2 \,|\, j_3, m_3 \rangle \,, \tag{A.2}$$

which also have to fulfill the conditions (A.1). Useful properties for the $3J$ symbols are given by

$$\begin{pmatrix} j_1 & j_2 & 0 \\ m_1 & m_2 & 0 \end{pmatrix} = \frac{(-1)^{j_1 - m_1}}{\sqrt{\dim(j_1)}} \delta_{j_1 j_2} \, \delta_{m_1 \, -m_2} \,, \tag{A.3}$$

and

$$\sum_{m_1 m_2} \begin{pmatrix} j_1 & j_2 & j \\ m_1 & m_2 & m \end{pmatrix} \begin{pmatrix} j_1 & j_2 & j' \\ m_1 & m_2 & m' \end{pmatrix} = \frac{1}{\dim(j)} \delta_{j j'} \, \delta_{m m'} \,, \tag{A.4}$$

which directly follow from the identities for matrix elements

$$\langle j_1, m_1; j_2, m_2 \,|\, 0{,}0 \rangle = \frac{(-1)^{j_1 - m_1}}{\sqrt{\dim(j_1)}} \delta_{j_1 j_2} \, \delta_{m_1 \, -m_2} \,,$$

and

$$\sum_{m_1 m_2} \langle j', m' \,|\, j_1, m_1; j_2, m_2 \rangle \, \langle j_1, m_1; j_2, m_2 \,|\, j, m \rangle = \delta_{j j'} \, \delta_{m m'} \,.$$

Furthermore it will be used that the $3J$-symbols are symmetric under cyclic permutations

$$\begin{pmatrix} j_1 & j_2 & j_3 \\ m_1 & m_2 & m_3 \end{pmatrix} = \begin{pmatrix} j_3 & j_1 & j_2 \\ m_3 & m_1 & m_2 \end{pmatrix} = \begin{pmatrix} j_2 & j_3 & j_1 \\ m_2 & m_3 & m_1 \end{pmatrix} \tag{A.5}$$

and changing the sign of all m_i will result in an overall factor

$$\begin{pmatrix} j_1 & j_2 & j_3 \\ m_1 & m_2 & m_3 \end{pmatrix} = (-1)^{j_1 + j_2 + j_3} \begin{pmatrix} j_1 & j_2 & j_3 \\ -m_1 & -m_2 & -m_3 \end{pmatrix} . \tag{A.6}$$

The Wigner $3J$-symbols are related to the Wigner D-matrices by the following condition

$$\int \mathrm{d}R \, D^{(j_1)}_{n_1 m_1}(R) \, D^{(j_2)}_{n_2 m_2}(R) \, D^{(j_3)}_{n_3 m_3}(R) = v \begin{pmatrix} j_1 & j_2 & j_3 \\ m_1 & m_2 & m_3 \end{pmatrix} \begin{pmatrix} j_1 & j_2 & j_3 \\ n_1 & n_2 & n_3 \end{pmatrix} . \tag{A.7}$$

The integral over R is the so-called Hurwitz integral over all generators of the group $SU(2)$ and the components of a Wigner D-matrix are the projection on the according states:

$$D^{(j)}_{nm}(R) := \langle j, n \,|\, U(R) \,|\, j, m \rangle \,. \tag{A.8}$$

For the proof of this identity one has to show that the Wigner D-matrices are orthogonal

$$\int \mathrm{d}R \, D^{(j_1)}_{n_1 m_1}(R) \, \left(D^{(j_2)}_{n_2 m_2}(R) \right)^* = \frac{v}{\dim(j_1)} \delta_{j_1 j_2} \, \delta_{n_1 n_2} \, \delta_{m_1 m_2} \tag{A.9}$$

and

$$\left(D^{(j_1)}_{nm}(h) \right)^* = D^{(j_1)}_{mn} \left(h^{-1} \right) = (-1)^{n-m} D^{(j_1)}_{-n-m}(h) \,. \tag{A.10}$$

Proof: Complex conjugated Wigner D-matrix.
The first part of equation (A.10) is relatively easy to see since it follows directly from the definition of $D^{(j)}_{nm}$ using the unitary property

$$\begin{aligned}\left(D^{(j)}_{nm}(h)\right)^* &:= \langle n \,|\, U(h) \,|\, m\rangle^* = \left\langle m \,\middle|\, U^\dagger(h) \,\middle|\, n \right\rangle = \left\langle m \,\middle|\, U^{-1}\,(h) \,\middle|\, n \right\rangle \\ &= D^{(j)}_{mn}\left(h^{-1}\right) .\end{aligned}$$

For the second part one has to use the explicit form of the $SU(2)$ representation in physics:

$$U(g) = \exp\left(ig\right) \quad \Rightarrow \quad U^{-1}(g) = \exp\left(-ig\right) = U(-g) .$$

The generators $g \in \mathfrak{su}(2)$ are defined by the operators J_z, J_+ and J_- with the action

$$\begin{aligned} J_z \cdot |j,m\rangle &= m\,|j,m\rangle \\ J_+ \cdot |j,m\rangle &= \lambda(m^2+m)\,|j,m+1\rangle \\ J_- \cdot |j,m\rangle &= \lambda(m^2-m)\,|j,m-1\rangle \ . \end{aligned}$$

Therefore one finds that

$$\langle j,m \,|\, J_z \,|\, j,m\rangle = m = \langle j,-m \,|\, -J_z \,|\, j,-m\rangle$$

and

$$\langle j,m\pm1 \,|\, J_\pm \cdot \,|\, j,m\rangle = \lambda(m^2 \pm m) = -\,\langle j,-m \,|\, -J_\pm \cdot \,|\, j,-(m\pm1)\rangle \ ,$$

since $m^2 \pm m = (-(m\pm1))^2 \pm (-(m\pm1))$, which is making it possible to identify the transposed matrix elements with non-transposed negative elements:

$$\left(D^{(j)}_{nm}\,(h)\right)^* = D^{(j)}_{mn}\,(-h) = (-1)^{n-m} D^{(j)}_{-n-m}\,(h) \ .$$

This is true since each term of a representation corresponds to a combination

$$\begin{aligned}&\langle j,m \,|\, J_- \,|\, j,m+1\rangle \,\langle j,m+1 \,|\, J_z \,|\, j,m+1\rangle \cdots \langle j,n+1 \,|\, J_+ \,|\, j,n\rangle \\ =&(-1)\,\langle j,-m-1 \,|\, -J_- \,|\, j,-m\rangle \,\langle j,-m-1 \,|\, -J_z \,|\, j,-m-1\rangle \cdots (-1)\,\langle j,-n \,|\, -J_+ \,|\, j,-n-1\rangle \ .\end{aligned}$$

Note that the factor $(-1)^{n-m}$ is correct since J_z does not change the sign and additional combinations of J_-J_+ correspond to a $(-1)^2$. Therefore one obtains equation (A.10). □

Proof: Wigner D-matrix orthogonality.
The proof for the orthogonality of Wigner D-matrices follows [Wigner and Griffin, 1959] and uses Schur's Lemma. The proof only uses the unitaryness of $SU(2)$ at the end and therefore could be extended to other Lie groups.

Lemma. *If one finds a matrix M which commutes with two representations $D^{(j_1)}(R)$ and $D^{(j_2)}(R)$ of the group $SU(2)$ for all generators $R \in \mathfrak{su}(2)$, then the matrix M must be a null matrix for $j_1 \neq j_2$ or proportional to the identity*

$$D^{(j1)}(R)M = MD^{(j_2)}(R) \quad \forall\, R \in \mathfrak{su}(2) \quad \Rightarrow \quad M = c\,\mathbb{1}\,\delta_{j_1 j_2} . \tag{A.11}$$

Thus, the matrix M, defined by

$$M := \int \mathrm{d}R\, D^{(j_1)}(R) X D^{(j_2)}(R^{-1}) ,$$

where X is an arbitrary matrix such that the multiplication is well defined, fulfills Schur's lemma and thus must be proportional to the identity or null.

$$\begin{aligned} D^{(j_1)}(S)M &= \int \mathrm{d}R\, D^{(j_1)}(SR) X D^{(j_2)}(R^{-1}S^{-1}) D^{(j_2)}(S) \\ &= MD^{(j_2)}(S) \end{aligned}$$

where one has substituted $R \mapsto R' = SR$. Since this has to be true for all X, the matrix M is of the form $M = \delta_{j_1 j_2} c(X)\, \mathbb{1}$. Accordingly one gets the equation for the components

$$\delta_{j_1 j_2}\, \delta_{n_1 n_2}\, c(X) = \sum_{m_1 m_2} X_{m_1 m_2} \int \mathrm{d}R\, D^{(j_1)}_{n_1 m_1}(R) D^{(j_2)}_{m_2 n_2}(R^{-1})\,.$$

Since one has the freedom of choosing X, the constant $c(X)$ can be defined by $c(X) = \sum_{m_1 m_2} c_{m_1 m_2}(X) X_{m_1 m_2}$. As an example $X_{m_1 m_2} = \delta_{a m_1} \delta_{b m_2}$ fixes $c_{ab}(X) = c(X)$. This finally results in the equation

$$\delta_{j_1 j_2}\, \delta_{n_1 n_2}\, c_{m_1 m_2} = \int \mathrm{d}R\, D^{(j_1)}_{n_1 m_1}(R) D^{(j_2)}_{m_2 n_2}(R^{-1})\,.$$

Now choosing $n_1 = n = n_2$ and summing over all n results in a matrix multiplication on the left-hand-side

$$\begin{aligned}\delta_{j_1 j_2}\, c_{m_1 m_2} \dim(j_1) &= \int \mathrm{d}R \sum_n D^{(j_2)}_{m_2 n}(R^{-1}) D^{(j_1)}_{n m_1}(R) \\ &= \delta_{j_1 j_2}\, \delta_{m_1 m_2} \int \mathrm{d}R\,.\end{aligned}$$

Thus, if one defines the volume of the group $v = \int \mathrm{d}R$ one obtains

$$\begin{aligned}\int \mathrm{d}R\, D^{(j_1)}_{n_1 m_1}(R) D^{(j_2)}_{m_2 n_2}(R^{-1}) &= \int \mathrm{d}R\, D^{(j_1)}_{n_1 m_1}(R) \left(D^{(j_2)}_{n_2 m_2}(R)\right)^* \\ &= \frac{v}{\dim(j_1)} \delta_{j_1 j_2}\, \delta_{n_1 n_2}\, \delta_{m_1 m_2}\,,\end{aligned}$$

where it was used that the representation is unitary (A.10). □

Proof: Wigner D-matrix to Wigner 3J-symbol relation.
Acting with a unitary representation of $SU(2)$ on tensor states will result in

$$\langle j_1, n_1; j_2, n_2 \,|\, U(R) \,|\, j_1, m_1; j_2, m_2 \rangle = D^{(j_1)}_{n_1 m_1}(R) D^{(j_2)}_{n_2 m_2}(R)\,.$$

On the other hand, when inserting two identity operators $\mathbb{1} = \sum_{jm} |j, m\rangle \langle j, m|$ one obtains

$$\begin{aligned}D^{(j_1)}_{n_1 m_1}(R) D^{(j_2)}_{n_2 m_2}(R) &= \sum_{jj'} \sum_{mn} \langle j_1, n_1; j_2, n_2 \,|\, j', n\rangle \langle j', n \,|\, U(R) \,|\, j, m\rangle \langle j, m \,|\, j_1, m_1; j_2, m_2\rangle \\ &= \sum_{j} \sum_{mn} \langle j_1, n_1; j_2, n_2 \,|\, j, n\rangle\, D^{(j)}_{nm}(R)\, \langle j, m \,|\, j_1, m_1; j_2, m_2\rangle \\ &= \sum_{j} \sum_{mn} \dim(j)\, (-1)^N \begin{pmatrix} j_1 & j_2 & j \\ n_1 & n_2 & -n \end{pmatrix} D^{(j)}_{nm}(R) \begin{pmatrix} j_1 & j_2 & j \\ m_1 & m_2 & -m \end{pmatrix},\end{aligned}$$

with $N = 2j_1 - 2j_2 + m + n$. It was used that Clebsch-Gordan coefficients are real. Multiplying this equation with the matrix $\left(D^{(j_3)}_{n_3 m_3}(R)\right)^*$, integrating over R and using the orthogonality relation (A.9) one gets

$$\int \mathrm{d}R\, D^{(j_1)}_{n_1 m_1}(R)\, D^{(j_2)}_{n_2 m_2}(R)\, \left(D^{(j_3)}_{n_3 m_3}(R)\right)^* = v(-1)^N \begin{pmatrix} j_1 & j_2 & j_3 \\ n_1 & n_2 & -n_3 \end{pmatrix} \begin{pmatrix} j_1 & j_2 & j_3 \\ m_1 & m_2 & -m_3 \end{pmatrix}.$$

If one furthermore uses the second part of (A.10) and substitutes m_3,$n_3 \mapsto -m_3, -n_3$ one gets the final result

$$\int \mathrm{d}R\, D^{(j_1)}_{n_1 m_1}(R)\, D^{(j_2)}_{n_2 m_2}(R)\, D^{(j_3)}_{n_3 m_3}(R) = v \begin{pmatrix} j_1 & j_2 & j_3 \\ n_1 & n_2 & n_3 \end{pmatrix} \begin{pmatrix} j_1 & j_2 & j_3 \\ m_1 & m_2 & m_3 \end{pmatrix},$$

since $2(j_1 - j_2 + m) \in 2\mathbb{Z}$ because of the Clebsch-Gordan conditions (A.1) one can conclude that $j_1 - j_2 + m \in \mathbb{Z}$. □

A.3 Baryonic states in contracted $SU(4)$ symmetry

To find the relation

$$|B;K\rangle := |I,i;J,j;K\rangle \ ,$$

one can start by expressing the $SU(4)_C$ weights such that they properly transform under isospin transformations

$$|I\,,i\,,m\,;\,K\,,k\rangle := \int \mathrm{d}g\, D^{(I)}_{mi}\left(g^{-1}\right) U_I\,(g)\,|X_0\,;\,K\,,k\rangle \ . \tag{A.12}$$

Therefore the isospin transformation is given by

$$\begin{aligned}
U_I(h)\,|I\,,i\,,m\,;\,K\,,k\rangle &= \int \mathrm{d}g\, D^{(I)}_{mi}\left(g^{-1}\right) U_I\,(h)\,U_I\,(g)\,|X_0\,;\,K\,,k\rangle \\
&= \int \mathrm{d}g\, D^{(I)}_{mi}\left(g^{-1}\right) U_I(hg)\,|X_0\,;\,K\,,k\rangle \\
&= \int \mathrm{d}g'\, D^{(I)}_{mi}\left((g')^{-1}h\right) U_I(g')\,|X_0\,;\,K\,,k\rangle \\
&= \sum_{i'} \int \mathrm{d}g'\, D^{(I)}_{mi'}\left((g')^{-1}\right) D^{(I)}_{i'i}\,(h)\,U_I(g')\,|X_0\,;\,K\,,k\rangle \\
&= \sum_{i'} |I\,,i'\,,m\,;\,K\,,k\rangle\, D^{(I)}_{i'i}\,(h) \ .
\end{aligned}$$

The normalization of this states is given by

$$\begin{aligned}
\langle I',i'_3,m';K,k'\,|\,I,i_3,m;K,k\rangle &= \int \mathrm{d}g' \int \mathrm{d}g\, \left(D^{(I')}_{m'i'_3}\left((g')^{-1}\right)\right)^* D^{(I)}_{mi_3}\left(g^{-1}\right) \delta\left(g'g^{-1}\right) \delta_{kk'} \\
&= \delta_{kk'} \int \mathrm{d}g\, \left(D^{(I')}_{m'i'_3}(g)\right)^* D^{(I)}_{mi_3}\,(g) \\
&= \frac{h}{\dim(I)} \delta_{II'}\,\delta_{kk'}\,\delta_{ii'}\,\delta_{mm'} \ ,
\end{aligned} \tag{A.13}$$

where the normalization of $SU(4)_C$ states (4.48) and the orthogonality of Wigner D-matrices (A.9) was used. Furthermore it is important to mention that conjugating of states (dagger operation) acts as a complex conjugation for Fock-space scalars like the Wigner D-matrices.

Next, one should analyze the spin transformation of the states defined by (A.12). Applying a spin transformation one obtains

$$\begin{aligned}
U_J(h)\,|I,i_3,m;K,k\rangle &= \int \mathrm{d}g\, D^{(I)}_{mi_3}\left(g^{-1}\right) U_I(g)U_J(h)\,|X_0\,;\,K\,,k\rangle \\
&= \sum_{k'} \int \mathrm{d}g\, D^{(I)}_{mi_3}\left(g^{-1}\right) U_I(g)U_I^\dagger(h)U_K(h)\,|X_0\,;\,K\,,k\rangle \\
&= \sum_{k'} \int \mathrm{d}g\, D^{(I)}_{mi_3}\left(g^{-1}\right) U_I(gh^{-1})\,|X_0\,;\,K\,,k'\rangle\, D^{(K)}_{k'k}(h) \\
&= \sum_{k'm'} D^{(I)}_{mm'}\left(h^{-1}\right) |I,i_3,m';K,k'\rangle\, D^{(K)}_{k'k}(h) \\
&= \sum_{k'm'} |I,i_3,m';K,k'\rangle\, D^{(K)}_{k'k}(h) \left(D^{(I)}_{m'm}\,(h)\right)^* \ ,
\end{aligned}$$

where (A.10) was used. Accordingly one can see that these states transform under spin rotation as a $2K+1$ dimensional $SU(2)$-representation in the k' component and as $2I+1$ dimensional $SU(2)$-complex-conjugated-representation in the m' component. Therefore the states defined by

$$|I,i;J,j;K\rangle := \sum_{km} c^{IJK}_{mjk}\ |I,i,m;K,k\rangle \ . \tag{A.14}$$

have to transform according to

$$\sum_{kmj'} c^{IJK}_{mj'k}\,|I,i,m;K,k\rangle\,D^{(J)}_{j'j}(h) \stackrel{!}{=} \sum_{kk'mm'} c^{IJK}_{mjk}\,|I,i_3,m';K,k'\rangle\,D^{(K)}_{k'k}(h)\left(D^{(I)}_{m'm}(h)\right)^* .$$

Multiplying with another spin matrix $\left(D^{(J)}_{ab}(h)\right)^*$, relabeling the sums, integrating over h and using the orthogonality condition (A.9) one obtains

$$\frac{v}{\dim(J)}\,c^{IJK}_{mak}\,\delta_{jb} = \sum_{k'm'} c^{IJK}_{m'jk'}\int \mathrm{d}h\,D^{(K)}_{kk'}(h)\left(D^{(I)}_{mm'}(h)\right)^*\left(D^{(J)}_{ab}(h)\right)^* ,$$

which can be simplified by using (A.10), (A.7), (A.6), dividing by v, setting $b = j$ and summing over all j

$$\begin{aligned} c^{IJK}_{mak} &= \sum_{k'm'j} c^{KJI}_{k'jm'}(-1)^{m+a-m'-j}\begin{pmatrix} I & J & K \\ m & a & -k\end{pmatrix}\begin{pmatrix} I & J & K \\ m' & j & -k'\end{pmatrix} \\ &= e^{i\pi k}\begin{pmatrix} I & J & K \\ m & a & -k\end{pmatrix} c\,, \end{aligned}$$

where the sum over the $3J$-symbol and the Clebsch-Gordan coefficient is expressed as the constant c (which is in principle depending on the dimension of the representations). The constant c can be found by requiring the proper normalization of the baryonic states

$$|I,i_3;J,j_3;K\rangle = c\sum_{km} e^{i\pi k}\begin{pmatrix} I & J & K \\ m & j & -k\end{pmatrix}|I,i,m;K,k\rangle\ . \tag{A.15}$$

The normalization can be found by solving

$$\begin{aligned} \delta_{II'}\,\delta_{ii'}\,\delta_{JJ'}\,\delta_{jj'} = |\,c\,|^2 \sum_{kk'mm'} e^{i\pi(k-k')}&\begin{pmatrix} I' & J' & K \\ m' & j' & -k'\end{pmatrix}\begin{pmatrix} I & J & K \\ m & j & -k\end{pmatrix} \\ &\times\langle I',i_3',m';K,k'\,|\,I,i_3,m;K,k\rangle \\ \stackrel{(A.13)}{=}\ \frac{v}{\dim(I)}\,|\,c_N\,|^2\,\delta_{II'}\,\delta_{ii'}&\sum_{km}\begin{pmatrix} I & J' & K \\ m & j' & -k\end{pmatrix}\begin{pmatrix} I & J & K \\ m & j & -k\end{pmatrix} \\ \stackrel{(A.4)}{=}\ \frac{v}{\dim(I)\dim(J)}\,|\,c_N\,|^2\,&\delta_{II'}\,\delta_{ii'}\,\delta_{JJ'}\,\delta_{jj'}\,. \end{aligned}$$

The normalized states are thus given by

$$\begin{aligned} |I,i;J,j;K\rangle &= \sqrt{\frac{\dim(I)\dim(J)}{v}}\sum_{km} e^{i\pi k}\begin{pmatrix} I & J & K \\ m & j & -k\end{pmatrix}|I,i,m;K,k\rangle \qquad (A.16) \\ &= \sqrt{\frac{\dim(I)\dim(J)}{v}}\sum_{km} e^{i\pi k}\begin{pmatrix} I & J & K \\ m & j & -k\end{pmatrix}\int \mathrm{d}g\,D^{(I)}_{mi}\left(g^{-1}\right)U_I(g)\,|X_0\,;\,K\,,k\rangle\ . \end{aligned}$$

A.4 Matrix elements of spin-isospin operator

The matrix element of the spin-isospin operators

$$\left\langle I',i';J',j';K'\right|\left.X_0^{ia}\right|\left.I,i_3;J,j_3;K\right\rangle \tag{A.17}$$

are proportional to the following sums

$$\sum_{kk'mm'} e^{i\pi(k-k')}\begin{pmatrix} I' & J' & K' \\ m' & j' & -k'\end{pmatrix}\begin{pmatrix} I & J & K \\ m & j & -k\end{pmatrix}\langle I',i',m';K',k'\,|\,X_0^{na}\,|\,I,i,m;K,k\rangle\ . \tag{A.18}$$

Evaluating the matrix element in the X_0 basis one obtains

$$\begin{aligned}
&\langle I',i',m';K',k' \,|\, X_0^{na} \,|\, I,i,m;K,k\rangle \\
&= \int \mathrm{d}g \int \mathrm{d}h \left(D^{(I')}_{m'i'}\left(h^{-1}\right)\right)^* D^{(I)}_{mi}\left(g^{-1}\right) \left\langle X_0;K',k' \,\middle|\, U_I^\dagger(h) X_0^{na} U_I(g) \,\middle|\, X_0;K,k\right\rangle \\
&= \sum_b \int \mathrm{d}g \int \mathrm{d}h \left(D^{(I')}_{m'i'}\left(h^{-1}\right)\right)^* D^{(I)}_{mi}\left(g^{-1}\right) D^{(1)}_{ab}(h) \left\langle X_0;K',k' \,\middle|\, X_0^{nb} U_I^\dagger(h) U_I(g) \,\middle|\, X_0;K,k\right\rangle \\
&= \sum_b \int \mathrm{d}g\, D^{(I')}_{i'm'}(g) \left(D^{(I)}_{im}(g)\right)^* D^{(1)}_{ab}(g)\, \delta_{KK'}\, \delta_{kk'}\, \delta_{nb}\ ,
\end{aligned}$$

where the normalization of the states, the inverse transformation behavior of X_0^{ia} and the explicit form of $X_0^{ia} = \mathrm{diag}(1,1,1)$ was used. Using identity (A.10) and (A.7) the sum finally becomes

$$\delta_{KK'} \sum_{kmm'} (-1)^{i-m} \begin{pmatrix} I' & J' & K \\ m' & j' & -k \end{pmatrix} \begin{pmatrix} I & J & K \\ m & j & -k \end{pmatrix} \begin{pmatrix} I' & 1 & I \\ m' & n & -m \end{pmatrix} \begin{pmatrix} I' & 1 & I \\ i' & a & -i \end{pmatrix} . \tag{A.19}$$

The last equation is proofing that one is not able to mix different K sectors with a spin-isospin operation. To resolve this equation for the $K = 0$ sector, one can transfer the $3J$-symbols back to Clebsch-Gordon matrix elements using identity

$$\begin{pmatrix} I & J & 0 \\ m & j & 0 \end{pmatrix} = \frac{(-1)^{I-m}}{\sqrt{\dim(I)}} \delta_{IJ}\, \delta_{m\,-j}\,.$$

The final result for the matrix Element is therefore given by

$$\langle I',i';J',j';0 \,|\, X_0^{na} \,|\, I,i;J,j;0\rangle = \frac{\sqrt{\dim(J)\dim(J')}}{v} \begin{pmatrix} J' & 1 & J \\ -j' & n & j \end{pmatrix} \begin{pmatrix} I' & 1 & I \\ i' & a & -i \end{pmatrix} , \tag{A.20}$$

for representations with $I = J$ and $I' = J'$. Furthermore one can proof that this relation forms the $SU(4) \to SU(2) \otimes SU(2)$ algebra for states with $I' = I = 1/2 = J = J'$. The equation (A.20) can be factorized as

$$\begin{aligned}
\langle I,i';J,j';0 \,|\, X_0^{na} \,|\, I,i;J,j;0\rangle &= \langle I,i' \,|\, X_0^a \,|\, I,i\rangle \, \langle J,j' \,|\, X_0^n \,|\, J,j\rangle \\
&\overset{(A.2)}{=} \frac{(-1)^a}{\sqrt{3}} \langle I,-i';I,i \,|\, 1,a\rangle \, \frac{(-1)^n}{\sqrt{3}} \langle J,j';J,-j;\,|\, 1,n\rangle\ .
\end{aligned}$$

Explicitly creating the representations one gets that states, as a tensor product of $D^{(1/2)} \otimes D^{(1/2)}$, are proportional to the direct sum $D^{(1)} \oplus D^{(0)}$. The states in the three-dimensional spin-one representation hereby generate the $SU(2)$ algebra in form of Pauli matrices

$$\begin{aligned}
\delta_{i'\uparrow}\,\delta_{i\downarrow} &= \left\langle \tfrac{1}{2},-i';\tfrac{1}{2},i \,\middle|\, 1,-1\right\rangle &&\mapsto \quad \tau^+ = \tfrac{1}{2}\left(\tau^1 + i\tau^2\right) \\
\delta_{i'\downarrow}\,\delta_{i\uparrow} &= \left\langle \tfrac{1}{2},-i';\tfrac{1}{2},i \,\middle|\, 1,1\right\rangle &&\mapsto \quad \tau^- = \tfrac{1}{2}\left(\tau^1 - i\tau^2\right)\ . \\
\tfrac{1}{\sqrt{2}}\left(\delta_{i'\uparrow}\,\delta_{i\uparrow} + \delta_{i'\downarrow}\,\delta_{i\downarrow}\right) &= \left\langle \tfrac{1}{2},-i';\tfrac{1}{2},i \,\middle|\, 1,0\right\rangle &&\mapsto \quad \mathbb{1}
\end{aligned}$$

Accordingly the set of operators corresponding to the pure nucleonic matrix elements of X_0^{ia} spans the basis

$$\left\langle N' \,\middle|\, X_0^{ia} \,\middle|\, N\right\rangle \in \left\{\sigma^+,\sigma^-,\mathbb{1}\right\} \otimes \left\{\tau^+,\tau^-,\mathbb{1}\right\}\ , \tag{A.21}$$

which generates the complete embedding $SU(2) \otimes SU(2) \mapsto SU(4)$ since e.g.

$$\left[\, J^+\,,\, J^-\,\right] := \left[\, \sigma^+ \otimes \mathbb{1}\,,\, \sigma^- \otimes \mathbb{1}\,\right] = \left[\, \sigma^+\,,\, \sigma^-\,\right] \otimes \mathbb{1} = \sigma^3 \otimes \mathbb{1} =: J^3\,.$$

B Pion exchange diagrams

B.1 Two-pion exchange diagrams

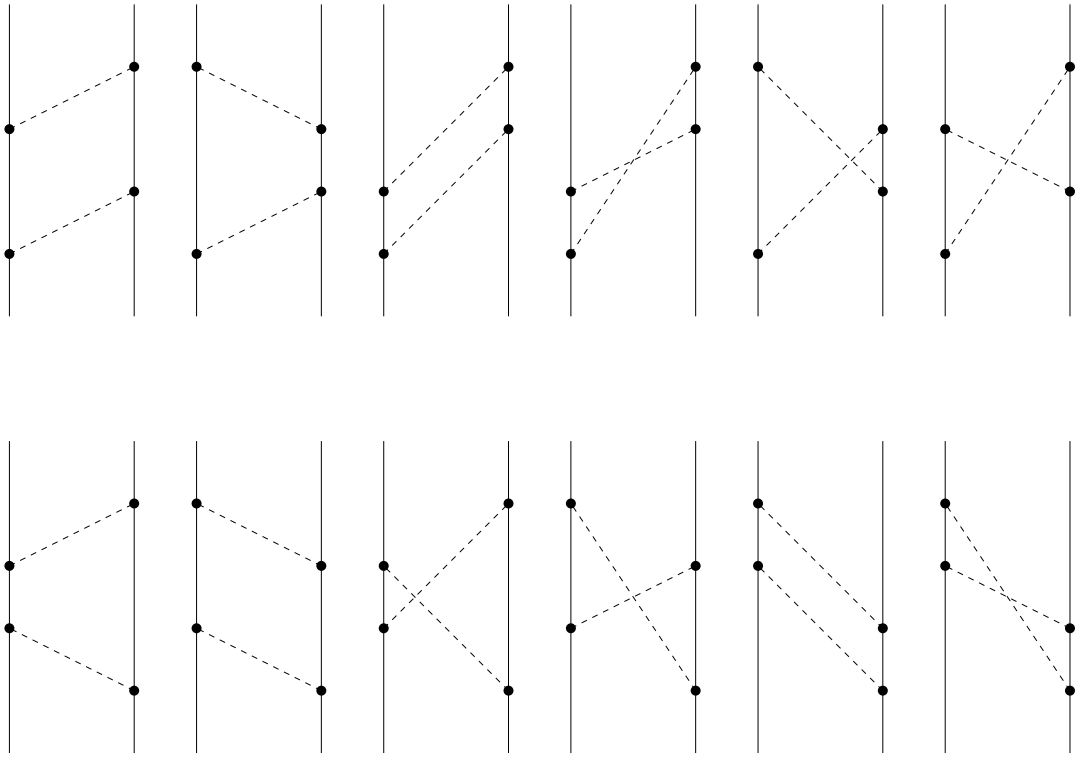

Figure B.1: Diagrams contributing to the two-pion exchange ($\nu = 2$) without seagull vertices (at order g_A^4).

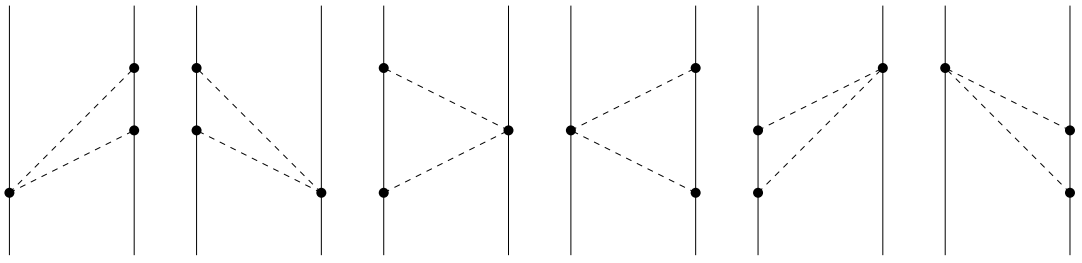

Figure B.2: Diagrams contributing to the two-pion exchange ($\nu = 2$) with one seagull vertex (at order g_A^2).

B.2 Three-pion exchange diagrams

B.2.1 Diagrams without seagull vertex

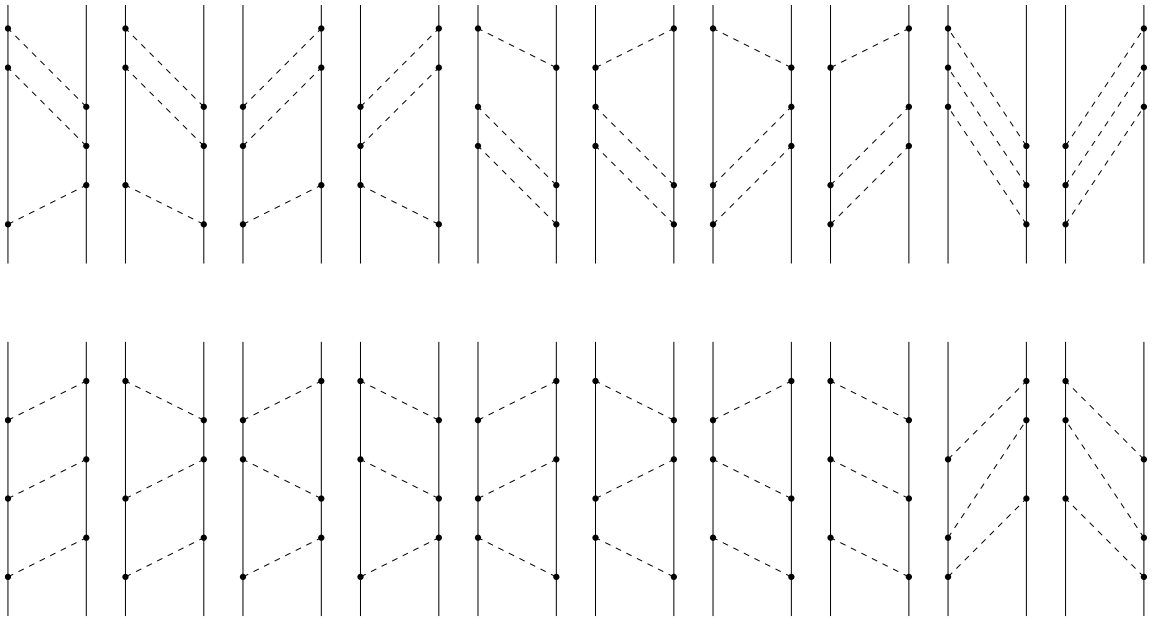

Figure B.3: Double-box diagrams contributing to the three-pion exchange at order g_A^6.

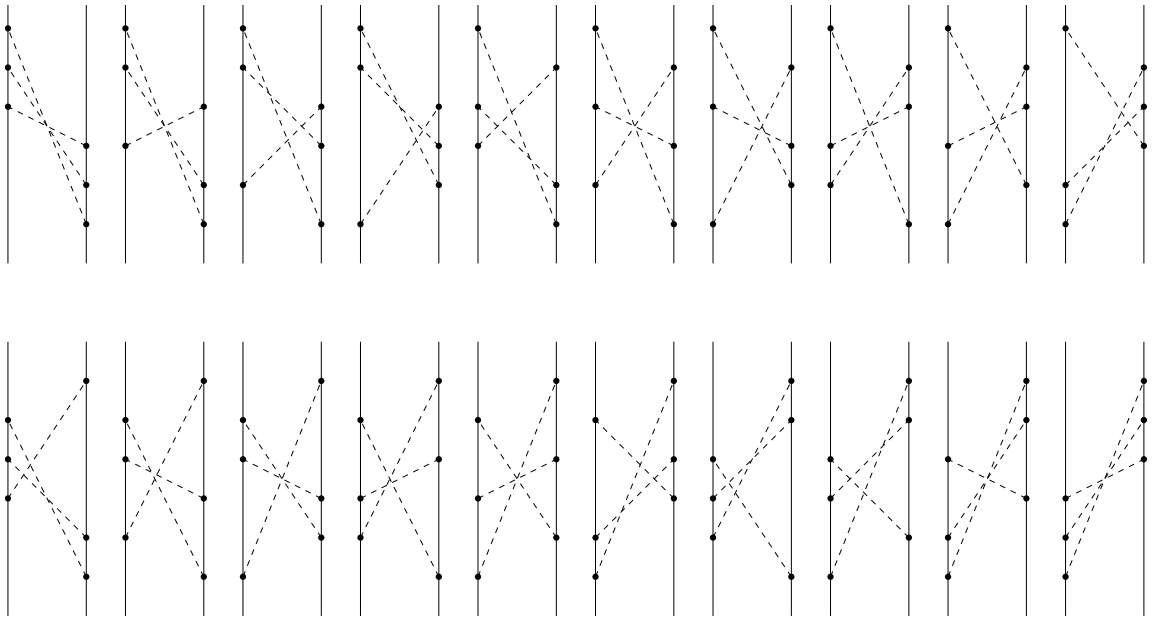

Figure B.4: Slashed cross-box diagrams contributing to the three-pion exchange at order g_A^6.

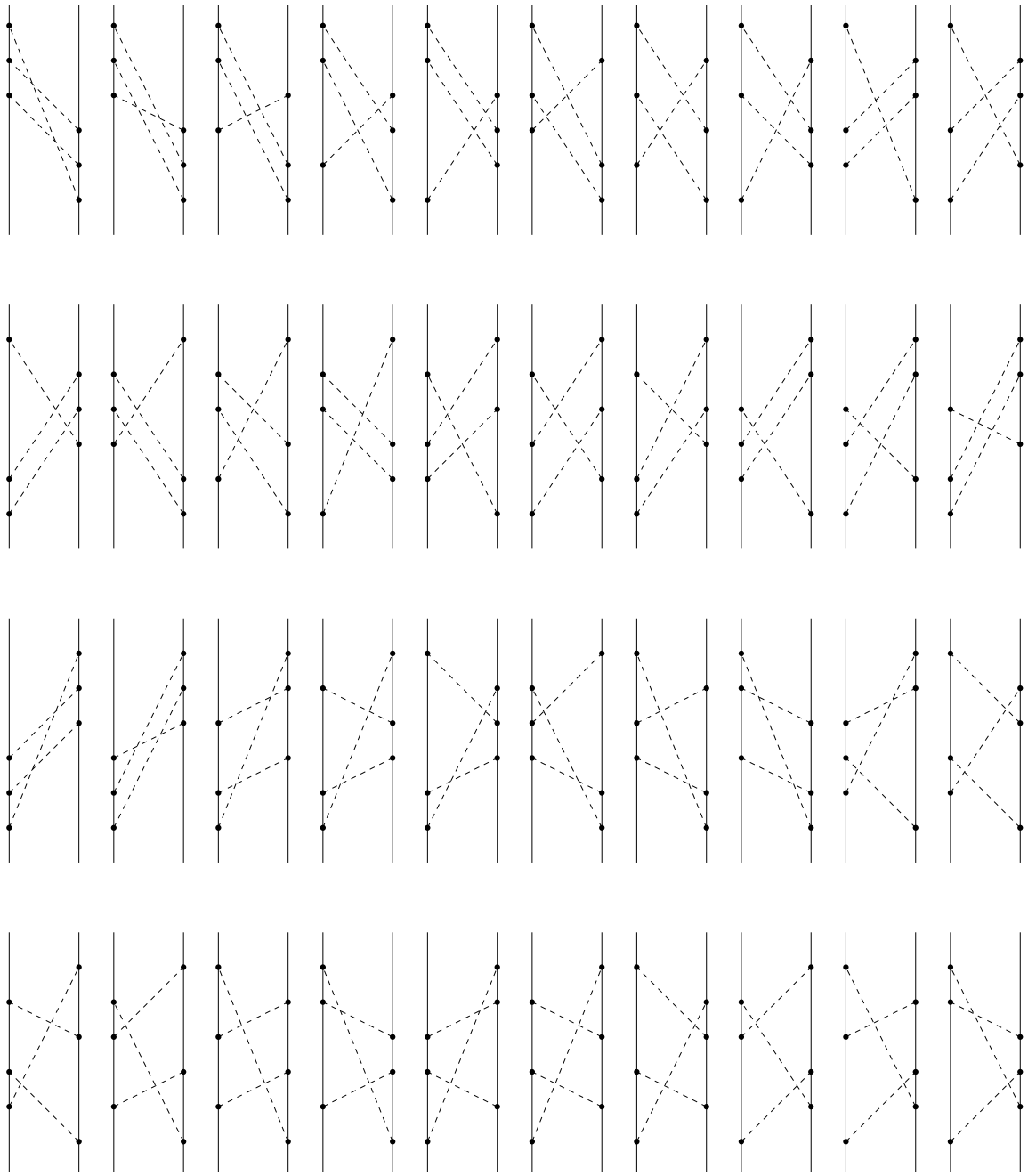

Figure B.5: Slashed box diagrams contributing to the three-pion exchange at order g_A^6.

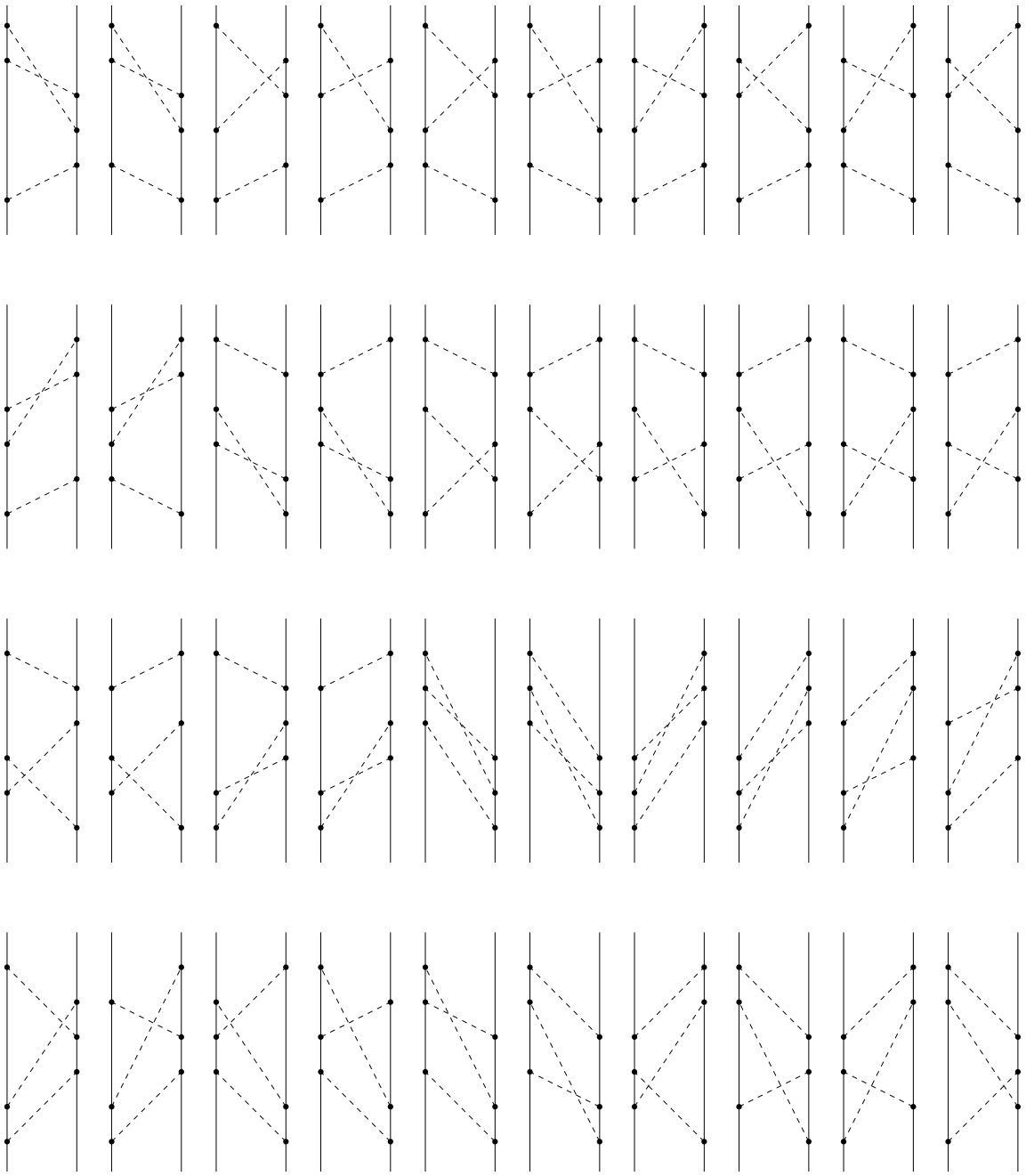

Figure B.6: Diagrams with just one crossed pion-line contributing to the three-pion exchange at order g_A^6.

B.2.2 Diagrams with one seagull vertex

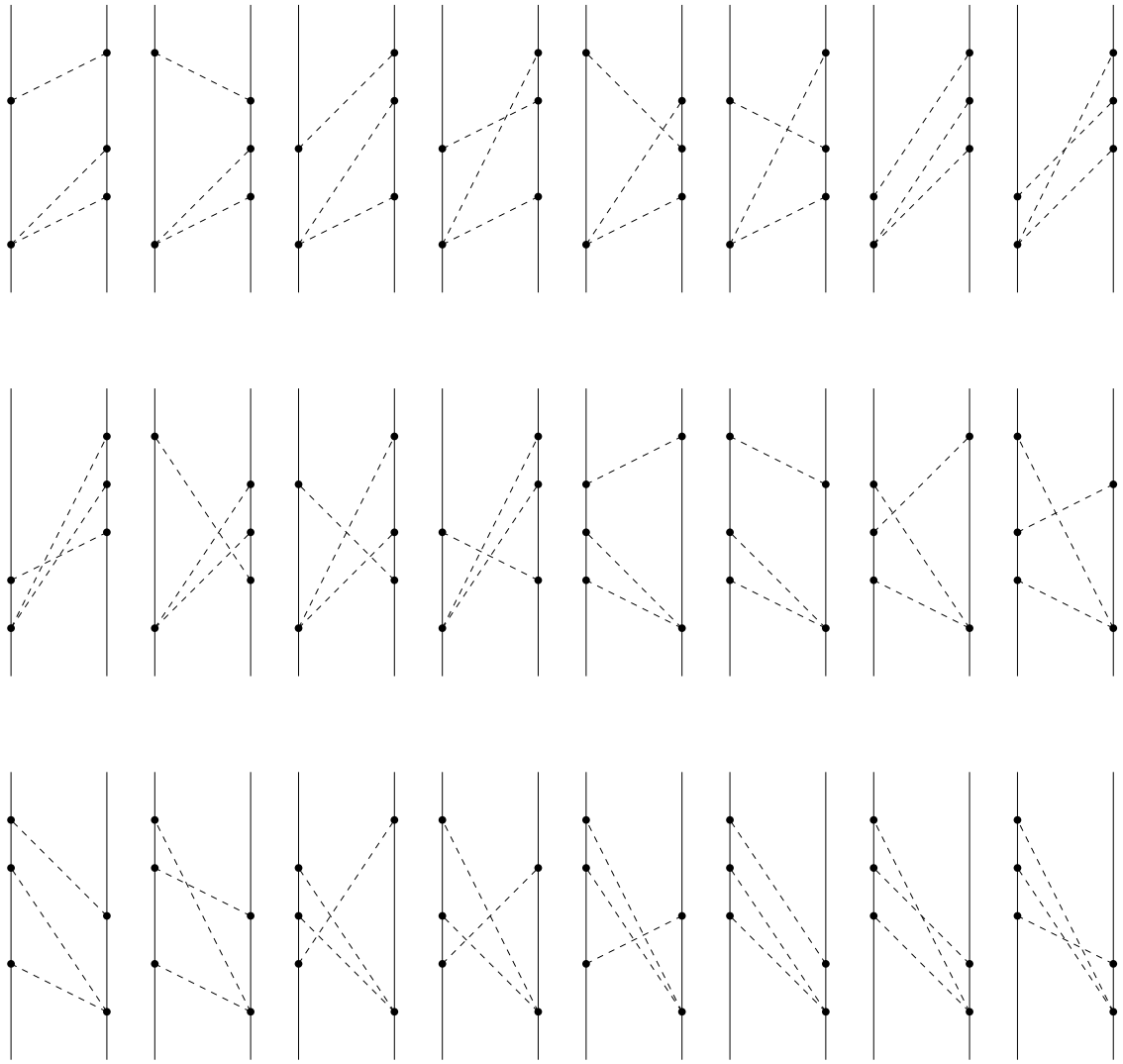

Figure B.7: Diagrams contributing to the three-pion exchange at order g_A^4 with seagull pion-exchange as first exchange.

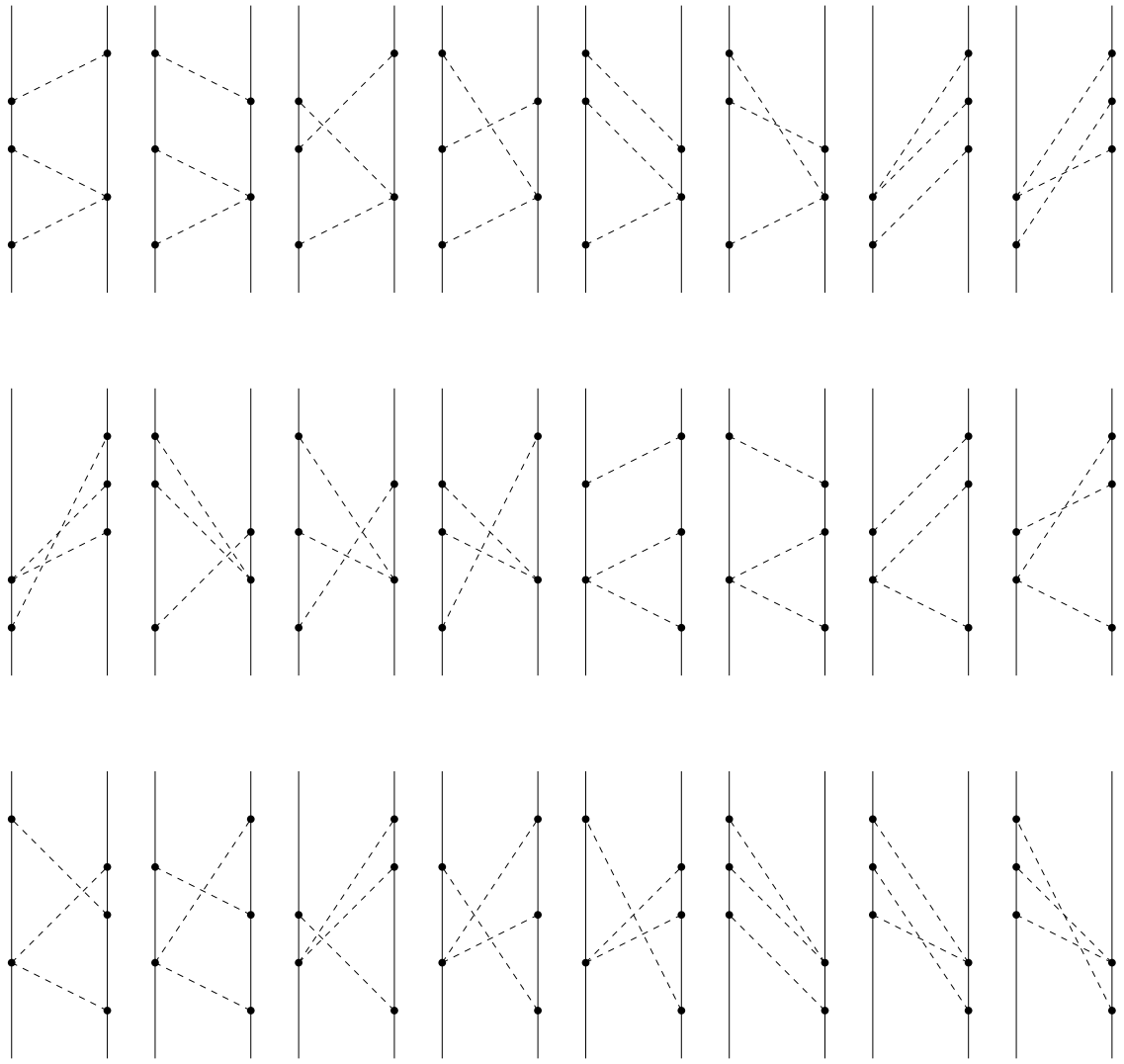

Figure B.8: Diagrams contributing to the three-pion exchange at order g_A^4 with seagull pion-exchange as second exchange.

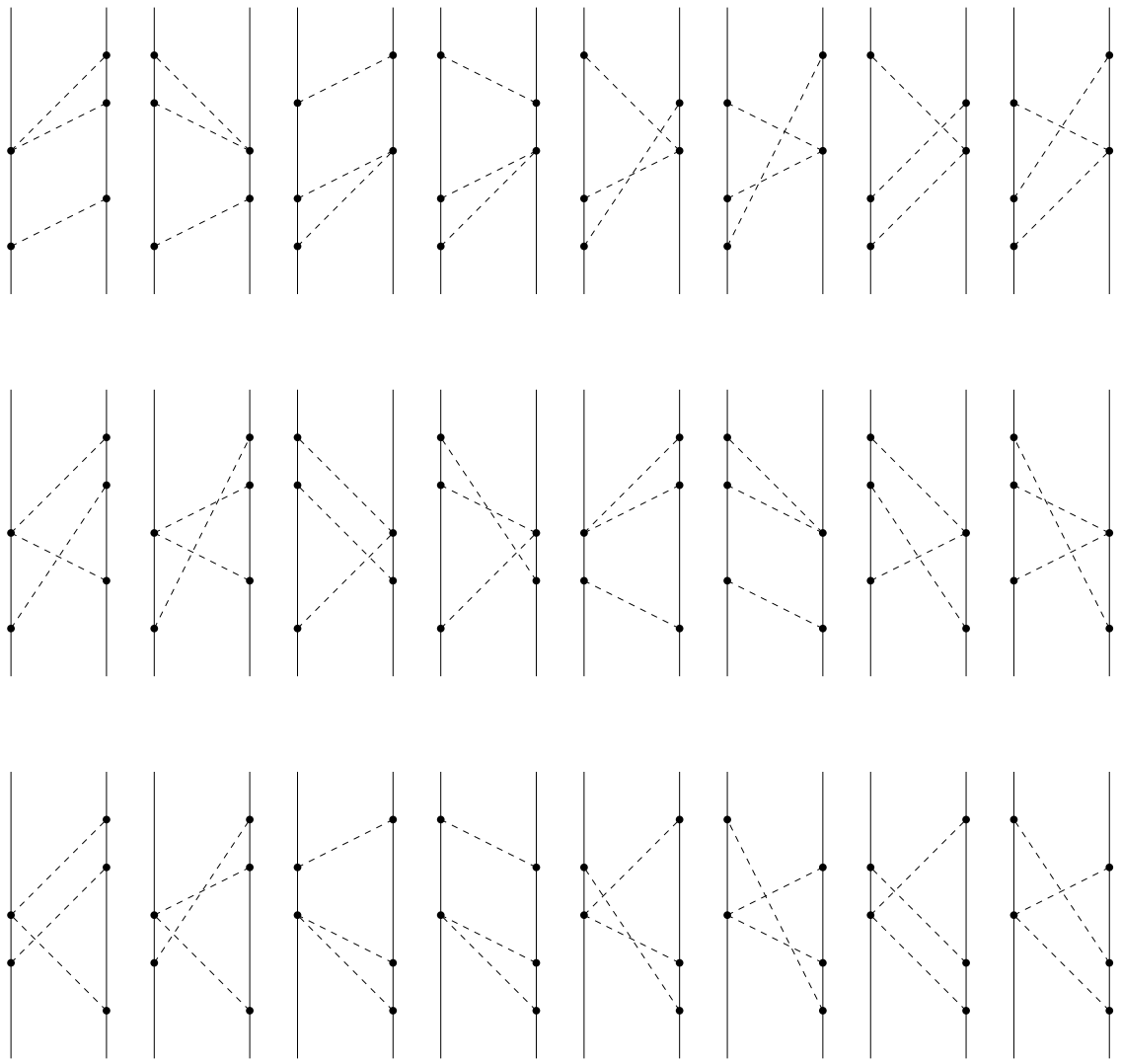

Figure B.9: Diagrams contributing to the three-pion exchange at order g_A^4 with seagull pion-exchange as third exchange.

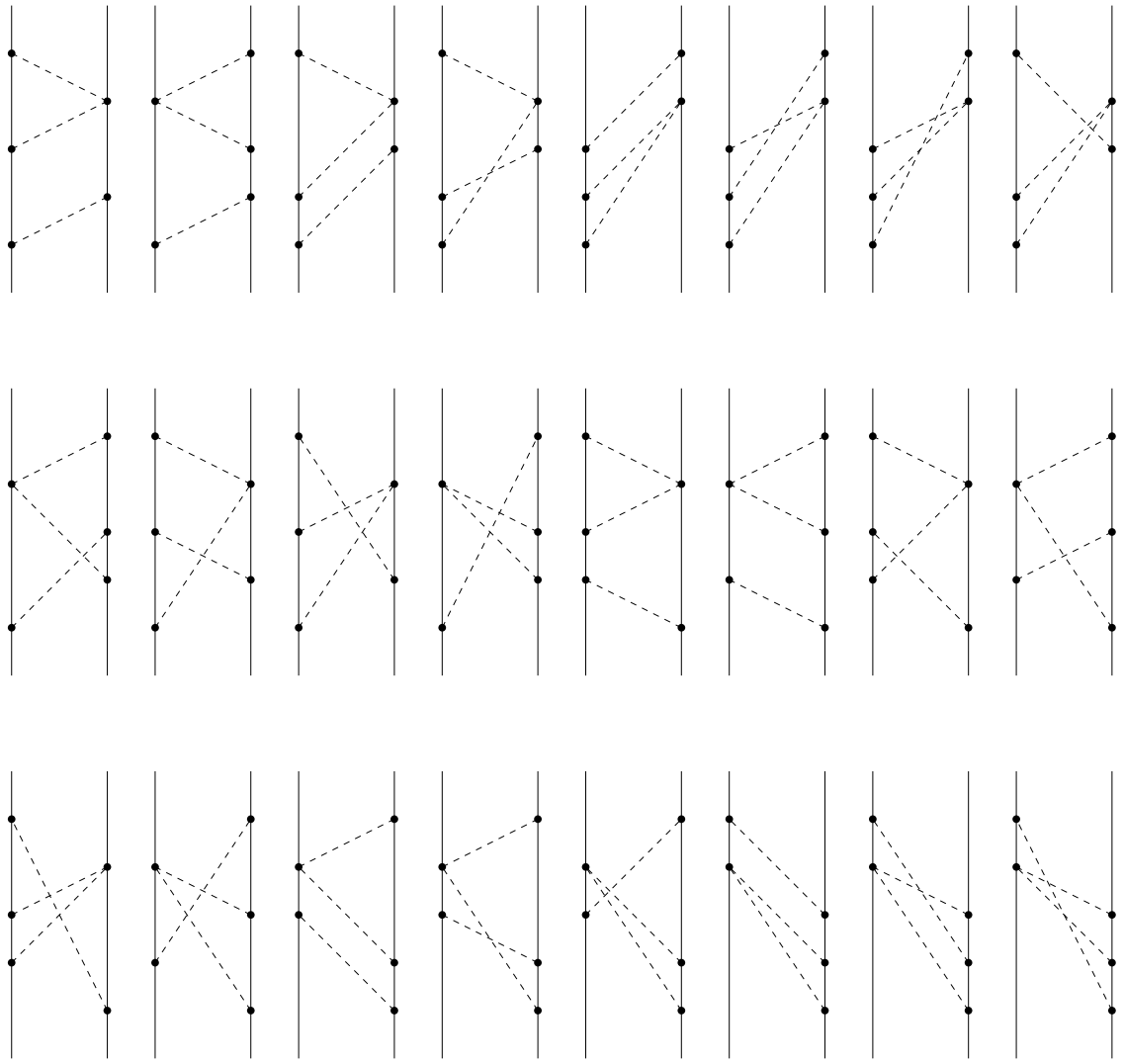

Figure B.10: Diagrams contributing to the three-pion exchange at order g_A^4 with seagull pion-exchange as second last exchange.

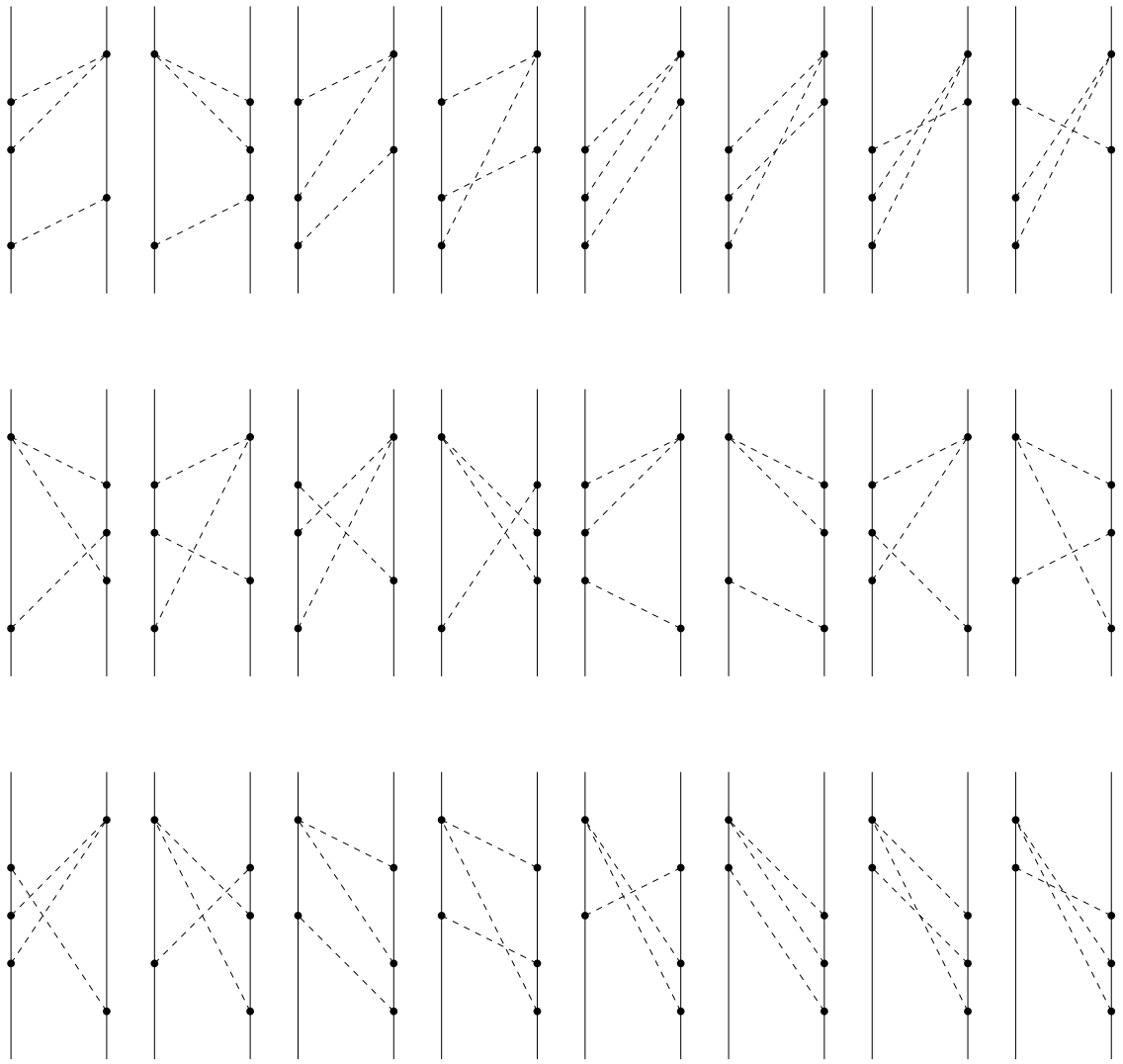

Figure B.11: Diagrams contributing to the three-pion exchange at order g_A^4 with seagull pion-exchange as last exchange.

B.2.3 Diagrams with two seagull vertices

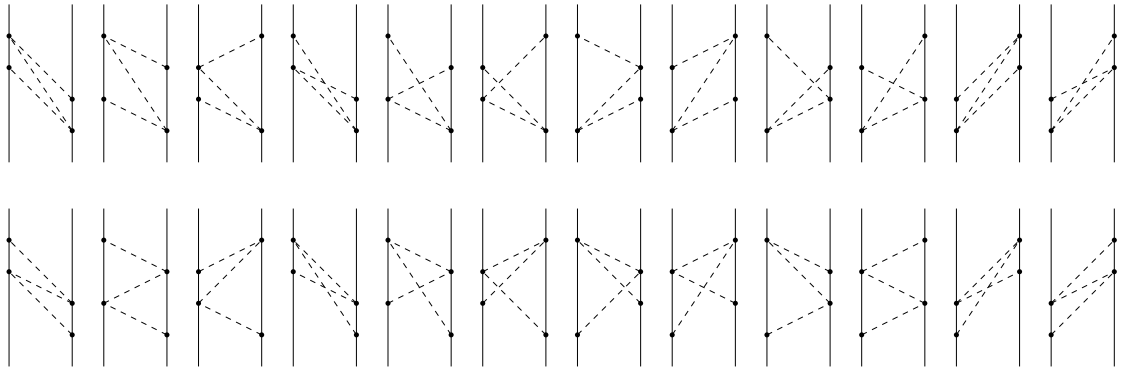

Figure B.12: Diagrams contributing to the three-pion exchange at order g_A^2.

Bibliography

[Banerjee et al., 2002] Banerjee, M. K., Cohen, T. D., and Gelman, B. A. (2002). The Nucleon nucleon interaction and large N(c) QCD. *Phys.Rev.*, C65:034011.

[Belitsky and Cohen, 2002] Belitsky, A. V. and Cohen, T. (2002). The Large N(c) nuclear potential puzzle. *Phys.Rev.*, C65:064008.

[Beringer et al., 2012] Beringer, J. et al. (2012). Review of Particle Physics (RPP). *Phys.Rev.*, D86:010001.

[Callan et al., 1969] Callan, C. G., Coleman, S., Wess, J., and Zumino, B. (1969). Structure of phenomenological lagrangians. ii. *Phys. Rev.*, 177:2247–2250.

[Cohen, 2002] Cohen, T. D. (2002). Resolving the large N(c) nuclear potential puzzle. *Phys.Rev.*, C66:064003.

[Coleman et al., 1969] Coleman, S., Wess, J., and Zumino, B. (1969). Structure of phenomenological lagrangians. i. *Phys. Rev.*, 177:2239–2247.

[Dashen et al., 1994] Dashen, R. F., Jenkins, E. E., and Manohar, A. V. (1994). The 1/N(c) expansion for baryons. *Phys.Rev.*, D49:4713.

[Epelbaum, 2007] Epelbaum, E. (2007). Four-nucleon force using the method of unitary transformation. *Eur.Phys.J.*, A34:197–214.

[Epelbaum, 2010] Epelbaum, E. (2010). Nuclear Forces from Chiral Effective Field Theory: A Primer.

[Epelbaum et al., 1998] Epelbaum, E., Gloeckle, W., and Meissner, U.-G. (1998). Nuclear forces from chiral Lagrangians using the method of unitary transformation. 1. Formalism. *Nucl.Phys.*, A637:107–134.

[Epelbaum et al., 2003] Epelbaum, E., Meissner, U.-G., and Gloeckle, W. (2003). Nuclear forces in the chiral limit. *Nucl.Phys.*, A714:535–574.

[Haag, 1958] Haag, R. (1958). Quantum field theories with composite particles and asymptotic conditions. *Phys. Rev.*, 112:669–673.

[Jenkins, 1998] Jenkins, E. E. (1998). Large N(c) baryons. *Ann.Rev.Nucl.Part.Sci.*, 48:81–119.

[Kaplan and Manohar, 1997] Kaplan, D. B. and Manohar, A. V. (1997). The Nucleon-nucleon potential in the 1/N(c) expansion. *Phys.Rev.*, C56:76–83.

[Kaplan and Savage, 1996] Kaplan, D. B. and Savage, M. J. (1996). The Spin flavor dependence of nuclear forces from large n QCD. *Phys.Lett.*, B365:244–251.

[Messiah, 1981] Messiah, A. (1981). *Quantum Mechanics*. Number Bd. 2 in Quantum Mechanics. North-Holland.

[Okubo, 1954] Okubo, S. (1954). Diagonalization of Hamiltonian and Tamm-Dancoff Equation. *Prog.Theor.Phys.*, 12:603.

[Okubo and Marshak, 1958] Okubo, S. and Marshak, R. (1958). Velocity dependence of the two-nucleon interaction. *Annals of Physics*, 4(2):166 – 179.

[Peskin and Schroeder, 1995] Peskin, M. E. and Schroeder, D. V. (1995). An Introduction to quantum field theory.

[Scherer and Schindler, 2012] Scherer, S. and Schindler, M. R. (2012). A Primer for Chiral Perturbation Theory. *Lect.Notes Phys.*, 830:pp.1–338.

['t Hooft, 1974] 't Hooft, G. (1974). A Planar Diagram Theory for Strong Interactions. *Nucl.Phys.*, B72:461.

[Weinberg, 1968] Weinberg, S. (1968). Nonlinear realizations of chiral symmetry. *Phys. Rev.*, 166:1568–1577.

[Weinberg, 1979] Weinberg, S. (1979). Phenomenological lagrangians. *Physica A: Statistical Mechanics and its Applications*, 96(12):327 – 340.

[Wigner and Griffin, 1959] Wigner, E. and Griffin, J. (1959). *Group Theory and Its Application to the Quantum Mechanics of Atomic Spectra*. Pure and applied Physics. Academic Press.

[Witten, 1979] Witten, E. (1979). Baryons in the 1/N Expansion. *Nucl.Phys.*, B160:57.

[Zee, 2003] Zee, A. (2003). Quantum field theory in a nutshell.